6-25-2021

Comparison of promoter, DNA vector, and cationic carrier for efficient transfection of hMSCs from multiple donors and tissue sources

Tyler Kozisek

Andrew Hamann

Luke Samuelson

Miguel Fudolig

Angela K. Pannier

Molecular Therapy
Nucleic Acids
Original Article

Comparison of promoter, DNA vector, and cationic carrier for efficient transfection of hMSCs from multiple donors and tissue sources

Tyler Kozisek,[1] Andrew Hamann,[1] Luke Samuelson,[1] Miguel Fudolig,[2] and Angela K. Pannier[1]

[1]Department of Biological Systems Engineering, University of Nebraska-Lincoln, Lincoln, NE, USA; [2]Department of Statistics, University of Nebraska-Lincoln, Lincoln, NE, USA

Human mesenchymal stem cells (hMSCs) are primary cells with high clinical relevance that could be enhanced through genetic modification. However, gene delivery, particularly through nonviral routes, is inefficient. To address the shortcomings of nonviral gene delivery to hMSCs, our lab has previously demonstrated that pharmacological "priming" of hMSCs with clinically approved drugs can increase transfection in hMSCs by modulating transfection-induced cytotoxicity. However, even with priming, hMSC transfection remains inefficient for clinical applications. This work takes a complementary approach to addressing the challenges of transfecting hMSCs by systematically investigating key transfection parameters for their effect on transgene expression. Specifically, we investigated two promoters (cytomegalovirus [CMV] and elongation factor 1 alpha), four DNA vectors (plasmid, plasmid with no F1 origin, minicircle, and mini-intronic plasmid), two cationic carriers (Lipofectamine 3000 and Turbofect), and four donors of hMSCs from two tissues (adipose and bone marrow) for efficient hMSC transfection. Following systematic comparison of each variable, we identified adipose-derived hMSCs transfected with mini-intronic plasmids containing the CMV promoter delivered using Lipofectamine 3000 as the parameters that produced the highest transfection levels. The data presented in this work can guide the development of other hMSC transfection systems with the goal of producing clinically relevant, genetically modified hMSCs.

INTRODUCTION

Human mesenchymal stem cells (hMSCs) are under extensive research for applications in cell and gene therapeutics[1,2] due to their ease of isolation from multiple adult tissues,[3] their multipotent differentiation potential,[4] and their ability to home to sites of injury and reduce inflammation upon transplantation.[5,6] These therapeutic properties could be enhanced or expanded through genetic modification accomplished via delivery of exogenous genes, e.g., delivery of a DNA vector encoding for differentiation factors to enhance hMSC tissue engineering applications.[7] Genetic modification of hMSCs can be accomplished via viral or nonviral methods.[8,9] While viral transduction is efficient, it suffers from safety issues related to immunogenicity and insertional mutagenesis.[9,10] Nonviral gene delivery, which typically consists of condensing an anionic DNA vector with a cationic carrier to form nano-sized complexes that are capable of *in vitro* transfection,[11] overcomes many challenges associated with viral methods; however, nonviral gene delivery suffers from inefficiency, especially in hMSCs.[12]

To address the shortcomings of nonviral gene delivery to hMSCs, our group has demonstrated that pharmacological "priming" of cells prior to or simultaneously with application of nonviral DNA complexes can improve transfection in hMSCs.[13–16] Specifically, we have shown that the glucocorticoid, dexamethasone, can significantly increase transfection efficiency and transgene expression in multiple donors of hMSCs from different tissues, relative to a vehicle control (VC),[13] by modulating transfection-induced stress pathways and apoptosis.[14,15] Additionally, we have expanded our hMSC transfection priming library by screening a collection of 707 FDA approved drugs for drug repurposing[17] and identified new candidate priming agents that can significantly improve transfection compared to a VC.[16] However, even with priming, nonviral gene delivery to hMSCs remains inefficient for clinical applications.

In addition to priming strategies to improve transfection in hMSCs, research has shown that many factors can contribute to the success of nonviral gene delivery systems, such as the promoter sequence,[18] DNA vector,[19–22] bacterial elements,[19] cationic carrier,[23] hMSC donor,[24] and hMSC tissue source.[13–15] Two common promoters, the viral cytomegalovirus (CMV) promoter and the endogenous elongation factor 1 alpha (EF1a) promoter, have shown varying degrees of transfection outcomes in hMSCs.[14,25] For example, we have shown increased transfection in hMSCs with a DNA vector containing the viral CMV promoter compared to a DNA vector containing the EF1a promoter,[14] while others have shown the opposite in hMSCs when using those promoters in different DNA vectors.[25] In addition to promoters, the DNA vectors themselves, and in particular the

Received 13 January 2021; accepted 25 June 2021;
https://doi.org/10.1016/j.omtn.2021.06.018.

Correspondence: Angela K. Pannier, Department of Biological Systems Engineering, University of Nebraska-Lincoln, Lincoln, NE, USA.
E-mail: apannier2@unl.edu

Table 1. DNA vector information

Vector Name	Transgene	Promoter	Bacterial elements
CMV	Fusion protein of EGFP and luciferase	CMV	pUC origin of replication
EF1a		EF1a	F1 origin of replication
			Kanamycin resistance marker
CMV No F1		CMV	pUC origin of replication
EF1a No F1		EF1a	Kanamycin resistance marker
MC CMV		CMV	None
MC EF1a		EF1a	
MIP CMV		CMV	pUC origin of replication
MIP EF1a		EF1a	RNA-OUT selectable marker

bacterial elements contained within the DNA vectors (e.g., bacterial origins of replication, like the F1 origin,[26] and antibiotic resistance genes) can modulate transfection. For example, minicircle vectors (MCs), which do not contain any bacterial elements, have shown increased transfection efficiency in hMSCs compared to conventional plasmids[7] that contain bacterial elements. Alternatively, mini-intronic plasmids (MIPs), which include bacterial elements within an engineered intron, have shown enhanced transfection *in vitro* and *in vivo* compared to conventional plasmids, possibly due to the inclusion of an intron.[19,22] However, MIPs have not been investigated in the context of hMSC transfection. In addition to vector elements, different cationic carriers, such as polymers or lipids, have shown varying degrees of transfection in hMSCs.[23] Beyond DNA vector and cationic carrier, hMSC donor and tissue source (i.e., adipose or bone marrow) can affect transfection success as well.[13–15,24]

However, even with the above studies, these variables and their effects on nonviral gene delivery to hMSCs have yet to be systematically examined, and thus the objective of this work was to investigate four DNA vectors (plasmid DNA, plasmid DNA with no F1 origin of replication, MIPs, and MCs) and two promoters (CMV and EF1a), complexed with two commercially available cationic carriers (Lipofectamine 3000 and Turbofect) for their effects on transfection in hMSCs from four donors derived from two tissue sources (adipose- and bone-marrow-derived). This work systematically studies the key aspects of nonviral gene delivery systems as they pertain to hMSCs and offers insight into design parameters that can be exploited and further explored to develop efficient gene delivery systems for cells of high clinical significance.

RESULTS

The objective of this study was to investigate the effects of different promoters, DNA vectors, and cationic carriers on transfection in hMSCs from different donors and tissues. Specifically, we investigated two promoters (CMV and EF1a; Table 1) and four DNA vectors (plasmid, plasmid with no F1 origin of replication, MC, and MIP; Table 1; Figure 1), delivered using two commercially available cationic carriers (Turbofect [polymer-mediated] and Lipofectamine 3000 [lipid-mediated]) to cells from four hMSC donors (D1, D2, D3, and D4; Table S1) derived from two tissue sources (bone-marrow-derived and adipose-derived; Table S1) in order to identify transfection parameters that significantly ($p < 0.05$) affect transfection efficiency and transgene production in hMSCs. The effects on transfection efficiency were assayed by fluorescence imaging of an expressed transgenic fusion protein of enhanced green fluorescent protein (EGFP) with luciferase, normalized by total cell count (Hoechst 33342, nuclei stain), to obtain transfection efficiencies for all conditions. Imaging results were then verified by a chemical assay for transgenic luciferase activity, in relative light units (RLUs), normalized by total cellular protein values (RLU/mg Protein). It is important to note that due to the varying sizes of DNA vectors and promoters tested, both mass of DNA delivered and DNA copy number (i.e., molarity of transgene) were normalized for each promoter and cationic carrier in order to properly compare conditions (Table 2).

Given all of the variables above, this study tested 64 conditions, in triplicate on duplicate days ($n = 6$), to identify key transfection parameters (Tables 1; Table S1) that modulate hMSC transfection efficiency (Figures 2A and 2C) and transgene production (Figures 2B and 2D). Both outcomes varied widely as a function of each parameter, e.g., D3 bone-marrow-derived hMSCs (hBMSCs) transfected with the conventional CMV plasmid complexed with Turbofect produced transfection efficiencies around 35%, the highest of our study (Figure 2A), while D2 adipose-derived hMSCs (hAMSCs) transfected with CMV MIP complexed with Lipofectamine 3000 produced the highest transgenic luciferase activity of our study (Figure 2D). When comparing fold change differences between all possible comparisons (Figures S1 and S2), D1 hAMSCs transfected with EF1a MIP vectors complexed with Lipofectamine 3000 increased transfection efficiency almost 2-fold and transgenic luciferase activity by more than 6-fold compared to D1 hAMSCs transfected with the conventional CMV plasmid complexed with Lipofectamine 3000 (Figures S1A and S2A, respectively). However, given the multitude of parameters and combinations studied, data analysis was performed to assess whether there were any significant interactions between variables. Analyzing the transfection data as a negative binomial identified all two-way interactions as significant (Table S3), therefore, further analysis of the effects of each individual parameter on transfection outcomes was conducted, as described next.

Promoter selection can affect transfection in hMSCs

In order to understand promoter effects on hMSC transfection, transgene expression data (i.e., number EGFP-positive cells and total cells counts) were grouped by promoter (CMV or EF1a) for all hMSCs (D1, D2, D3, and D4), cationic carriers (Turbofect and Lipofectamine 3000), and DNA vectors (plasmid, no F1, MC, and MIP) and depicted as scatterplots of total cell counts versus number of EGFP-positive cells (Figure 3). These plots were sectioned into four quadrants for each promoter as described in the methods and legend for Figure 3. Analyzing transfection data as a function of promoter revealed differences between the CMV and EF1a promoters, as the CMV promoter resulted in eight conditions (transfection efficiencies for conditions in which hAMSCs were transfected with MIPs; Figure 3A) out of 192 total conditions/replicates in quadrant 2 (Q2; i.e., high transgene expression and low total cell counts), whereas the EF1a promoter

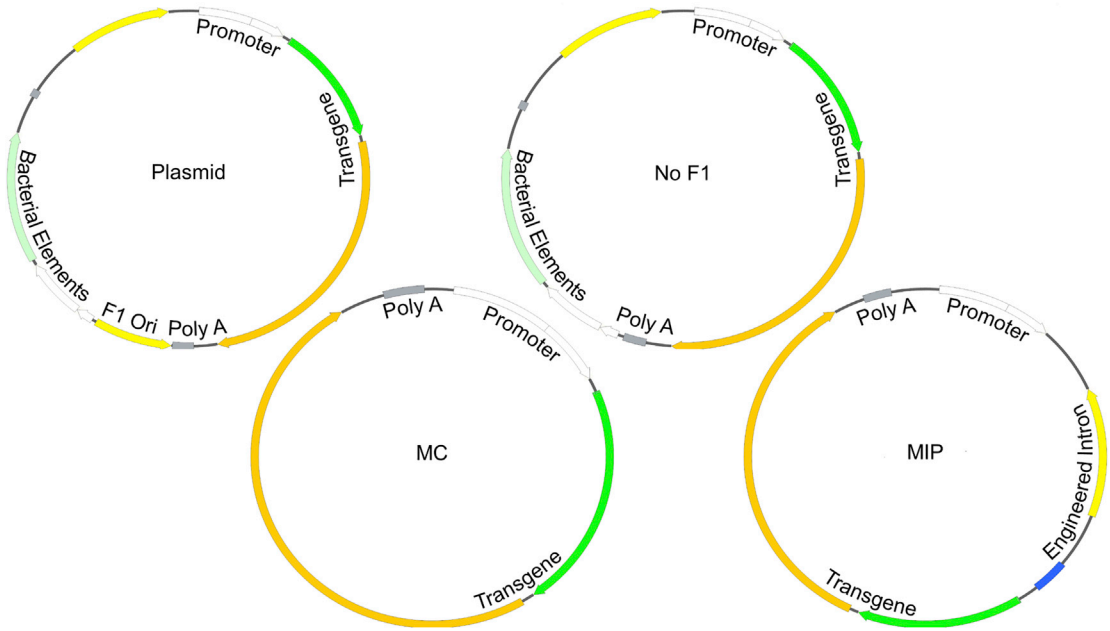

Figure 1. Representative schematics of DNA vectors investigated in this study

DNA vector diagrams are not to scale. DNA vector diagrams were created with SnapGene. F1 Ori, F1 origin of replication; poly(A), polyadenylation signal; MC, minicircle; MIP, mini-intronic plasmid.

resulted in no conditions in Q2 (Figure 3B). Furthermore, both promoters resulted in a majority of the transfection conditions within Q3 (i.e., low transgene expression and low total cell counts). Analyzing EGFP-positive cell counts as a negative binomial variable, with total cell counts as an offset term, showed that in terms of promoter effects, the CMV promoter resulted in significantly higher EGFP-positive cell counts than the EF1a promoter at the same total cell count within vector ($p < 0.0001$, Table S4), cationic carrier ($p < 0.0001$, Table S5), and donor ($p < 0.0001$, Table S6).

DNA vector bacterial elements affect transfection in hMSCs

In a similar manner used to compare promoters, transgene expression data (i.e., number of EGFP-positive cells and total cell counts) were grouped by the bacterial elements contained within each DNA vector (Table 1; Figure 4). Transgene expression data for the 16 conventional plasmid conditions, which contain the most bacterial elements (Table 1), were analyzed (i.e., CMV and EF1a; Table 1; Figure 2). Conditions in which hMSCs were transfected with conventional plasmids generally had transgene expression data in Q3 (i.e., low transgene expression and low total cell counts; Figure 4A). Removal of the F1 origin of replication from the conventional plasmid (No F1) resulted in more transfection conditions with higher EGFP-positive cell counts (i.e., Q1, more transgene expression) or higher total cell counts (i.e., Q4; Figure 4B) compared to conventional plasmids; however, conditions in which hMSCs were transfected with No F1 vectors generally had transgene expression data within Q3 (Figure 4B). Transgene expression data for the 16 MC conditions were also analyzed (Table 1; Figure 2). Conditions in which hMSCs were transfected with MCs generally produced transgene expression data that were within Q3 (i.e., low transgene expression and low total cell counts; Figure 4C). Conditions where hMSCs were transfected with MCs also produced a lower number of EGFP-positive cells (Figure 4C) compared to conditions where hMSCs were transfected with either conventional plasmids or No F1 vectors (Figures 4A and 4B, respectively). Finally, the transgene expression data for the 16 MIP conditions (Table 1; Figure 2) were analyzed. Conditions in which hMSCs were transfected with MIPs generally produced transgene expression data that were within Q3 (i.e., low transgene expression and low total cell counts; Figure 4D); however, conditions where hMSCs were transfected with MIPs produced more transgene expression data that were within Q2 (i.e., high transgene expression and high total cell counts; Figure 4D) compared to conditions where hMSCs were transfected with conventional plasmids (Figure 4A), No F1 vectors (Figure 4B), and MCs (Figure 4C). Analyzing EGFP-positive cell counts as a negative binomial variable with total cell counts as an offset term, indicated significant differences in EGFP-positive cell counts between vectors at the same total cell count within promoter ($p < 0.01$, Table S7), cationic carrier ($p < 0.0001$, Table S8), and donor ($p < 0.05$, Table S9). Furthermore, MIP vectors resulted in significantly higher EGFP-positive cell counts compared to all other vectors tested in hMSCs ($p < 0.001$, Table S9), except for D4 hMSCs transfected with plasmids ($p < 0.07$, Figure 4; Table S9).

Cationic carrier can affect hMSC transfection

In a similar manner used to compare promoters and bacterial elements, transgene expression data (i.e., number of EGFP-positive cells

Table 2. Normalization of DNA vector mass and moles of transgene

Vector name	Vector size (kbp)	Normalized expression cassette fraction	Fraction of expressionless vector for 1 μg/μL stocks
CMV	6.3	1	0
EF1a	6.9	1	0
CMV No F1	5.9	0.94	0.06
EF1a No F1	6.5	0.94	0.06
MC CMV	3.3	0.52	0.48
MC EF1a	3.9	0.57	0.43
MIP CMV	4.7	0.75	0.25
MIP EF1a	5.4	0.78	0.22

Kbp, kilobase pairs

and total cell counts) were grouped for the two commercially available cationic carriers (Figure 5). Conditions that made use of Turbofect, a polymer-based cationic carrier, generally had transgene expression data within Q3 (i.e., low transgene expression and low total cell counts; Figure 5A), however, seven transfection conditions (conditions in which hAMSCs were transfected with MIP CMV vectors) of the 192 conditions/replicates were contained within Q2 (i.e., high transgene expression and high total cell counts; Figure 5A). Conditions that made use of Lipofectamine 3000, a lipid-based cationic carrier, had one condition within Q2 (D1 hAMSC transfected with MIP CMV vectors; Figure 5B) but similar to Turbofect, the 64 conditions that made use of Lipofectamine 3000 (Figure 2) generally produced transgene expression data within Q3 (Figure 5B). Furthermore, analyzing EGFP-positive cell counts as a negative binomial variable, with total cell counts as an offset term, indicated a significant difference in EGFP-positive cell counts between Lipofectamine 3000 and Turbofect at the same total cell count within promoter ($p < 0.05$, Table S10), vector ($p < 0.01$, Table S11), and donor ($p < 0.01$, Table S12); however, due to our experimental design, it is difficult to conclude with any statistical confidence that Lipofectamine 3000 results in more EGFP-positive cells than Turbofect specifically between donors.

hMSC donor and tissue source can affect transfection

In a similar manner used to analyze promoters, bacterial elements, and cationic carriers, transgene expression data (i.e., number of EGFP-positive cell counts and total cell counts) for each hMSC donor and tissue source were grouped (Table S1; Figure 6). Transfection of hAMSCs generally resulted in transgene expression data within Q3 and Q4 (i.e., low transgene expression and varying total cell counts; Figure 6A) while transfection of hBMSCs resulted in all but one condition within Q3 (D4 hBMSCs transfected with No F1 CMV vector; Figure 6B). We further separated the transgene expression data by hMSC donor within each scatterplot in order to investigate transfection as a function of donor variability. For the two donors of hAMSCs, D1 (orange symbols) had transfection conditions with fewer EGFP-positive cells but higher total cell counts when compared to transfection conditions for D2 (Figure 6A; yellow symbols). However, there was little difference in transgene expression data between the two donors of hBMSCs (Figure 6B). Analyzing EGFP-positive cell counts as a negative binomial variable, with total cell counts as an offset term, indicated a significant difference in EGFP-positive cell counts between donors within promoter ($p < 0.05$, Table S13), vector ($p < 0.05$, Table S14), and cationic carrier ($p < 0.05$, Table S15); however, due to our experimental design in which we blocked by donor, further interpretation of statistical analysis on donor effects is not appropriate.

DISCUSSION

hMSCs are primary cells isolated from a variety of tissue with high clinical relevance,[1,2] which could be enhanced through genetic modification. However, gene delivery, particularly through nonviral routes, is inefficient.[8,12–16,24] We have previously reported enhanced nonviral gene delivery to hMSCs by priming with pharmacologic agents,[16] specifically with the glucocorticoid dexamethasone;[13–15] however, work remains to improve nonviral gene delivery to hMSCs, in particular through evaluation of key variables of the nonviral gene delivery system. This work systematically compares the key variables of nonviral gene delivery systems (e.g., DNA vector type, DNA vector bacterial elements, promoter, cationic carrier, and donor and tissue source) and the effects of these variables on transfection outcomes. The transfection outcomes varied widely for all 64 conditions tested (Tables 1; Table S1; Figure 2), therefore, deliberate grouping of variables was conducted in order to study the effects of each variable on hMSC transfection.

In order to investigate the effects of DNA vector modification on hMSC transfection, we first aggregated imaging transfection data (i.e., number of EGFP-positive cells and total cell counts) for all conditions tested and analyzed a single variable at a time. The first variable that we investigated was promoter used to drive expression of the transgene. The two promoters tested in this work (i.e., CMV and EF1a) are widely used promoters for gene delivery shown to produce high levels of transfection in numerous cell types.[25,27] Even so, the CMV promoter has shown significantly increased transfection levels compared to the EF1a promoter, especially in hMSCs.[14] Consistent with other published work, in this work, the CMV promoter did result in significantly increased EGFP-positive cell counts compared to the EF1a promoter when only the effects of the promoter were analyzed (Figure 3; Table S4–S6). This significant increase in transfection by the CMV promoter compared to the EF1a promoter may be from increased transcription of the transgene, as Antonova and colleagues have shown that the CMV promoter produces more transgenic mRNA transcripts compared to other promoters in mouse and primary human fibroblasts.[28] However, in this current report there was no significant increase in transgenic mRNA transcripts in hAMSCs from the CMV promoter compared to the EF1a promoter for any of the conditions tested at either 12 or 24 h after delivery of the transgene (Figure S3). While not significant, we did observe slight increases in transgenic mRNA transcripts in hAMSCs transfected with CMV DNA vectors compared to hAMSCs transfected with the same DNA vector with the EF1a promoter. However, these increases in transgenic mRNA transcripts likely do not contribute to the

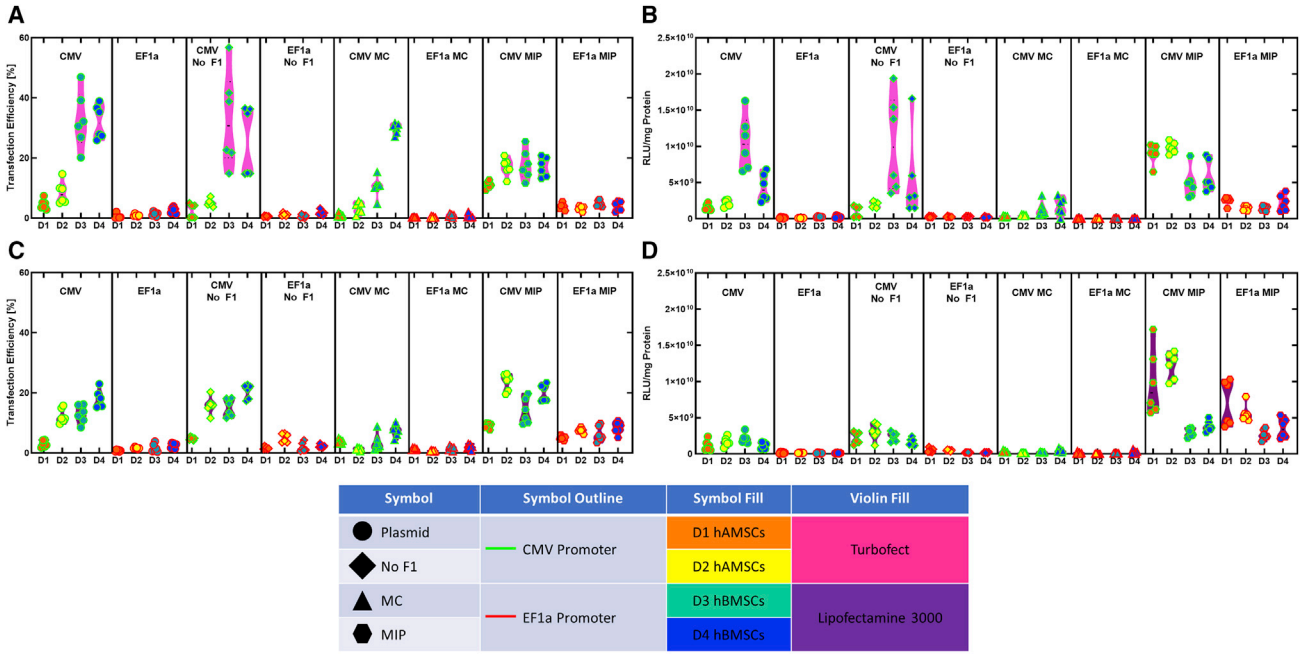

Figure 2. Transfection efficiency and production of transgene for all 64 conditions tested

(A) Violin plots of transfection efficiency for the 32 transfection conditions where Turbofect was used as the cationic carrier. (B) Violin plots of transgenic luciferase activity normalized to total protein amounts for the 32 transfection conditions where Turbofect was used as the cationic carrier. (C) Violin plots of transfection efficiency for the 32 transfection conditions where Lipofectamine 3000 was used as the cationic carrier. (D) Violin plots of transgenic luciferase activity normalized to total protein amounts for the 32 conditions that Lipofectamine 3000 was used as the cationic carrier. Parameters are identified within the legend provided.

significant increases in transfection efficiency and transgenic luciferase activity that we observed, and others have reported,[14] from the CMV promoter compared to the EF1a promoter. While this current study confirms that the CMV promoter produces more transfection than the EF1a promoter in hMSCs from multiple donors and tissue sources, the mechanism of enhancement for the CMV promoter needs further investigation.

Next, we investigated the effects of bacterial elements contained within the DNA vector for their effect on transfection outcomes in hMSCs. Conventional plasmids contain bacterial origins of replication and typically an antibiotic resistance gene for selection of plasmid-harboring bacteria during plasmid propagation. These bacterial components, while necessary for DNA vector production, have often been associated with an innate immune response through recognition of pathogen associated molecular patterns (PAMPs; e.g., unmethylated cytosine-phosphate-guanine [CpG]) by pattern recognition receptors (PPRs),[29,30] which may lead to transgene silencing.[31,32] Therefore, research into the development of highly efficient nonviral gene delivery systems has focused on removing bacterial elements from nonviral vectors.[8,29] While the experiments in this present work were not designed to study transgene silencing (i.e., transfection was assayed at a single time point following addition of DNA vectors), we did observe slight increases in transgenic luciferase activity when the F1 origin of replication (i.e., bacterial element) was removed from conventional plasmids, compared to conventional plasmids (Figures 2B and 2D). The F1 origin of replication is used in conventional plasmids to replicate and package single-stranded DNA into phages;[33] however, the F1 origin of replication is not necessary for conventional plasmid production or expression in mammalian cells. Furthermore, Johnson and colleagues[26] observed significant increases in bactofection (i.e., delivery of genetic cargo to mammalian cells using bacteria) of human breast cancer cells when the bacteria were harboring plasmids with no F1 origin of replication, presumably by rescuing DNA-induced stress. Therefore, removal of nonessential bacterial elements within DNA vectors may increase transfection in various cell types, particularly in hMSCs.

While removal of all bacterial elements is improbable for conventional plasmid production, Chen and colleagues[34] developed a DNA vector devoid of all bacterial elements, termed MCs, and showed increased transgene expression *in vivo* compared to conventional plasmids. MCs are devoid of all bacterial elements, while also having the ability to be propagated in engineered bacteria, through excision and recombination of the expression cassette from a parental plasmid, leaving a DNA vector that contains a promoter, transgene, and a terminator sequence.[34] MCs have since been shown to enhance transfection in hMSCs,[7,25,35–37] as well as stem cells from other species,[38,39] compared to conventional plasmids; however, in this current study, MCs produced the lowest transfection efficiencies and transgene expression observed, regardless of cationic carrier, promoter, donor, or hMSC tissue source (Figures 2, 3, 4, 5, and 6). The large

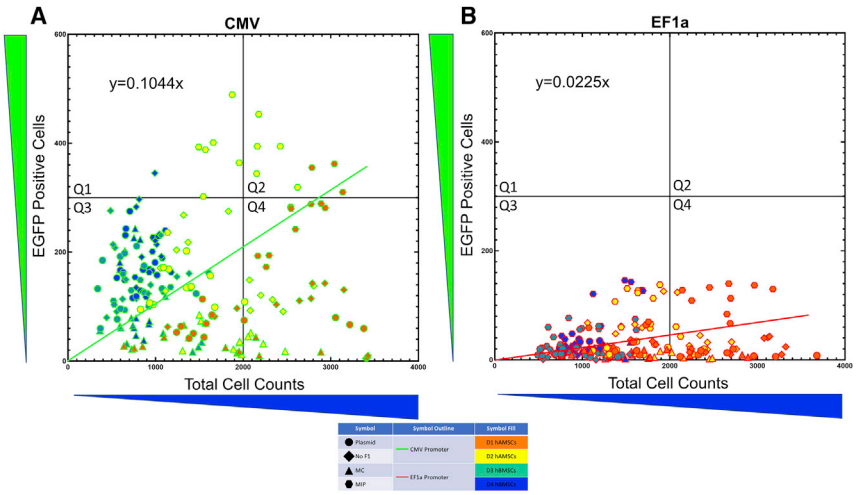

Figure 3. Transgene expression data as a function of DNA vector promoter in human mesenchymal stem cells (hMSCs)

(A) Scatterplot showing aggregated EGFP-positive cells and total cell counts for all transfection conditions (Table S1; Table 1) with the CMV promoter in all donors of hMSCs. (B) Scatterplot showing aggregated EGFP-positive cells and total cell counts for all transfection conditions (Table S1; Table 1) with the EF1a promoter in all donors of hMSCs. Quadrant 1 (Q1) represents high transgene expression but low total cell counts, which could be attributed to either transfection-induced toxicity and/or a reduction in proliferation. Q2 represents high transgene expression with high total cell counts, which could be attributed to either minimal transfection-induced toxicity and/or minimal reduction in proliferation. Q3 represents both low transgene expression and low total cell counts. Lastly, Q4 represents low transgene expression but high total cell counts. It should be noted that these quadrants were partitioned using the highest number of EGFP-positive cells and total cell counts that were observed in this current study; therefore, these quadrant boundaries should not be used to evaluate conditions and data from other studies. Lines represent the Poisson regression line that best fits the data. Parameters are identified within the legend provided.

discrepancy in transfection outcomes from MCs observed in this current study compared to other published studies may be from our normalization of both moles of expression cassette (i.e., transgene) and mass of DNA delivered (Table 2). For example, Mun and colleagues[25] observed higher transfection efficiencies in hAMSCs and hBMSCs using an EGFP expressing MC compared to an EGFP expressing plasmid when equal moles of expression cassette were delivered (i.e., higher mass of plasmid delivered than mass of MC). Alternatively, Boura and colleagues[36] delivered equal mass of MCs (i.e., higher molarity of expression cassette for MCs compared to plasmid) encoding for human leukocyte antigen-G1 (HLA-G1) to hBMSCs as plasmids carrying HLA-G1 and observed significantly higher expression of HLA-G1 from MCs in hBMSCs compared to a plasmid with the same promoter. Furthermore, Zimmermann and colleagues[7] showed significantly more alkaline phosphatase (ALP) activity in hBMSCs transfected with a bone morphogenetic protein 2 (BMP2) encoding MC compared to a conventional plasmid encoding BMP2, when equal mass of DNA was delivered (i.e., higher molarity of expression cassette for MCs compared to plasmid); however, when equal moles of expression cassette was delivered (i.e., higher mass of plasmid delivered than mass of MCs), BMP2 encoding MCs produced the same levels of ALP activity compared to BMP2 encoding plasmids. Indeed, we have observed increased transfection in hMSCs with MCs compared to conventional plasmids when equal mass of DNA vector was delivered but not equal moles of expression cassette (T.K., unpublished data); however, delivering equal mass of vectors with drastically different sizes is not a fair comparison as there will always be higher concentrations of expression cassette for the smaller vector (i.e., MC) than the larger vector (i.e., conventional plasmid), potentially increasing the probability of successful transfection for the smaller vector. Furthermore, delivering equal moles of expression cassette is also not a fair comparison for DNA vectors with drastically different sizes as the larger vector (i.e., conventional plasmid) will always have more mass of DNA than the smaller vector (i.e., MC), potentially leading to more toxicity than the smaller vector, as Zimmermann and colleagues observed a significant decrease in viability for conventional plasmids compared to MCs when equal moles of transgene were delivered (i.e., higher mass of conventional plasmid).[7] Therefore, we recommend that both moles of transgene and mass of DNA delivered need to be normalized in order to robustly compare DNA vectors with drastically different sizes. However, whether the transfection by MC observed in other studies is due to the lack of bacterial elements or the vectors' small size compared to conventional plasmids, or whether the lack of transfection observed in this work is due to lower copy numbers of the expression cassette for a given mass of DNA delivered, needs further investigation.

Another DNA vector with reduced bacterial components, which retains the ability to propagate in conventional bacteria, was developed by the Kay Lab.[19] These vectors, termed MIPs, contain all bacterial elements necessary for vector propagation in an engineered intron within the expression cassette.[19] The idea to incorporate bacterial elements within an engineered intron in the expression cassette stemmed from observations of *in vivo* transgene silencing when the extragenic space between the 5′ and 3′ ends of the expression cassette was greater than 1 kb.[31] The authors hypothesized that shortening the extragenic space between the 5′ and 3′ ends of the expression cassette could allow for more efficient gene looping, a mechanism in which the promoter and terminator regions are juxtaposed in a transcription-dependent manner,[40] thereby promoting efficient transcriptional elongation and recycling of RNA polymerase II from the terminator to the promoter. Their hypothesis that shortening the extragenic

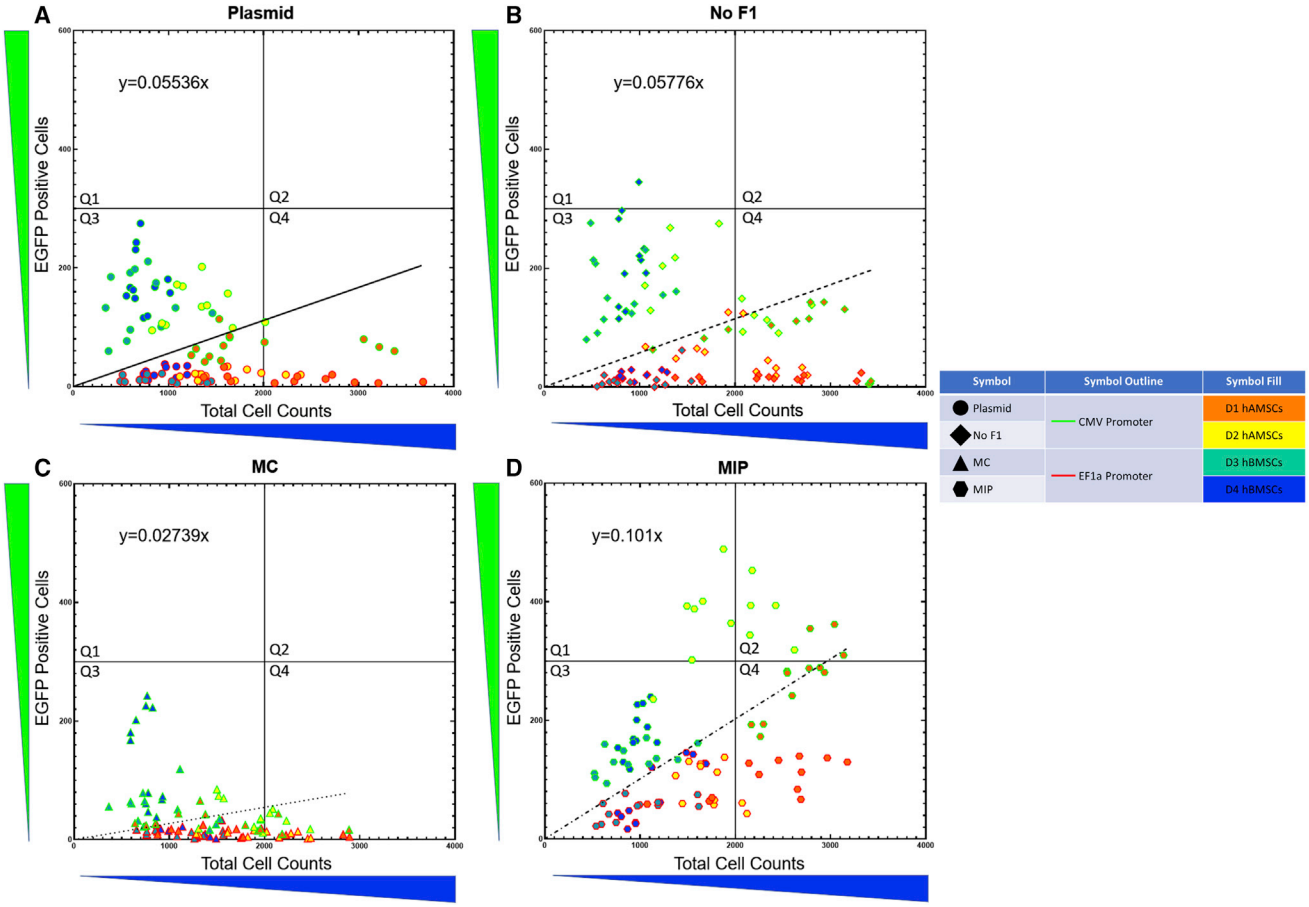

Figure 4. Transgene expression data as a function of DNA vector bacterial elements in hMSCs

(A) Scatterplot showing aggregated EGFP-positive cells and total cell counts for all plasmid vector conditions in all donors of hMSCs. (B) Scatterplot showing aggregated EGFP-positive cells and total cell counts for all plasmid conditions with the F1 origin of replication removed (No F1) in all donors of hMSCs. (C) Scatterplot showing aggregated EGFP-positive cells and total cell counts for all MC vector conditions in all donors of hMSCs. (D) Scatterplot showing aggregated EGFP-positive cells and total cell counts for all MIP conditions in all donors of hMSCs. Q1 represents high transgene expression but low total cell counts, which could be attributed to either transfection-induced toxicity and/or a reduction in proliferation. Q2 represents high transgene expression with high total cell counts, which could be attributed to either minimal transfection-induced toxicity and/or minimal reduction in proliferation. Q3 represents both low transgene expression and low total cell counts. Lastly, Q4 represents low transgene expression but high total cell counts. It should be noted that these quadrants were partitioned using the highest number of EGFP-positive cells and total cell counts that were observed in this current study, therefore, these quadrant boundaries should not be used to evaluate conditions and data from other studies. Lines represent the Poisson regression line that best fits the data. Parameters are identified within the legend provided.

space would allow for more efficient gene looping was never verified, but Lu and colleagues[19] did observe enhanced transfection with MIPs in mice and in human cells compared to plasmids and MCs. Indeed, MIPs produced the highest transfection efficiencies and transgene expression in this current study in both donors of hAMSCs compared to all other vectors, regardless of cationic carrier or promoter (Figures 2, 3, 4, 5, and 6). Additionally, we observed significantly more transgenic mRNA transcripts from hAMSCs transfected with MIP EF1a compared to hAMSCs transfected with either CMV or EF1a plasmids at 24 h (Figure S3); however, similar results were not observed for hAMSCs transfected with MIP CMV (Figure S3). The high transfection levels from MIPs observed in this current study, as well as other published work,[19,22,41] may be from the inclusion of an intron within the expression cassette, as others have shown increased transgene expression[42] or mRNA transcripts[43] when introns were inserted into the expression cassette. Introns have long been thought of as superfluous genetic material and were traditionally removed from transgenes prior to ligating into a DNA vector; however, introns have been shown to play vital roles in transgene expression, such as transcription,[43] polyadenylation,[44] and mRNA export and decay,[45] as well as translational efficiency.[46] Given the transfection levels observed in this current study by MIPs, as well as the transgenic mRNA transcript levels at 12 and 24 h after transfection, it is plausible that the engineered intron within the expression cassette of MIPs might be promoting transcription[42,43] or limiting mRNA decay (i.e., significantly higher transgenic mRNA transcripts for MIPs in

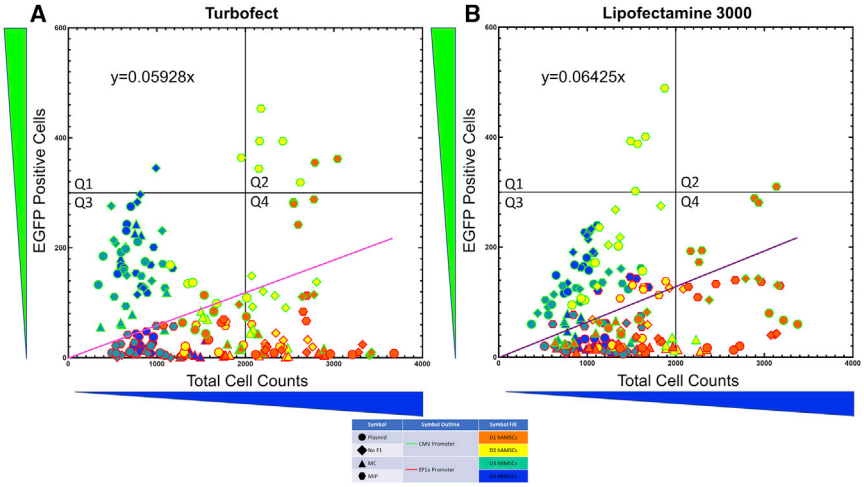

Figure 5. Transgene expression data as a function of cationic carrier in hMSCs

(A) Scatterplot showing aggregated EGFP-positive cells and total cell counts for all transfection conditions where the polymer transfection reagent Turbofect was used as the cationic carrier in all donors of hMSCs. (B) Scatterplot showing aggregated EGFP-positive cells and total cell counts for all vectors where the lipid transfection reagent Lipofectamine 3000 was used as the cationic carrier in all donors of hMSCs. Q1 represents high transgene expression but low total cell counts, which could be attributed to either transfection-induced toxicity and/or a reduction in proliferation. Q2 represents high transgene expression with high total cell counts, which could be attributed to either minimal transfection-induced toxicity and/or minimal reduction in proliferation. Q3 represents both low transgene expression and low total cell counts. Lastly, Q4 represents low transgene expression but high total cell counts. It should be noted that these quadrants were partitioned using the highest number of EGFP-positive cells and total cell counts that were observed in this current study, therefore, these quadrant boundaries should not be used to evaluate conditions and data from other studies. Lines represent the Poisson regression line that best fits the data. Parameters are identified within the legend provided.

D1 hAMSCs compared to both the CMV and EF1a conventional plasmid, regardless of promoter used; Figures S3B and S3D) or are enhancing translation in hAMSCs[42] (i.e., higher transfection efficiency and transgene expression by MIPs compared to other vectors tested regardless of promoter or cationic carrier in hAMSCs; Figure 4). However, in hBMSCs, increases in transfection efficiency and transgene expression by MIPs were only observed when the EF1a promoter was used (Figure 2), possibly due to the incorporation of a second intron within the EF1a promoter[42] or differences in intron processing by the cells.[47] However, studies comparing transcription and translation efficiency differences from either gene looping or incorporation of one or more introns are needed to fully elucidate the transfection enhancements observed by MIPs in hMSCs.

In addition to the above transfection parameters, research has shown that polymer- and lipid-mediated nonviral gene delivery efficacy can be dependent on cationic carrier formulation; however, limited research has been conducted on how polymer- and lipid-mediated transfection can be affected by different DNA vectors,[48] in particular within the context of hMSCs from multiple donors and tissue sources. Here, two commercially available transfection reagents were used, which represent both lipid- and polymer-based systems: Lipofectamine 3000 and Turbofect, respectively. These commercially available transfection reagents were chosen as they are readily available, widely used, and have shown moderate levels of transfection in hMSCs[14–16,24] (T.K., A.H., and L.S., unpublished data). This study did not include other modes of delivery (e.g., electroporation) given the complexities involved in comparing carrier-based systems to physical methods, but future studies should investigate other delivery strategies in the context of the parameters investigated here.

In this current study, there were differences in transfection efficiencies and transgene production between the two cationic carriers (Figure 2) and Poisson regressions of aggregated transgene expression data for each cationic carrier showed slight differences in overall transfection trends (Figure 5). Indeed, others have shown differences in transfection outcomes in hMSCs between polymer- and lipid-based systems, with either polymer-[49] or lipid-based[23] systems producing the highest transgene expression. Furthermore, we observed significantly different total cell ratios for tested cationic carriers (Turbofect total cell count divided by the total cell count for the same condition complexed with Lipofectamine 3000, which is an indirect measure of toxicity and/or proliferative effects of Turbofect relative to Lipofectamine 3000) between hAMSCs and hBMSCs (Figure S4), highlighting another transfection parameter that needs to be carefully considered in a hMSC nonviral gene delivery system. Indeed, our previous studies on hMSC transfection with lipid-based cationic carriers extensively characterized both cellular proliferation (through metabolic studies)[13] and transfection-induced toxicity,[15] and showed that rescuing transfection-induced metabolic shut down and toxicity could enhance transfection efficiency and transgene production.[13,15]. Taken together, cationic carrier selection does not have a large effect on overall transfection outcomes; however, transfection and total cell counts, which are an indirect measure of cytotoxicity and/or proliferative nature, can be optimized if the cationic carrier is selected based on hMSC tissue source.

Finally, hMSCs can be harvested from multiple tissues in the adult human body[50,51] and, due to their immunomodulatory effects,[5,52] have the potential for allogenic use,[53] making both donor and tissue source pertinent variables in this study. hMSCs have been shown to have

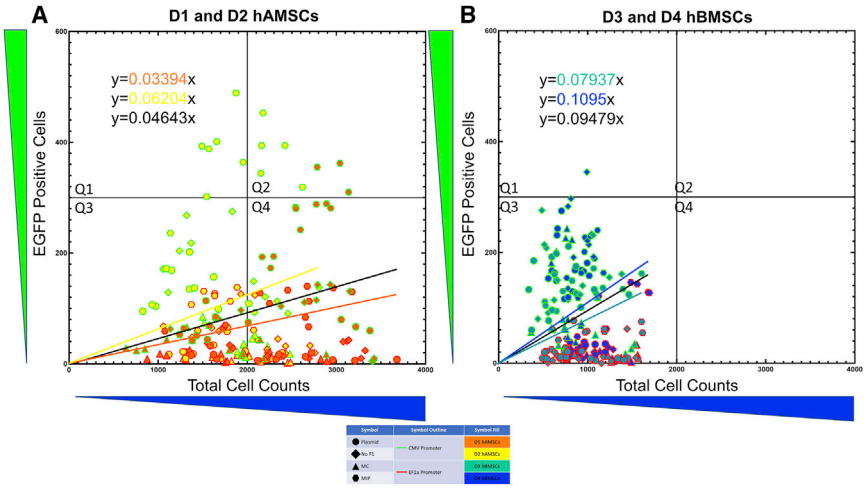

Figure 6. Transgene expression data as a function of hMSC tissue source and donor

(A) Scatterplot showing aggregated EGFP-positive cells and total cell counts for all transfection conditions in both donors of adiposed-derived hMSCs (hAMSCs). (B) Scatterplot showing aggregated EGFP-positive cells and total cell counts for all transfection conditions in both donors of bone-marrow-derived hMSCs (hBMSCs). Q1 represents high transgene expression but low total cell counts, which could be attributed to either transfection-induced toxicity and/or a reduction in proliferation. Q2 represents high transgene expression with high total cell counts, which could be attributed to either minimal transfection-induced toxicity and/or minimal reduction in proliferation. Q3 represents both low transgene expression and low total cell counts. Lastly, Q4 represents low transgene expression but high total cell counts. It should be noted that these quadrants were partitioned using the highest number of EGFP-positive cells and total cell counts that were observed in this current study; therefore, these quadrant boundaries should not be used to evaluate conditions and data from other studies. Lines represent the Poisson regression line that best fits the data. Parameters are identified within the legend provided.

large variability in gene expression, proliferative capacity, differentiation capacity, and transfection efficacy between the donor and tissue source from which they were obtained;[13–15,24,50,54] however, these parameters have not been studied in depth as they pertain to DNA vector modifications and transfection outcomes.[13,14] Here, the data show discrepancies in trends between transfection outcomes for each condition between the different donors and tissue sources (Figure 2), which may be partly attributed to the different proliferation rates between hMSCs from different donors and tissue source.[50] Generally, hAMSCs have higher proliferation rates compared to hBMSCs,[50] which may increase nuclear internalization of DNA vectors due to the increased nuclear breakdown, thereby giving hAMSCs a higher probability of successful transfection compared to hBMSCs. The slower proliferating hBMSCs may have lower probabilities of successful transfection due to less nuclear breakdown but have a higher DNA vector-to-cell ratio due to their lower cell numbers compared to hAMSCs (Figure 6), possibly causing an increase in transfection-induced toxicity (Figure S4) due to the higher DNA vector dose, as others have observed.[55] However, further studies are needed in order to elucidate the discrepancies in transfection efficiency and transgene expression observed in this study between different conditions on a hMSC donor and tissue source basis.

Conclusions

This work systematically investigated the effects of DNA vector modifications (i.e., promoter, bacterial element quantities, and positions within the vector) on transfection in hMSCs from different donors and tissue sources using two commercially available cationic carriers. Analyzing each variable separately, we observed differences in transfection outcomes based on promoter selection, DNA vector, and cationic carrier, as well as donor and tissue source. Notably, we observed the highest levels of transgene expression when MIPs, complexed with Lipofectamine 3000, were delivered to hAMSCs and transgene production was under control of the CMV promoter. Furthermore, the presented data provide valuable insight into the importance of hMSC donor and tissue source variability as they pertain to DNA vector modifications for nonviral gene delivery. This work demonstrates that transfection parameters may need to be tuned in an application- and patient-specific manner in order to achieve efficient transfection in hMSCs for clinical therapies.

MATERIALS AND METHODS

Cell culture

Cryopreserved hMSCs from four human donors and two tissue sources were purchased at passage two from Lonza (Lonza, Walkersville, MD, USA) and were used at passage six (see Table S1 for donor information). Adipose-derived hMSCs (hAMSCs) were positive for CD13, CD29, CD44, CD73, CD90, CD105, CD166, and negative for CD14, CD31, and CD45 cell surface markers. Bone-marrow-derived hMSCs (hBMSCs) were positive for CD29, CD44, CD105, and CD166 and negative for CD14, CD34, and CD45 cell surface markers. hMSCs were passaged and cultured in hMSC media, consisting of minimum essential medium alpha (MEM Alpha; GIBCO, Grand Island, NY, USA) supplemented with 10% heat-inactivated fetal bovine serum (FBS; GIBCO), 6 mM L-Glutamine (GIBCO), and 1% penicillin-streptomycin (Pen-Strep; 10,000 U/mL; GIBCO), and incubated at 37°C with 5% CO_2 until confluent. At confluence, hMSC media was removed and cells were washed with 1× phosphate-buffered saline (PBS) prior to the addition of 0.25% trypsin-ethylenediamine tetraacetic acid (EDTA; GIBCO) for cellular dissociation. After dissociation, an equal volume of hMSC media was added and total cellular suspension was removed for subsequent cell pelleting via

centrifugation to remove trypsin-EDTA. Cells were resuspended in warm hMSC media and counted via trypan blue exclusion using a hemocytometer prior to diluting in hMSC media for seeding, as described next.

For seeding of hAMSCs, cells were dissociated and counted, as described above, and 100 μL of 4.5×10^4 cells/mL cell suspension (4,500 cells/well; D1 and D2) was added to each well of clear bottom, black walled, 96-well plates (Corning Life Sciences, Corning, NY, USA). Immediately following seeding, plates were incubated at 37°C and 5% CO_2 and allowed to culture for 24 h. For seeding of hBMSCs, cells were dissociated and counted, as described above, and 100 μL of 4×10^4 cells/mL cell suspension (4,000 cells/well; D3 & D4) was added to each well of clear bottom, black walled, 96-well plates (Corning Life Sciences). Immediately following seeding, plates were incubated at 37°C and 5% CO_2 and allowed to culture for 48 h. The different seeding densities and culture times for hAMSCs (4.5×10^4 cells/mL, 24 h) and hBMSCs (4×10^4 cells/mL, 48 hours) were selected so all experimental conditions were at ~80% confluence before transfecting, as described below.

DNA vectors

All DNA vectors used in this screen encode for a fusion protein of EGFP and firefly luciferase (EGFPLuc, Figure 1 and Table 1). pTubb3-MC was a gift from Juan Belmonte (Addgene plasmid #87112; http://n2t.net/addgene:87112; RRID: Addgene_87112)[56] and was used to clone minicircle (MC) vectors MC.EGFPLuc-CMV, MC.EGFPLuc-EF1a, and MC.Expressionless (Genscript, Piscataway, NJ, USA). MIP 247 CoMIP 4in1 with shRNA p53 was a gift from Mark Kay and Joseph Wu (Addgene plasmid #63726; http://n2t.net/addgene:63726; RRID: Addgene_63726)[22] and was used to clone MIP vectors MIP.EGFPLuc-CMV, MIP.EGFPLuc-EF1a, and MIP.Expressionless (Genscript). The F1 origin of replication was removed from EGFPLuc-CMV (Clontech, Mountain View, CA, USA) and pEGFPLuc-EF1a (Genscript) in order to clone pEGFPLuc-CMV No F1 and pEGFPLuc-EF1a No F1, respectively (Genscript). MC vectors (MC.EGFPLuc-CMV, MC.EGFPLuc-EF1a, and MC.Expressionless) were propagated in the bacterial strain ZYCY10P3S2T (System Biosciences, Palo Alto, CA) under kanamycin selection following a published protocol,[57] with minor changes. Briefly, 100 mL of Terrific Broth (TB; Invitrogen) was inoculated with bacterial strain ZYCY10P3S2T containing MC vectors and cultured overnight at 37°C with shaking at 250 RPM. The overnight culture was then mixed with minicircle induction mix comprising 100 mL of Luria-Bertani broth (LB; Becton Dickinson, Franklin Lakes, NJ, USA), 4 mL of 1N NaOH, and 100 μL of 20% L-arabinose, and cultured for 5 h at 32°C with shaking at 250 RPM. All MIP vectors (MIP.EGFPLuc-CMV, MIP.EGFPLuc-EF1a, and MIP.Expressionless) were propagated in RNA-OUT competent cells (Nature Technologies, Lincoln, NE, USA)[58] using 6% sucrose selection media. All plasmids (pEGFPLuc-CMV, pEGFPLuc-CMV No F1, pEGPFLuc-EF1a, and pEGFPLuc-EF1a) were propagated in DH5α e. coli. (Invitrogen, Carlsbad, CA, USA) under kanamycin selection. All DNA vectors were isolated and purified using a Purelink High Purity Endotoxin free plasmid purification kit (Invitrogen). DNA quality and yield were measured using a Nanodrop (Thermo Fisher Scientific) and all DNA vectors were resuspended in Tris EDTA (TE) buffer at a concentration of 1 μg/μL.

In order to compare DNA vectors, an equal amount of transgene (i.e., molarity of expression cassette) and DNA mass was delivered to hMSCs for each DNA vector. Molarity of expression cassette for each DNA vector was normalized by dividing the size of each DNA vector (in kilobase pairs) by the size of the largest DNA vector (in kilobase pairs) for each promoter. DNA mass was then equalized by adding the remaining fraction of corresponding expressionless vector to make all DNA vector stocks be 1 μg/μL (Table 2).

hMSC transfection

24 h after seeding of hAMSCs, or 48 h after seeding of hBMSCs, as described above, all DNA vectors were complexed with either Lipofectamine 3000 (Invitrogen) at a DNA:lipid ratio of 1:2 in serum free Opti-MEM media (Invitrogen) following the manufacturer's protocol or complexed with Turbofect (Thermo Fisher Scientific) at a DNA:polymer ratio of 1:4 in serum free Opti-MEM media following manufacturer's protocol. After complex formation, 0.07 μg of Lipofectamine 3000 complexed DNA vector in 6.7 μL of Opti-MEM or 0.07 μg of Turbofect complexed DNA vector in 11.1 μL of Opt-MEM was delivered to each well, and plates were briefly centrifuged to ensure mixing of complexes with the hMSC media. Media were removed immediately after centrifugation and replaced with fresh, warmed, hMSC media lacking complexes. Following complex delivery, hMSCs were placed into incubators at 37°C and 5% CO_2 and allowed to culture for 48 h.

Cell staining and high content imaging for transfection efficiency assessment

48 h after delivery of complexes, cells were stained with Hoechst 33342 (Sigma-Aldrich, St. Louis, MO, USA) to enable nuclei counts for assessment of EGFP transfection efficiencies. After removing culture media from the cells, 50 μL of staining solution (1 μg/mL of Hoechst in hMSC media) was added to each well and incubated for 25 min at 37°C and 5% CO_2. After incubation, staining solution was removed, and cells were rinsed with 20 μL of 1× PBS on a multi-purpose rotator for 5 min, after which the rinse was removed and 100 μL of 1× PBS was added to each well for subsequent imaging.

Images of each well were acquired with a Cytation 1 Cell Imaging System (Biotek, Winooski, VT, USA), equipped with a laser autofocus cube and GFP (EGFP transgene production) and DAPI (nuclei count via Hoechst) filter cubes paired with 465 nm and 365 nm LED cubes, respectively. Two images, spaced 150 μm apart vertically, were taken of each well in each fluorescent channel, in addition to phase contrast images, using a 4× objective. Consistent fluorescence excitation LED intensity and camera exposure settings were used to allow for comparison of image intensities between wells in the same plate. After imaging, cells were washed with PBS and lysed with 150 μL per well of

1× reporter lysis buffer (Promega, Madison, WI, USA) by incubating at room temp for 10 min prior to storage at −80°C.

Assessment of transfection efficiency and transgene expression levels

Gen5 software (Biotek) was used for image preprocessing and deconvolution (to subtract background fluorescence from captured digital images), as well as object analysis (e.g., EGFP-positive cells and cell nuclei) in order to calculate transfection efficiencies. Object analysis identified objects of interest in all channels by their fluorescence intensity and size. DAPI and GFP intensity thresholds were set at 5,000 and 1,000 relative fluorescent units (RFUs), respectively, and minimum and maximum object size were set at 12 and 50 (DAPI) and 12 and 150 (GFP).

Transfection efficiency was calculated by dividing the number of EGFP objects (cells producing transgene) by the number of DAPI objects (cell nuclei) in the same well. Transgenic luciferase activity levels were quantified by measuring luciferase luminescence in RLUs with a Luciferase Assay kit (Promega) and a luminometer (Turner Designs, Sunnyvale, CA, USA). RLUs were normalized to total protein amount determined with a Pierce bicinchoninic acid (BCA) colorimetric assay (Pierce, Rockford, IL, USA) using an Epoch plate reader (Biotek) to measure absorbance at 562 nm.

Quantification of transgenic mRNA

To quantify relative mRNA transcript copy numbers of the EGFPLuc transgene from each DNA vector, we seeded D6 hAMSCs at 4.5×10^4 cells/mL (4,500 cells/well), as described above, and cultured at 37°C and 5% CO_2. 24 h after seeding, D1 hAMSCs were transfected with DNA vectors complexed with Turbofect transfection reagent, as described above. 12 and 24 h following transfection, mRNA was isolated for each condition using SingleShot Cell Lysis Kit (Bio-Rad, Hercules, CA, USA) following the manufacturer's protocol. Isolated mRNA was then reverse transcribed using iScript cDNA Synthesis Kit (Bio-Rad) following the manufacturer's protocol. qRT-PCR was performed on a QuantStudio 6 Flex Real-Time PCR System (Applied Biosystems, Foster City, CA, USA) with Power SYBR Green Master Mix (Thermo Fisher Scientific) and relative expression was calculated by the ΔΔCt method normalizing to the endogenous control RPL13A. See Table S2 for primer sequences (Integrated DNA Technologies, Coralville, IA, USA).

Data analysis and statistics

In this study, two promoters in eight DNA vectors complexed with two commercially available transfection reagents were investigated in four donors of hMSCs from two tissue sources (64 conditions). Our experimental design for this study was a split-plot design with the whole plot factor being the cationic carrier and the split plot factor being vector × promoter after blocking by donor. All data are reported as the mean of triplicate values for each condition on duplicate days (n = 6), except where noted. In order to compare each variable tested, the EGFP cell counts and total cell counts for all 64 conditions tested (Figure 2) were aggregated for that particular variable and presented in scatterplots (Figures 3, 4, 5, and 6) divided into four quadrants. Q1 represents high transgene expression but low total cell counts (which could be attributed to either transfection-induced toxicity and/or a reduction in proliferation). Q2 represents high transgene expression with high total cell counts (which could be attributed to either minimal transfection-induced toxicity and/or minimal reduction in proliferation). Q3 represents both low transgene expression and low total cell counts. Lastly, Q4 represents low transgene expression but high total cell counts. It should be noted that these quadrants were partitioned using the highest number of EGFP-positive cells and total cell counts that were observed in this current study; therefore, these quadrant boundaries should not be used to evaluate conditions and data from other studies. Poisson regressions, with the line forced through the origin, were performed for each scatterplot (i.e., variable) in order to visually identify differences in EGFP cell counts versus total cell counts for each variable tested. EGFP-positive cell count data represented in the scatterplots were analyzed as a negative binomial variable with the total cell counts as an offset term. Kenward-Roger adjustment was used on the degrees of freedom to account for the multiple error levels in the analysis. Transfection efficiency and transgenic luciferase activity fold changes were calculated for all pairwise comparisons for each donor by dividing the six transgene expression values for each column condition by the average (n = 6 for each condition) of the row condition (Figures S1 and S2). Relative transgenic mRNA transcript fold-changes were analyzed using an ANOVA with Dunnett's post hoc test. Statistical significance was accepted for p values less than 0.05. Statistics were evaluated using Prism GraphPad software (GraphPad Software, La Jolla, CA, USA) and SAS/STAT 14.2 software, version 9.4 of the SAS system for Windows. Copyright 2016 SAS Institute SAS and all other SAS Institute product or service names are registered trademarks or trademarks of SAS Institute (SAS Institute, Cary, NC, USA).

SUPPLEMENTAL INFORMATION

Supplemental information can be found online at https://doi.org/10.1016/j.omtn.2021.06.018.

ACKNOWLEDGMENTS

We would like to thank the National Institutes of Health (1 DP2 EB025760-01, 3 DP2 EB025760-01S1) for funding. The contents of this publication are the sole responsibility of the authors and do not necessarily represent the official views of the NIH. We would also like to thank Dr. Stephen D. Kachman and Kory Heier for their assistance with the statistical analysis.

AUTHOR CONTRIBUTIONS

Conceptualization, T.K. and A.K.P.; Methodology, T.K.; Investigation, T.K., A.H., L.S., and M.F.; Writing – Original Draft, T.K.; Writing – Review & Editing, T.K., A.H., L.S., M.F., and A.K.P.; Funding Acquisition, A.K.P.

DECLARATION OF INTERESTS

The authors declare no competing interests.

REFERENCES

1. Hosseini, S.A., Mohammadi, R., Noruzi, S., Mohamadi, Y., Azizian, M., Mousavy, S.M., Ghasemi, F., Hesari, A., Sahebkar, A., Salarinia, R., et al. (2018). Stem cell- and gene-based therapies as potential candidates in Alzheimer's therapy. J. Cell. Biochem. *119*, 8723–8736.
2. Lo Furno, D., Mannino, G., and Giuffrida, R. (2018). Functional role of mesenchymal stem cells in the treatment of chronic neurodegenerative diseases. J. Cell. Physiol. *233*, 3982–3999.
3. Ullah, I., Subbarao, R.B., and Rho, G.J. (2015). Human mesenchymal stem cells - current trends and future prospective. Biosci. Rep. *35*, e00191.
4. Goff, L.A., Boucher, S., Ricupero, C.L., Fenstermacher, S., Swerdel, M., Chase, L.G., Adams, C.C., Chesnut, J., Lakshmipathy, U., and Hart, R.P. (2008). Differentiating human multipotent mesenchymal stromal cells regulate microRNAs: prediction of microRNA regulation by PDGF during osteogenesis. Exp Hematol *36*, 1354–1369.
5. Gebler, A., Zabel, O., and Seliger, B. (2012). The immunomodulatory capacity of mesenchymal stem cells. Trends Mol. Med. *18*, 128–134.
6. Leng, Z., Zhu, R., Hou, W., Feng, Y., Yang, Y., Han, Q., Shan, G., Meng, F., Du, D., Wang, S., et al. (2020). Transplantation of ACE2-mesenchymal stem cells improves the outcome of patients with COVID-19 pneumonia. Aging Dis. *11*, 216–228.
7. Zimmermann, A., Hercher, D., Regner, B., Frischer, A., Sperger, S., Redl, H., and Hacobian, A. (2020). Evaluation of BMP-2 Minicircle DNA for Enhanced Bone Engineering and Regeneration. Curr. Gene Ther. *20*, 55–63.
8. Hamann, A., Nguyen, A., and Pannier, A.K. (2019). Nucleic acid delivery to mesenchymal stem cells: a review of nonviral methods and applications. J. Biol. Eng. *13*, 7.
9. Oggu, G.S., Sasikumar, S., Reddy, N., Ella, K.K.R., Rao, C.M., and Bokara, K.K. (2017). Gene delivery approaches for mesenchymal stem cell therapy: strategies to increase efficiency and specificity. Stem Cell Rev. Rep. *13*, 725–740.
10. Nayerossadat, N., Maedeh, T., and Ali, P.A. (2012). Viral and nonviral delivery systems for gene delivery. Adv. Biomed. Res. *1*, 27.
11. Jin, L., Zeng, X., Liu, M., Deng, Y., and He, N. (2014). Current progress in gene delivery technology based on chemical methods and nano-carriers. Theranostics *4*, 240–255.
12. Santos, J.L., Pandita, D., Rodrigues, J., Pêgo, A.P., Granja, P.L., and Tomás, H. (2011). Non-viral gene delivery to mesenchymal stem cells: methods, strategies and application in bone tissue engineering and regeneration. Curr. Gene Ther. *11*, 46–57.
13. Kelly, A.M., Plautz, S.A., Zempleni, J., and Pannier, A.K. (2016). Glucocorticoid cell priming enhances transfection outcomes in adult human mesenchymal stem cells. Mol. Ther. *24*, 331–341.
14. Hamann, A., Broad, K., Nguyen, A., and Pannier, A.K. (2019). Mechanisms of unprimed and dexamethasone-primed nonviral gene delivery to human mesenchymal stem cells. Biotechnol. Bioeng. *116*, 427–443.
15. Hamann, A., Kozisek, T., Broad, K., and Pannier, A.K. (2020). Glucocorticoid Priming of Nonviral Gene Delivery to Human Mesenchymal Stem Cells Increases Transfection by Reducing Induced Stresses. Mol. Ther. Methods Clin. Dev.
16. Kozisek, T., Hamann, A., Nguyen, A., Miller, M., Plautz, S., and Pannier, A.K. (2020). High-throughput screening of clinically approved drugs that prime nonviral gene delivery to human Mesenchymal stem cells. J. Biol. Eng. *14*, 16.
17. McCarthy, A. (2010). The NIH Molecular Libraries Program: identifying chemical probes for new medicines, http://nihsmr.evotec.com/evotec/.
18. Zheng, C., and Baum, B.J. (2005). Evaluation of viral and mammalian promoters for use in gene delivery to salivary glands. Mol. Ther. *12*, 528–536.
19. Lu, J., Zhang, F., and Kay, M.A. (2013). A mini-intronic plasmid (MIP): a novel robust transgene expression vector in vivo and in vitro. Mol. Ther. *21*, 954–963.
20. Darquet, A.M., Cameron, B., Wils, P., Scherman, D., and Crouzet, J. (1997). A new DNA vehicle for nonviral gene delivery: supercoiled minicircle. Gene Ther. *4*, 1341–1349.
21. Argyros, O., Wong, S.P., Fedonidis, C., Tolmachov, O., Waddington, S.N., Howe, S.J., Niceta, M., Coutelle, C., and Harbottle, R.P. (2011). Development of S/MAR minicircles for enhanced and persistent transgene expression in the mouse liver. J. Mol. Med. (Berl.) *89*, 515–529.
22. Diecke, S., Lu, J., Lee, J., Termglinchan, V., Kooreman, N.G., Burridge, P.W., Ebert, A.D., Churko, J.M., Sharma, A., Kay, M.A., and Wu, J.C. (2015). Novel codon-optimized mini-intronic plasmid for efficient, inexpensive, and xeno-free induction of pluripotency. Sci. Rep. *5*, 8081.
23. Cheung, W.Y., Hovey, O., Gobin, J.M., Muradia, G., Mehic, J., Westwood, C., and Lavoie, J.R. (2018). Efficient nonviral transfection of human bone marrow mesenchymal stromal cells shown using placental growth factor overexpression. Stem Cells Int. *2018*, 1310904.
24. Hamann, A., Thomas, A.K., Kozisek, T., Farris, E., Lück, S., Zhang, Y., and Pannier, A.K. (2020). Screening a chemically defined extracellular matrix mimetic substrate library to identify substrates that enhance substrate-mediated transfection. Exp. Biol. Med. (Maywood) *245*, 606–619.
25. Mun, J.-Y., Shin, K.K., Kwon, O., Lim, Y.T., and Oh, D.-B. (2016). Minicircle microporation-based non-viral gene delivery improved the targeting of mesenchymal stem cells to an injury site. Biomaterials *101*, 310–320.
26. Johnson, S.A., Ormsby, M.J., McIntosh, A., Tait, S.W.G., Blyth, K., and Wall, D.M. (2019). Increasing the bactofection capacity of a mammalian expression vector by removal of the f1 ori. Cancer Gene Ther. *26*, 183–194.
27. Raup, A., Jérôme, V., Freitag, R., Synatschke, C.V., and Müller, A.H. (2016). Promoter, transgene, and cell line effects in the transfection of mammalian cells using PDMAEMA-based nano-stars. Biotechnol. Rep. (Amst.) *11*, 53–61.
28. Antonova, D.V., Alekseenko, I.V., Siniushina, A.K., Kuzmich, A.I., and Pleshkan, V.V. (2020). Searching for Promoters to Drive Stable and Long-Term Transgene Expression in Fibroblasts for Syngeneic Mouse Tumor Models. Int. J. Mol. Sci. *21*, 6098.
29. Hardee, C.L., Arévalo-Soliz, L.M., Hornstein, B.D., and Zechiedrich, L. (2017). Advances in non-viral DNA vectors for gene therapy. Genes (Basel) *8*, 65.
30. Tan, Y., Li, S., Pitt, B.R., and Huang, L. (1999). The inhibitory role of CpG immunostimulatory motifs in cationic lipid vector-mediated transgene expression in vivo. Hum. Gene Ther. *10*, 2153–2161.
31. Lu, J., Zhang, F., Xu, S., Fire, A.Z., and Kay, M.A. (2012). The extragenic spacer length between the 5′ and 3′ ends of the transgene expression cassette affects transgene silencing from plasmid-based vectors. Mol. Ther. *20*, 2111–2119.
32. Chen, Z.Y., He, C.Y., Meuse, L., and Kay, M.A. (2004). Silencing of episomal transgene expression by plasmid bacterial DNA elements in vivo. Gene Ther. *11*, 856–864.
33. Russel, M., and Model, P. (1989). Genetic analysis of the filamentous bacteriophage packaging signal and of the proteins that interact with it. J. Virol. *63*, 3284–3295.
34. Chen, Z.-Y., He, C.-Y., Ehrhardt, A., and Kay, M.A. (2003). Minicircle DNA vectors devoid of bacterial DNA result in persistent and high-level transgene expression in vivo. Mol. Ther. *8*, 495–500.
35. Narsinh, K.H., Jia, F., Robbins, R.C., Kay, M.A., Longaker, M.T., and Wu, J.C. (2011). Generation of adult human induced pluripotent stem cells using nonviral minicircle DNA vectors. Nat. Protoc. *6*, 78–88.
36. Boura, J.S., Vance, M., Yin, W., Madeira, C., Lobato da Silva, C., Porada, C.D., and Almeida-Porada, G. (2014). Evaluation of gene delivery strategies to efficiently overexpress functional HLA-G on human bone marrow stromal cells. Mol. Ther. Methods Clin. Dev. *2014*, 1.
37. Jia, F., Wilson, K.D., Sun, N., Gupta, D.M., Huang, M., Li, Z., Panetta, N.J., Chen, Z.Y., Robbins, R.C., Kay, M.A., et al. (2010). A nonviral minicircle vector for deriving human iPS cells. Nat. Methods *7*, 197–199.
38. Bandara, N., Gurusinghe, S., Chen, H., Chen, S., Wang, L.X., Lim, S.Y., and Strappe, P. (2016). Minicircle DNA-mediated endothelial nitric oxide synthase gene transfer enhances angiogenic responses of bone marrow-derived mesenchymal stem cells. Stem Cell Res. Ther. *7*, 48.
39. Tidd, N., Michelsen, J., Hilbert, B., and Quinn, J.C. (2017). Minicircle mediated gene delivery to canine and equine mesenchymal stem cells. Int. J. Mol. Sci. *18*, 819.
40. O'Sullivan, J.M., Tan-Wong, S.M., Morillon, A., Lee, B., Coles, J., Mellor, J., and Proudfoot, N.J. (2004). Gene loops juxtapose promoters and terminators in yeast. Nat. Genet. *36*, 1014–1018.
41. Colluru, V.T., Zahm, C.D., and McNeel, D.G. (2016). Mini-intronic plasmid vaccination elicits tolerant LAG3^{+} CD8^{+} T cells and inferior antitumor responses. OncoImmunology *5*, e1223002.

42. Nott, A., Meislin, S.H., and Moore, M.J. (2003). A quantitative analysis of intron effects on mammalian gene expression. RNA *9*, 607–617.

43. Furger, A., O'Sullivan, J.M., Binnie, A., Lee, B.A., and Proudfoot, N.J. (2002). Promoter proximal splice sites enhance transcription. Genes Dev. *16*, 2792–2799.

44. Niwa, M., Rose, S.D., and Berget, S.M. (1990). In vitro polyadenylation is stimulated by the presence of an upstream intron. Genes Dev. *4*, 1552–1559.

45. Le Hir, H., Gatfield, D., Izaurralde, E., and Moore, M.J. (2001). The exon-exon junction complex provides a binding platform for factors involved in mRNA export and nonsense-mediated mRNA decay. EMBO J. *20*, 4987–4997.

46. Matsumoto, K., Wassarman, K.M., and Wolffe, A.P. (1998). Nuclear history of a pre-mRNA determines the translational activity of cytoplasmic mRNA. EMBO J. *17*, 2107–2121.

47. Xu, Y., Zhao, W., Olson, S.D., Prabhakara, K.S., and Zhou, X. (2018). Alternative splicing links histone modifications to stem cell fate decision. Genome Biol. *19*, 133.

48. Rahimi, P., Mobarakeh, V.I., Kamalzare, S., SajadianFard, F., Vahabpour, R., and Zabihollahi, R. (2018). Comparison of transfection efficiency of polymer-based and lipid-based transfection reagents. Bratisl. Lek Listy *119*, 701–705.

49. Yang, F., Green, J.J., Dinio, T., Keung, L., Cho, S.-W., Park, H., Langer, R., and Anderson, D.G. (2009). Gene delivery to human adult and embryonic cell-derived stem cells using biodegradable nanoparticulate polymeric vectors. Gene Ther. *16*, 533–546.

50. Mohamed-Ahmed, S., Fristad, I., Lie, S.A., Suliman, S., Mustafa, K., Vindenes, H., and Idris, S.B. (2018). Adipose-derived and bone marrow mesenchymal stem cells: a donor-matched comparison. Stem Cell Res. Ther. *9*, 168.

51. Zazzeroni, L., Lanzoni, G., Pasquinelli, G., and Ricordi, C. (2017). Considerations on the harvesting site and donor derivation for mesenchymal stem cells-based strategies for diabetes. CellR4 Repair Replace Regen Reprogram *5*, e2435.

52. Wada, N., Gronthos, S., and Bartold, P.M. (2013). Immunomodulatory effects of stem cells. Periodontol. 2000 *63*, 198–216.

53. Oliva, A.A., McClain-Moss, L., Pena, A., Drouillard, A., and Hare, J.M. (2019). Allogeneic mesenchymal stem cell therapy: A regenerative medicine approach to geroscience. Aging Med. (Milton) *2*, 142–146.

54. Qadan, M.A., Piuzzi, N.S., Boehm, C., Bova, W., Moos, M., Jr., Midura, R.J., Hascall, V.C., Malcuit, C., and Muschler, G.F. (2018). Variation in primary and culture-expanded cells derived from connective tissue progenitors in human bone marrow space, bone trabecular surface and adipose tissue. Cytotherapy *20*, 343–360.

55. Wang, W., Li, W., Ou, L., Flick, E., Mark, P., Nesselmann, C., Lux, C.A., Gatzen, H.H., Kaminski, A., Liebold, A., et al. (2011). Polyethylenimine-mediated gene delivery into human bone marrow mesenchymal stem cells from patients. J. Cell. Mol. Med. *15*, 1989–1998.

56. Suzuki, K., Tsunekawa, Y., Hernandez-Benitez, R., Wu, J., Zhu, J., Kim, E.J., Hatanaka, F., Yamamoto, M., Araoka, T., Li, Z., et al. (2016). In vivo genome editing via CRISPR/Cas9 mediated homology-independent targeted integration. Nature *540*, 144–149.

57. Kay, M.A., He, C.-Y., and Chen, Z.-Y. (2010). A robust system for production of minicircle DNA vectors. Nat. Biotechnol. *28*, 1287–1289.

58. Luke, J., Carnes, A.E., Hodgson, C.P., and Williams, J.A. (2009). Improved antibiotic-free DNA vaccine vectors utilizing a novel RNA based plasmid selection system. Vaccine *27*, 6454–6459.

OMTN, Volume *26*

Supplemental information

Comparison of promoter, DNA vector, and cationic carrier for efficient transfection of hMSCs from multiple donors and tissue sources

Tyler Kozisek, Andrew Hamann, Luke Samuelson, Miguel Fudolig, and Angela K. Pannier

Table S1: hMSC Donor Information				
Donor ID	Tissue Source	Age	Sex	Ethnicity/Race
D1	Adipose	22	M	Black
D2	Adipose	42	F	Black
D3	Bone Marrow	22	M	Not provided
D4	Bone Marrow	31	M	Black

Table S2: Sequences of Primers Used in qRT-PCR	
EGFP Forward	5'-ACGTAAACGGCCACAAGTTC-3'
EGFP Reverse	5'-AAGTCGTGCTGCTTCATGTG-3'
RPL-13A Forward	5'-CCTGGAGGAGAAGAGGAAAGAGA-3'
RPL-13A Reverse	5'-TTGAGGACCTCTGTGTATTTGTCAA-3'

Table S3: Type III Tests of Fixed Effects				
Effect	DF	Den DF	F Value	Pr > F
Cationic Carrier	1	4.134	15.05	0.0168
Donor	3	4.001	10.12	0.0244
Promoter	1	330.7	1455.64	<.0001
Vector	3	326	186.99	<.0001
Cationic Carrier*Donor	3	4.047	12.85	0.0156
Cationic Carrier*Promoter	1	321.4	85.87	<.0001
Cationic Carrier*Vector	3	310.9	8.16	<.0001
Donor*Promoter	3	321	18.07	<.0001
Donor*Vector	9	310	13.37	<.0001
Promoter*Vector	3	325.5	27.72	<.0001

EGFP positive cell counts for each effect (variable) were analyzed as a negative binomial with total cell count as an offset term. Kenward-Rogers adjustment was used on the degrees of freedom to account for the multiple error levels in our analysis. DF, degrees of freedom; Den DF, degrees of freedom associated with model errors; F-Value, F-test statistic; Pr > F, p-value associated with the F statistic. Significance was accepted at $p<0.05$.

Table S4: Pairwise Comparisons Between Promoters for Each Vector								
Vector	Promoter	_Promoter	Estimate	SE	DF	t Value	Pr > |t|	Adj P
Plasmid	CMV	EF1a	1.8122	0.09838	353	18.42	<.0001	<.0001
No F1	CMV	EF1a	1.9739	0.09191	316	21.48	<.0001	<.0001
MC	CMV	EF1a	1.8122	0.09838	353	18.42	<.0001	<.0001
MIP	CMV	EF1a	1.1076	0.08760	262.6	12.64	<.0001	<.0001

EGFP positive cell counts for each promoter were analyzed as a negative binomial with total cell count as an offset term. Promoter effects within each vector were compared using least square means with use of Tukey-Kramer to adjust for multiple comparisons. Estimate, logarithm of the ratio between the estimated responses for each promoter; SE, standard error; DF, degrees of freedom; t value, t-test statistic; Pr > |t|, p-value associated with the t statistic; Adj P, adjusted p-value. Significance was accepted at $p<0.05$.

Table S5: Pairwise Comparisons Between Promoters for Each Cationic Carrier

Cationic Carrier	Promoter	_Promoter	Estimate	SE	DF	t Value	Pr > |t|
Turbofect	CMV	EF1a	2.2020	0.06665	345.7	33.04	<.0001
Lipofectamine	CMV	EF1a	1.3440	0.06453	306.8	20.83	<.0001

EGFP positive cell counts for each promoter were analyzed as a negative binomial with total cell count as an offset term. Promoter effects within each cationic carrier were compared using least square means with use of Tukey-Kramer to adjust for multiple comparisons. Estimate, logarithm of the ratio between the estimated responses for each promoter; SE, standard error; DF, degrees of freedom; t value, t-test statistic; Pr > |t|, p-value associated with the t statistic. Significance was accepted at $p<0.05$.

Table S6: Pairwise Comparisons Between Promoters for Each Donor

Donor	Promoter	_Promoter	Estimate	SE	DF	t Value	Pr > |t|	Adj P
D1	CMV	EF1a	1.2843	0.09338	331.9	13.75	<.0001	<.0001
D2	CMV	EF1a	1.6203	0.09204	311.3	17.61	<.0001	<.0001
D3	CMV	EF1a	2.0922	0.09429	347.6	22.19	<.0001	<.0001
D4	CMV	EF1a	2.0951	0.09100	304.5	23.02	<.0001	<.0001

EGFP positive cell counts for each promoter were analyzed as a negative binomial with total cell count as an offset term. Promoter effects within each donor were compared using least square means with use of Tukey-Kramer to adjust for multiple comparisons. Estimate, logarithm of the ratio between the estimated responses for each promoter; SE, standard error; DF, degrees of freedom; t value, t-test statistic; Pr > |t|, p-value associated with the t statistic; Adj P, adjusted p-value. Significance was accepted at $p<0.05$.

Table S7: Pairwise Comparisons Between Vectors for Each Promoter

Promoter	Vector	_Vector	Estimate	SE	DF	t Value	Pr > |t|	Adj P
CMV	MC	MIP	-1.1961	0.08807	268.2	-13.58	<.0001	<.0001
CMV	MC	No F1	-0.8637	0.08838	272	-9.77	<.0001	<.0001
CMV	MC	Plasmid	-0.8924	0.08863	275	-10.07	<.0001	<.0001
CMV	MIP	No F1	0.3324	0.08651	250.1	3.84	0.0002	0.0009
CMV	MIP	Plasmid	0.3036	0.08677	253	3.50	0.0006	0.0031
CMV	No F1	Plasmid	-0.02875	0.08708	256.7	-0.33	0.7415	0.9876
EF1a	MC	MIP	-1.9006	0.09797	353	-19.40	<.0001	<.0001
EF1a	MC	No F1	-0.7020	0.1016	353	-6.91	<.0001	<.0001
EF1a	MC	Plasmid	-0.5063	0.1026	353	-4.93	<.0001	<.0001
EF1a	MIP	No F1	1.1987	0.09291	329.2	12.90	<.0001	<.0001
EF1a	MIP	Plasmid	1.3943	0.09413	347.9	14.81	<.0001	<.0001
EF1a	No F1	Plasmid	0.1956	0.09785	353	2.00	0.0463	0.1901

EGFP positive cell counts for each vector were analyzed as a negative binomial with total cell count as an offset term. Vector effects within each promoter were compared using least square means with use of Tukey-Kramer to adjust for multiple comparisons. Estimate, logarithm of the ratio between the estimated responses for each vector; SE, standard error; DF, degrees of freedom; t value, t-test statistic; Pr > |t|, p-value associated with the t statistic; Adj P, adjusted p-value. Significance was accepted at $p<0.05$. Red highlighted adjusted p-values indicate no significant difference at $\alpha=0.05$

Table S8: Pairwise Comparisons Between Vectors for Each Cationic Carrier

Cationic Carrier	Vector	_Vector	Estimate	SE	DF	t Value	Pr > |t|	Adj P
Turbofect	MC	MIP	-1.5044	0.09400	336.9	-16.00	<.0001	<.0001
Turbofect	MC	No F1	-0.5944	0.09662	353	-6.15	<.0001	<.0001
Turbofect	MC	Plasmid	-0.8299	0.09659	353	-8.59	<.0001	<.0001
Turbofect	MIP	No F1	0.9100	0.09115	303	9.98	<.0001	<.0001
Turbofect	MIP	Plasmid	0.6745	0.09114	303.4	7.40	<.0001	<.0001
Turbofect	No F1	Plasmid	-0.2355	0.09386	336.1	-2.51	0.0126	0.0604
Lipofectamine 3000	MC	MIP	-1.5923	0.09171	312.6	-17.36	<.0001	<.0001
Lipofectamine 3000	MC	No F1	-0.9712	0.09288	327.9	-10.46	<.0001	<.0001
Lipofectamine 3000	MC	Plasmid	-0.5689	0.09420	345.3	-6.04	<.0001	<.0001
Lipofectamine 3000	MIP	No F1	0.6211	0.08815	268.8	7.05	<.0001	<.0001
Lipofectamine 3000	MIP	Plasmid	1.0235	0.08956	285.5	11.43	<.0001	<.0001
Lipofectamine 3000	No F1	Plasmid	0.4023	0.09078	300.4	4.43	<.0001	<.0001

EGFP positive cell counts for each vector were analyzed as a negative binomial with total cell count as an offset term. Vector effects within each cationic carrier were compared using least square means with use of Tukey-Kramer to adjust for multiple comparisons. Estimate, logarithm of the ratio between the estimated responses for each vector; SE, standard error; DF, degrees of freedom; t value, t-test statistic; Pr > |t|, p-value associated with the t statistic; Adj P, adjusted p-value. Significance was accepted at $p<0.05$. Red highlighted adjusted p-values indicate no significant difference at $\alpha=0.05$

Table S9: Pairwise Comparisons Between Vectors for Each Donor

Donor	Vector	_Vector	Estimate	SE	DF	t Value	Pr > |t|	Adj P
D1	MC	MIP	-1.7418	0.1318	329.4	-13.22	<.0001	<.0001
D1	MC	No F1	-0.3901	0.1353	353	-2.88	0.0042	0.0216
D1	MC	Plasmid	-0.2420	0.1367	353	-1.77	0.0777	0.2898
D1	MIP	No F1	1.3517	0.1267	283.9	10.67	<.0001	<.0001
D1	MIP	Plasmid	1.4998	0.1283	298.4	11.69	<.0001	<.0001
D1	No F1	Plasmid	0.1481	0.1320	328.4	1.12	0.2624	0.6758
D2	MC	MIP	-2.3004	0.1325	328.6	-17.37	<.0001	<.0001
D2	MC	No F1	-1.5455	0.1338	340.6	-11.55	<.0001	<.0001
D2	MC	Plasmid	-1.2590	0.1355	353	-9.29	<.0001	<.0001
D2	MIP	No F1	0.7549	0.1242	264.7	6.08	<.0001	<.0001
D2	MIP	Plasmid	1.0413	0.1261	279.8	8.26	<.0001	<.0001
D2	No F1	Plasmid	0.2864	0.1277	292.2	2.24	0.0256	0.1142
D3	MC	MIP	-1.3379	0.1328	335	-10.08	<.0001	<.0001
D3	MC	No F1	-0.8160	0.1355	353	-6.02	<.0001	<.0001
D3	MC	Plasmid	-0.7892	0.1362	353	-5.79	<.0001	<.0001
D3	MIP	No F1	0.5220	0.1286	299.5	4.06	<.0001	0.0004
D3	MIP	Plasmid	0.5488	0.1294	306.3	4.24	<.0001	0.0002
D3	No F1	Plasmid	0.02683	0.1323	329	0.20	0.8394	0.9970
D4	MC	MIP	-0.8133	0.1273	290.7	-6.39	<.0001	<.0001
D4	MC	No F1	-0.3797	0.1298	310.1	-2.92	0.0037	0.0193
D4	MC	Plasmid	-0.5073	0.1296	309.4	-3.91	0.0001	0.0006
D4	MIP	No F1	0.4336	0.1269	284.9	3.42	0.0007	0.0040
D4	MIP	Plasmid	0.3060	0.1267	284.4	2.42	0.0164	0.0765
D4	No F1	Plasmid	-0.1276	0.1292	303.2	-0.99	0.3240	0.7565

EGFP positive cell counts for each vector were analyzed as a negative binomial with total cell count as an offset term. Vector effects within each donor were compared using least square means with use of Tukey-Kramer to adjust for multiple comparisons. Estimate, logarithm of the ratio between the estimated responses for each vector; SE, standard error; DF, degrees of freedom; t value, t-test statistic; Pr > |t|, p-value associated with the t statistic; Adj P, adjusted p-value. Significance was accepted at $p<0.05$. Red highlighted adjusted p-values indicate no significant difference at $\alpha=0.05$

Table S10: Pairwise Comparisons Between Cationic Carriers for Each Promoter

Promoter	Cationic Carrier	_Cationic Carrier	Estimate	SE	DF	t Value	Pr > |t|	Adj P
CMV	Lipofectamine 3000	Turbofect	-0.2017	0.07151	9.14	-2.82	0.0197	0.0197
EF1a	Lipofectamine 3000	Turbofect	0.6563	0.07772	12.74	8.45	<0.0001	<0.0001

EGFP positive cell counts for each cationic carrier were analyzed as a negative binomial with total cell count as an offset term. Cationic carrier effects within each promoter were compared using least square means with use of Tukey-Kramer to adjust for multiple comparisons. Estimate, logarithm of the ratio between the estimated responses for each cationic carrier; SE, standard error; DF, degrees of freedom; t value, t-test statistic; Pr > |t|, p-value associated with the t statistic. Significance was accepted at $p<0.05$.

Table S11: Pairwise Comparisons Between Cationic Carriers for Each Vector								
Vector	Cationic Carrier	_Cationic Carrier	Estimate	SE	DF	t Value	Pr > |t|	Adj P
Plasmid	Lipofectamine 3000	Turbofect	-0.08462	0.09949	32.95	-0.85	0.4012	0.4012
No F1	Lipofectamine 3000	Turbofect	0.5532	0.09832	31.46	5.63	<0.0001	<0.0001
MC	Lipofectamine 3000	Turbofect	0.1764	0.1038	38.9	1.7	0.0971	0.0971
MIP	Lipofectamine 3000	Turbofect	0.2643	0.09460	26.99	2.79	0.0095	0.0095
EGFP positive cell counts for each cationic carrier were analyzed as a negative binomial with total cell count as an offset term. Cationic carrier effects within each vector were compared using least square means with use of Tukey-Kramer to adjust for multiple comparisons. Estimate, logarithm of the ratio between the estimated responses for each cationic carrier; SE, standard error; DF, degrees of freedom; t value, t-test statistic; Pr > |t|, p-value associated with the t statistic. Significance was accepted at $p<0.05$. Red highlighted p-values indicate no significant difference at $\alpha=0.05$.								

Table S12: Pairwise Comparisons Between Cationic Carriers for Each Donor							
Donor	Cationic Carrier	_Cationic Carrier	Estimate	SE	DF	t Value	Pr > |t|
D1	Lipofectamine	Turbofect	0.5510	0.1174	4.157	4.69	0.0085
D2	Lipofectamine	Turbofect	0.6193	0.1163	4.006	5.33	0.0060
D3	Lipofectamine	Turbofect	-0.2048	0.1177	4.214	-1.74	0.1534
D4	Lipofectamine	Turbofect	-0.05621	0.1155	3.906	-0.49	0.6526
EGFP positive cell counts for each cationic carrier were analyzed as a negative binomial with total cell count as an offset term. Cationic carrier effects within each donor were compared using least square means with use of Tukey-Kramer to adjust for multiple comparisons. Estimate, logarithm of the ratio between the estimated responses for each cationic carrier; SE, standard error; DF, degrees of freedom; t value, t-test statistic; Pr > |t|, p-value associated with the t statistic. Significance was accepted at $p<0.05$. Red highlighted p-values indicate no significant difference at $\alpha=0.05$.							

Table S13: Pairwise Comparisons Between Donors for Each Promoter								
Promoter	Donor	_Donor	Estimate	SE	DF	t Value	Pr > |t|	Adj P
CMV	D1	D2	-0.6892	0.2325	4.565	-2.96	0.0351	0.1143
CMV	D1	D3	-1.2501	0.2325	4.566	-5.38	0.0039	0.0141
CMV	D2	D3	-0.5609	0.2322	4.546	-2.42	0.0655	0.2012
CMV	D4	D1	1.5946	0.2323	4.553	6.86	0.0014	0.0053
CMV	D4	D2	0.9054	0.2321	4.533	3.9	0.0138	0.0474
CMV	D4	D3	0.3445	0.2321	4.534	1.48	0.2037	0.5133
EF1a	D1	D2	-0.3532	0.236	4.852	-1.5	0.1966	0.5041
EF1a	D1	D3	-0.4423	0.2369	4.923	-1.87	0.1218	0.3474
EF1a	D2	D3	-0.0891	0.2366	4.9	-0.38	0.7223	0.9798
EF1a	D4	D1	0.7838	0.2358	4.832	3.32	0.022	0.0752
EF1a	D4	D2	0.4306	0.2355	4.81	1.83	0.1293	0.3634
EF1a	D4	D3	0.3415	0.2364	4.879	1.44	0.2095	0.5285

EGFP positive cell counts for each donor were analyzed as a negative binomial with total cell count as an offset term. Donor effects within each promoter were compared using least square means with use of Tukey-Kramer to adjust for multiple comparisons. Estimate, logarithm of the ratio between the estimated responses for each donor; SE, standard error; DF, degrees of freedom; t value, t-test statistic; Pr > |t|, p-value associated with the t statistic; Adj P, adjusted p-value. Significance was accepted at $p<0.05$. Red highlighted adjusted p-values indicate no significant difference at $\alpha=0.05$

Table S14: Pairwise Comparisons Between Donors for Each Vector

Vector	Donor	_Donor	Estimate	SE	DF	t Value	Pr > |t|	Adj P
Plasmid	D1	D2	-0.8555	0.2521	6.311	-3.39	0.0135	0.0509
Plasmid	D1	D3	-1.2511	0.2531	6.404	-4.94	0.0022	0.0088
Plasmid	D2	D3	-0.3956	0.252	6.3	-1.57	0.1652	0.4558
Plasmid	D4	D1	1.6229	0.252	6.298	6.44	0.0005	0.0023
Plasmid	D4	D2	0.7674	0.251	6.194	3.06	0.0214	0.0779
Plasmid	D4	D3	0.3718	0.2519	6.287	1.48	0.1882	0.5018
No F1	D1	D2	-0.9938	0.2504	6.14	-3.97	0.007	0.0272
No F1	D1	D3	-1.1298	0.2519	6.284	-4.49	0.0037	0.0148
No F1	D2	D3	-0.136	0.2507	6.17	-0.54	0.6065	0.9454
No F1	D4	D1	1.3472	0.2513	6.227	5.36	0.0015	0.0062
No F1	D4	D2	0.3534	0.2501	6.113	1.41	0.2066	0.5351
No F1	D4	D3	0.2174	0.2516	6.256	0.86	0.4195	0.8230
MC	D1	D2	0.1616	0.257	6.807	0.63	0.55	0.9195
MC	D1	D3	-0.7039	0.2565	6.754	-2.74	0.0298	0.1074
MC	D2	D3	-0.8655	0.2568	6.786	-3.37	0.0125	0.048
MC	D4	D1	1.3576	0.2541	6.506	5.34	0.0014	0.0056
MC	D4	D2	1.5192	0.2545	6.545	5.97	0.0007	0.003
MC	D4	D3	0.6537	0.2539	6.491	2.57	0.0393	0.1370
MIP	D1	D2	-0.397	0.2477	5.876	-1.6	0.1611	0.4438
MIP	D1	D3	-0.3001	0.2484	5.946	-1.21	0.2729	0.6446
MIP	D2	D3	0.09696	0.2484	5.941	0.39	0.7099	0.9780
MIP	D4	D1	0.4291	0.2481	5.915	1.73	0.1351	0.3875
MIP	D4	D2	0.03209	0.248	5.91	0.13	0.9013	0.9991
MIP	D4	D3	0.1291	0.2488	5.98	0.52	0.6226	0.9515

EGFP positive cell counts for each donor were analyzed as a negative binomial with total cell count as an offset term. Donor effects within each vector were compared using least square means with use of Tukey-Kramer to adjust for multiple comparisons. Estimate, logarithm of the ratio between the estimated responses for each donor; SE, standard error; DF, degrees of freedom; t value, t-test statistic; Pr > |t|, p-value associated with the t statistic; Adj P, adjusted p-value. Significance was accepted at $p<0.05$. Red highlighted adjusted p-values indicate no significant difference at $\alpha=0.05$

Table S15: Pairwise Comparisons Between Donors for Each Cationic Carrier								
Cationic Carrier	Donor	_Donor	Estimate	SE	DF	t Value	Pr > |t|	Adj P
Turbofect	D1	D2	-0.4871	0.2402	5.11	-2.03	0.0972	0.2897
Turbofect	D1	D3	-1.2241	0.2404	5.127	-5.09	0.0035	0.0132
Turbofect	D2	D3	-0.737	0.2402	5.113	-3.07	0.0271	0.0925
Turbofect	D4	D1	1.4928	0.2398	5.078	6.22	0.0015	0.0056
Turbofect	D4	D2	1.0057	0.2397	5.064	4.2	0.0083	0.0301
Turbofect	D4	D3	0.2687	0.2399	5.081	1.12	0.3127	0.6941
Lipofectamine 3000	D1	D2	-0.5553	0.239	5.003	-2.32	0.0677	0.2113
Lipofectamine 3000	D1	D3	-0.4683	0.2395	5.05	-1.96	0.1074	0.3142
Lipofectamine 3000	D2	D3	0.08698	0.2391	5.02	0.36	0.7309	0.9817
Lipofectamine 3000	D4	D1	0.8856	0.2389	5.003	3.71	0.0139	0.0492
Lipofectamine 3000	D4	D2	0.3303	0.2386	4.973	1.38	0.2252	0.5576
Lipofectamine 3000	D4	D3	0.4173	0.2391	5.019	1.74	0.1412	0.3926

EGFP positive cell counts for each donor were analyzed as a negative binomial with total cell count as an offset term. Donor effects within each cationic carrier were compared using least square means with use of Tukey-Kramer to adjust for multiple comparisons. Estimate, logarithm of the ratio between the estimated responses for each donor; SE, standard error; DF, degrees of freedom; t value, t-test statistic; Pr > |t|, p-value associated with the t statistic; Adj P, adjusted p-value. Significance was accepted at $p<0.05$. Red highlighted adjusted p-values indicate no significant difference at $\alpha=0.05$

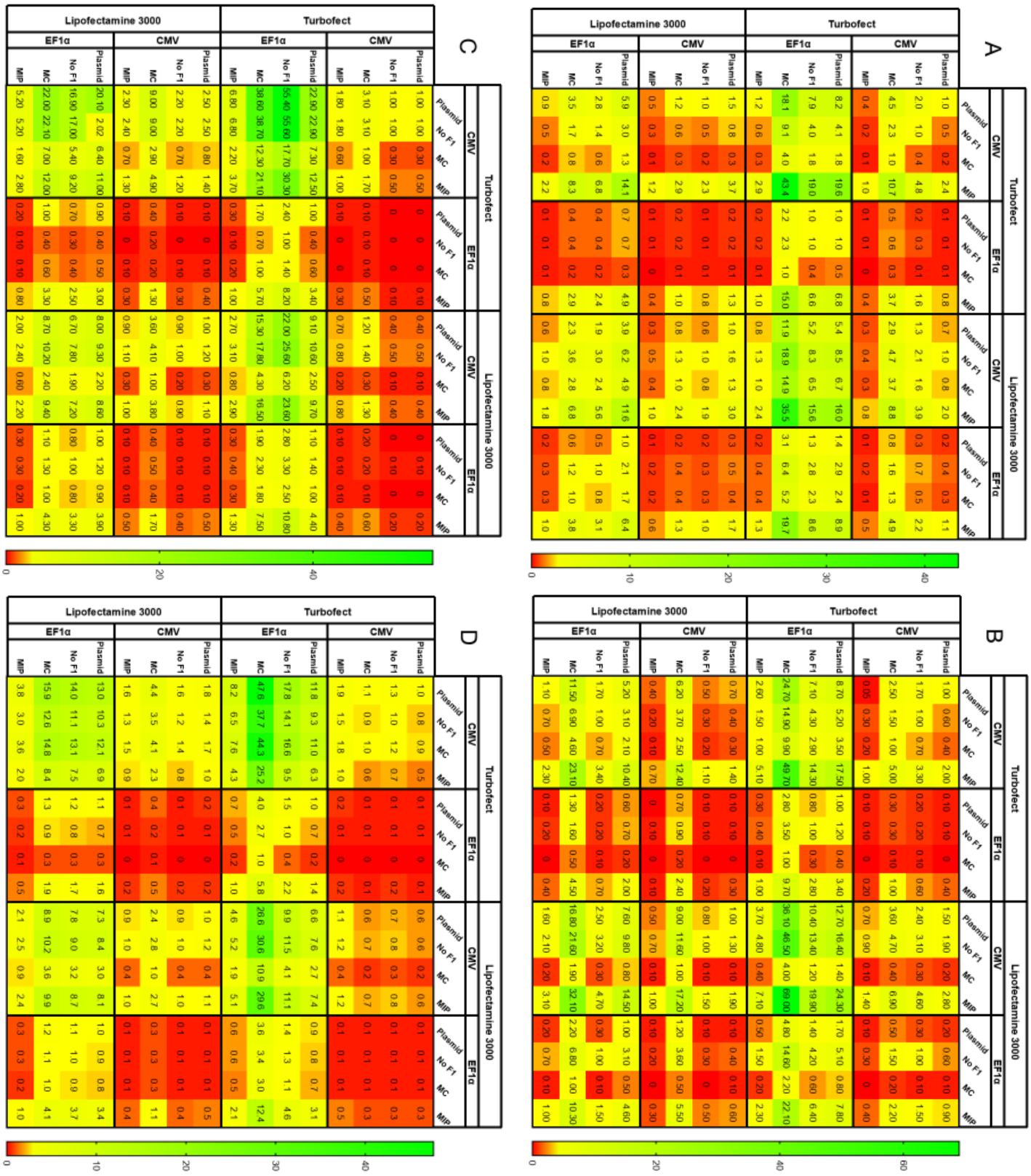

Figure S1. Donor specific transfection efficiency fold changes for all pairwise comparisons of transfection conditions. (A) Transfection efficiency fold changes for all pairwise comparisons of transfection

conditions in D1 hAMSCs. (B) Transfection efficiency fold changes for all pairwise comparisons of transfection conditions in D2 hAMSCs. (C) Transfection efficiency fold changes for all pairwise comparisons of transfection conditions in D3 hBMSCs. (D) Transfection efficiency fold changes for all pairwise comparisons of transfection conditions in D4 hBMSCs. Fold changes are presented relative to column conditions.

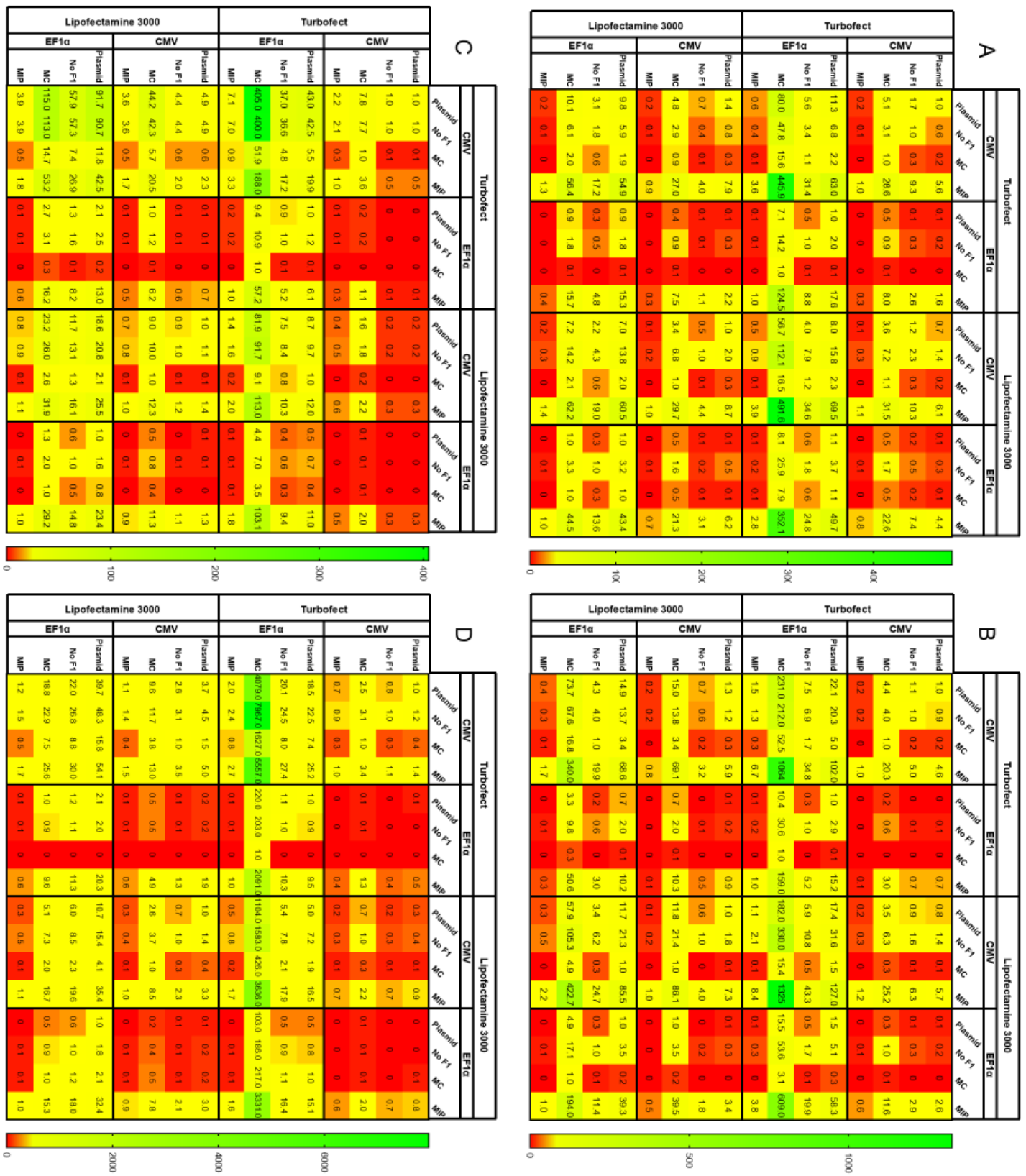

Figure S2. Donor specific transgenic luciferase activity fold changes for all pairwise comparisons of

transfection conditions. (A) Transgenic luciferase activity fold changes for all pairwise comparisons of transfection conditions in D1 hAMSCs. (B) Transgenic luciferase activity fold changes for all pairwise comparisons of transfection conditions in D2 hAMSCs. (C) Transgenic luciferase activity fold changes for all pairwise comparisons of transfection conditions in D3 hBMSCs. (D) Transgenic luciferase activity fold changes for all pairwise comparisons of transfection conditions in D4 hBMSCs. Fold changes are presented relative to column conditions.

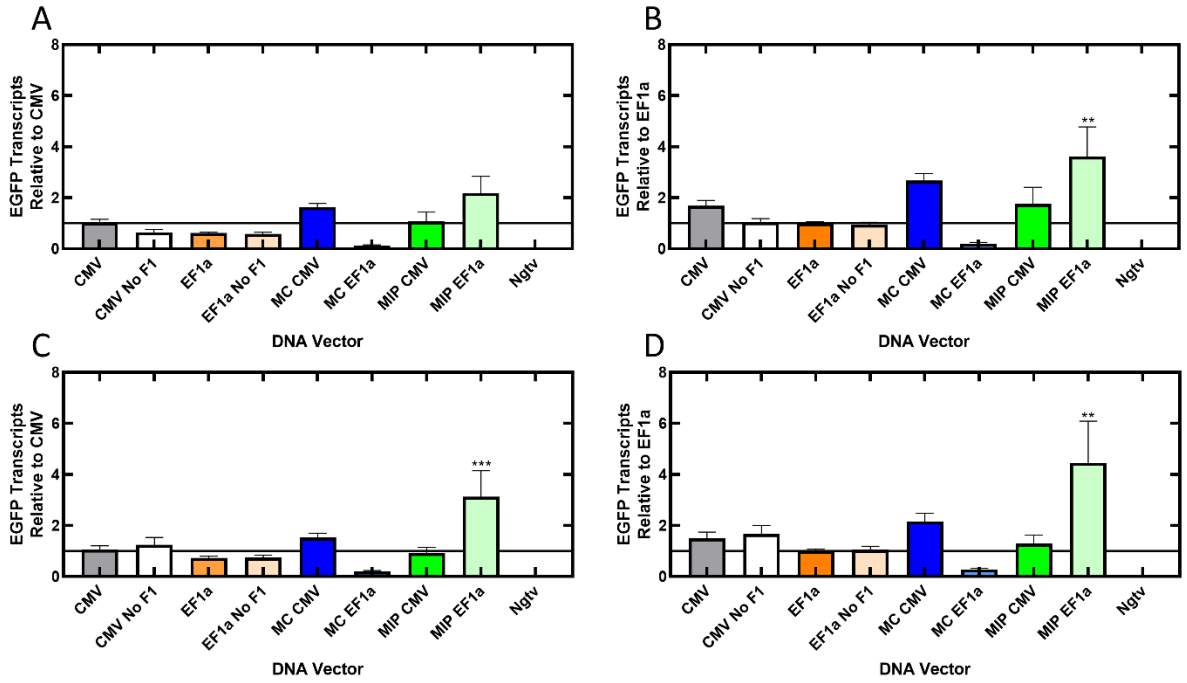

Figure S3. Relative transgenic mRNA transcripts at 12- and 24-hours following delivery of complexes as a function of DNA vector and promoter. (A) Transgenic mRNA transcripts, relative to the plasmid vector with the CMV promoter, for D1 hMSCs 12 hours after delivery of DNA vectors complexed with Turbofect. (B) Transgenic mRNA transcripts, relative to the plasmid vector with the EF1a promoter, for D1 hMSCs 12 hours after delivery of DNA vectors complexed with Turbofect. (C) Transgenic mRNA transcripts, relative to the plasmid vector with the CMV promoter, for D1 hMSCs 24 hours after delivery of DNA vectors complexed with Turbofect. (D) Transgenic mRNA transcripts, relative to the plasmid vector with the EF1a promoter, for D1 hMSCs 24 hours after delivery of DNA vectors complexed with Turbofect. Data in bar graphs are represented as mean ± SEM (n=6). *, $p<0.05$; **, $p<0.01$; ***, $p<0.001$; ****, $p<0.0001$.

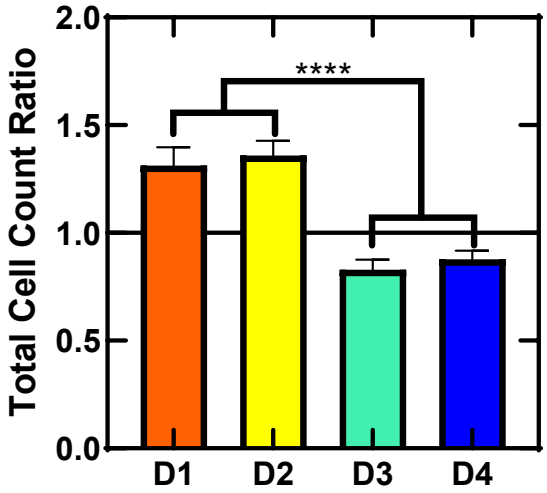

Figure S4. Cationic carrier effects on total cell counts in different donors of hMSCs derived from adipose tissue and bone marrow. Total cell counts for a DNA vector complexed with Turbofect were divided by total cell counts for the same DNA vector complexed with Lipofectamine 3000 for each donor to calculate total cell count ratios, which is an indirect measure of toxicity and/or proliferative effects of Turbofect relative to Lipofectamine 3000. Data in bar graphs are represented as mean ± SEM (n=48/donor). ****, $p<0.0001$

Molecular Therapy
Nucleic Acids
Original Article

Comparison of promoter, DNA vector, and cationic carrier for efficient transfection of hMSCs from multiple donors and tissue sources

Tyler Kozisek,[1] Andrew Hamann,[1] Luke Samuelson,[1] Miguel Fudolig,[2] and Angela K. Pannier[1]

[1]Department of Biological Systems Engineering, University of Nebraska-Lincoln, Lincoln, NE, USA; [2]Department of Statistics, University of Nebraska-Lincoln, Lincoln, NE, USA

Human mesenchymal stem cells (hMSCs) are primary cells with high clinical relevance that could be enhanced through genetic modification. However, gene delivery, particularly through nonviral routes, is inefficient. To address the shortcomings of nonviral gene delivery to hMSCs, our lab has previously demonstrated that pharmacological "priming" of hMSCs with clinically approved drugs can increase transfection in hMSCs by modulating transfection-induced cytotoxicity. However, even with priming, hMSC transfection remains inefficient for clinical applications. This work takes a complementary approach to addressing the challenges of transfecting hMSCs by systematically investigating key transfection parameters for their effect on transgene expression. Specifically, we investigated two promoters (cytomegalovirus [CMV] and elongation factor 1 alpha), four DNA vectors (plasmid, plasmid with no F1 origin, minicircle, and mini-intronic plasmid), two cationic carriers (Lipofectamine 3000 and Turbofect), and four donors of hMSCs from two tissues (adipose and bone marrow) for efficient hMSC transfection. Following systematic comparison of each variable, we identified adipose-derived hMSCs transfected with mini-intronic plasmids containing the CMV promoter delivered using Lipofectamine 3000 as the parameters that produced the highest transfection levels. The data presented in this work can guide the development of other hMSC transfection systems with the goal of producing clinically relevant, genetically modified hMSCs.

INTRODUCTION

Human mesenchymal stem cells (hMSCs) are under extensive research for applications in cell and gene therapeutics[1,2] due to their ease of isolation from multiple adult tissues,[3] their multipotent differentiation potential,[4] and their ability to home to sites of injury and reduce inflammation upon transplantation.[5,6] These therapeutic properties could be enhanced or expanded through genetic modification accomplished via delivery of exogenous genes, e.g., delivery of a DNA vector encoding for differentiation factors to enhance hMSC tissue engineering applications.[7] Genetic modification of hMSCs can be accomplished via viral or nonviral methods.[8,9] While viral transduction is efficient, it suffers from safety issues related to immunogenicity and insertional mutagenesis.[9,10] Nonviral gene delivery, which typically consists of condensing an anionic DNA vector with a cationic carrier to form nano-sized complexes that are capable of *in vitro* transfection,[11] overcomes many challenges associated with viral methods; however, nonviral gene delivery suffers from inefficiency, especially in hMSCs.[12]

To address the shortcomings of nonviral gene delivery to hMSCs, our group has demonstrated that pharmacological "priming" of cells prior to or simultaneously with application of nonviral DNA complexes can improve transfection in hMSCs.[13–16] Specifically, we have shown that the glucocorticoid, dexamethasone, can significantly increase transfection efficiency and transgene expression in multiple donors of hMSCs from different tissues, relative to a vehicle control (VC),[13] by modulating transfection-induced stress pathways and apoptosis.[14,15] Additionally, we have expanded our hMSC transfection priming library by screening a collection of 707 FDA approved drugs for drug repurposing[17] and identified new candidate priming agents that can significantly improve transfection compared to a VC.[16] However, even with priming, nonviral gene delivery to hMSCs remains inefficient for clinical applications.

In addition to priming strategies to improve transfection in hMSCs, research has shown that many factors can contribute to the success of nonviral gene delivery systems, such as the promoter sequence,[18] DNA vector,[19–22] bacterial elements,[19] cationic carrier,[23] hMSC donor,[24] and hMSC tissue source.[13–15] Two common promoters, the viral cytomegalovirus (CMV) promoter and the endogenous elongation factor 1 alpha (EF1a) promoter, have shown varying degrees of transfection outcomes in hMSCs.[14,25] For example, we have shown increased transfection in hMSCs with a DNA vector containing the viral CMV promoter compared to a DNA vector containing the EF1a promoter,[14] while others have shown the opposite in hMSCs when using those promoters in different DNA vectors.[25] In addition to promoters, the DNA vectors themselves, and in particular the

Received 13 January 2021; accepted 25 June 2021;
https://doi.org/10.1016/j.omtn.2021.06.018.

Correspondence: Angela K. Pannier, Department of Biological Systems Engineering, University of Nebraska-Lincoln, Lincoln, NE, USA.
E-mail: apannier2@unl.edu

Table 1. DNA vector information

Vector Name	Transgene	Promoter	Bacterial elements
CMV	Fusion protein of EGFP and luciferase	CMV	pUC origin of replication
EF1a		EF1a	F1 origin of replication
			Kanamycin resistance marker
CMV No F1		CMV	pUC origin of replication
EF1a No F1		EF1a	Kanamycin resistance marker
MC CMV		CMV	None
MC EF1a		EF1a	
MIP CMV		CMV	pUC origin of replication
MIP EF1a		EF1a	RNA-OUT selectable marker

bacterial elements contained within the DNA vectors (e.g., bacterial origins of replication, like the F1 origin,[26] and antibiotic resistance genes) can modulate transfection. For example, minicircle vectors (MCs), which do not contain any bacterial elements, have shown increased transfection efficiency in hMSCs compared to conventional plasmids[7] that contain bacterial elements. Alternatively, mini-intronic plasmids (MIPs), which include bacterial elements within an engineered intron, have shown enhanced transfection *in vitro* and *in vivo* compared to conventional plasmids, possibly due to the inclusion of an intron.[19,22] However, MIPs have not been investigated in the context of hMSC transfection. In addition to vector elements, different cationic carriers, such as polymers or lipids, have shown varying degrees of transfection in hMSCs.[23] Beyond DNA vector and cationic carrier, hMSC donor and tissue source (i.e., adipose or bone marrow) can affect transfection success as well.[13–15,24]

However, even with the above studies, these variables and their effects on nonviral gene delivery to hMSCs have yet to be systematically examined, and thus the objective of this work was to investigate four DNA vectors (plasmid DNA, plasmid DNA with no F1 origin of replication, MIPs, and MCs) and two promoters (CMV and EF1a), complexed with two commercially available cationic carriers (Lipofectamine 3000 and Turbofect) for their effects on transfection in hMSCs from four donors derived from two tissue sources (adipose- and bone-marrow-derived). This work systematically studies the key aspects of nonviral gene delivery systems as they pertain to hMSCs and offers insight into design parameters that can be exploited and further explored to develop efficient gene delivery systems for cells of high clinical significance.

RESULTS

The objective of this study was to investigate the effects of different promoters, DNA vectors, and cationic carriers on transfection in hMSCs from different donors and tissues. Specifically, we investigated two promoters (CMV and EF1a; Table 1) and four DNA vectors (plasmid, plasmid with no F1 origin of replication, MC, and MIP; Table 1; Figure 1), delivered using two commercially available cationic carriers (Turbofect [polymer-mediated] and Lipofectamine 3000 [lipid-mediated]) to cells from four hMSC donors (D1, D2, D3, and D4; Table S1) derived from two tissue sources (bone-marrow-derived and adipose-derived; Table S1) in order to identify transfection parameters that significantly ($p < 0.05$) affect transfection efficiency and transgene production in hMSCs. The effects on transfection efficiency were assayed by fluorescence imaging of an expressed transgenic fusion protein of enhanced green fluorescent protein (EGFP) with luciferase, normalized by total cell count (Hoechst 33342, nuclei stain), to obtain transfection efficiencies for all conditions. Imaging results were then verified by a chemical assay for transgenic luciferase activity, in relative light units (RLUs), normalized by total cellular protein values (RLU/mg Protein). It is important to note that due to the varying sizes of DNA vectors and promoters tested, both mass of DNA delivered and DNA copy number (i.e., molarity of transgene) were normalized for each promoter and cationic carrier in order to properly compare conditions (Table 2).

Given all of the variables above, this study tested 64 conditions, in triplicate on duplicate days ($n = 6$), to identify key transfection parameters (Tables 1; Table S1) that modulate hMSC transfection efficiency (Figures 2A and 2C) and transgene production (Figures 2B and 2D). Both outcomes varied widely as a function of each parameter, e.g., D3 bone-marrow-derived hMSCs (hBMSCs) transfected with the conventional CMV plasmid complexed with Turbofect produced transfection efficiencies around 35%, the highest of our study (Figure 2A), while D2 adipose-derived hMSCs (hAMSCs) transfected with CMV MIP complexed with Lipofectamine 3000 produced the highest transgenic luciferase activity of our study (Figure 2D). When comparing fold change differences between all possible comparisons (Figures S1 and S2), D1 hAMSCs transfected with EF1a MIP vectors complexed with Lipofectamine 3000 increased transfection efficiency almost 2-fold and transgenic luciferase activity by more than 6-fold compared to D1 hAMSCs transfected with the conventional CMV plasmid complexed with Lipofectamine 3000 (Figures S1A and S2A, respectively). However, given the multitude of parameters and combinations studied, data analysis was performed to assess whether there were any significant interactions between variables. Analyzing the transfection data as a negative binomial identified all two-way interactions as significant (Table S3), therefore, further analysis of the effects of each individual parameter on transfection outcomes was conducted, as described next.

Promoter selection can affect transfection in hMSCs

In order to understand promoter effects on hMSC transfection, transgene expression data (i.e., number EGFP-positive cells and total cells counts) were grouped by promoter (CMV or EF1a) for all hMSCs (D1, D2, D3, and D4), cationic carriers (Turbofect and Lipofectamine 3000), and DNA vectors (plasmid, no F1, MC, and MIP) and depicted as scatterplots of total cell counts versus number of EGFP-positive cells (Figure 3). These plots were sectioned into four quadrants for each promoter as described in the methods and legend for Figure 3. Analyzing transfection data as a function of promoter revealed differences between the CMV and EF1a promoters, as the CMV promoter resulted in eight conditions (transfection efficiencies for conditions in which hAMSCs were transfected with MIPs; Figure 3A) out of 192 total conditions/replicates in quadrant 2 (Q2; i.e., high transgene expression and low total cell counts), whereas the EF1a promoter

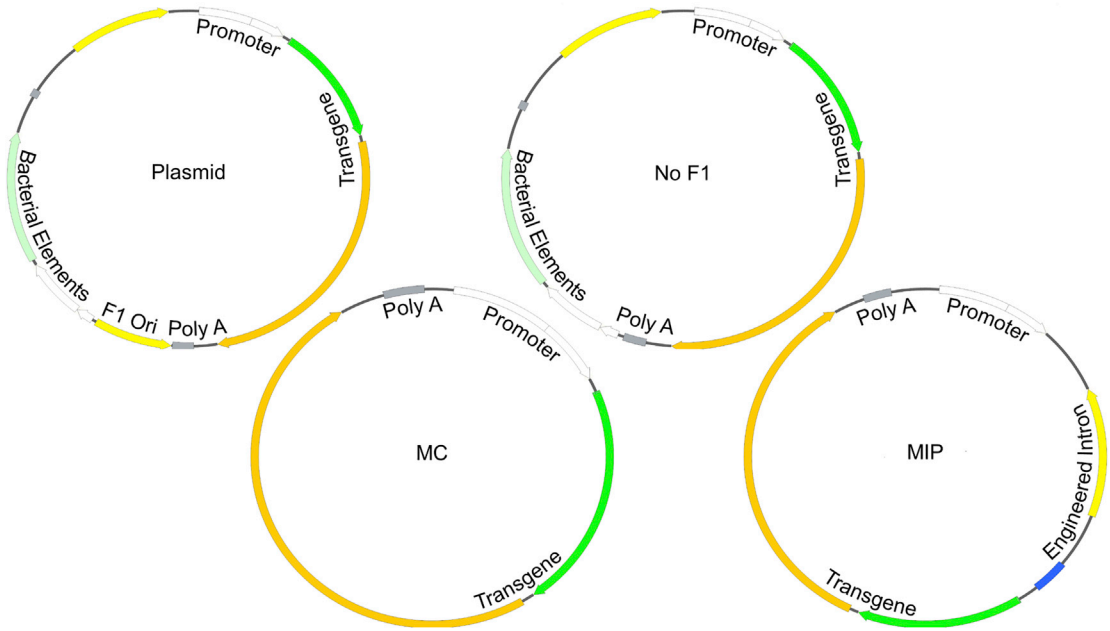

Figure 1. Representative schematics of DNA vectors investigated in this study

DNA vector diagrams are not to scale. DNA vector diagrams were created with SnapGene. F1 Ori, F1 origin of replication; poly(A), polyadenylation signal; MC, minicircle; MIP, mini-intronic plasmid.

resulted in no conditions in Q2 (Figure 3B). Furthermore, both promoters resulted in a majority of the transfection conditions within Q3 (i.e., low transgene expression and low total cell counts). Analyzing EGFP-positive cell counts as a negative binomial variable, with total cell counts as an offset term, showed that in terms of promoter effects, the CMV promoter resulted in significantly higher EGFP-positive cell counts than the EF1a promoter at the same total cell count within vector ($p < 0.0001$, Table S4), cationic carrier ($p < 0.0001$, Table S5), and donor ($p < 0.0001$, Table S6).

DNA vector bacterial elements affect transfection in hMSCs

In a similar manner used to compare promoters, transgene expression data (i.e., number of EGFP-positive cells and total cell counts) were grouped by the bacterial elements contained within each DNA vector (Table 1; Figure 4). Transgene expression data for the 16 conventional plasmid conditions, which contain the most bacterial elements (Table 1), were analyzed (i.e., CMV and EF1a; Table 1; Figure 2). Conditions in which hMSCs were transfected with conventional plasmids generally had transgene expression data in Q3 (i.e., low transgene expression and low total cell counts; Figure 4A). Removal of the F1 origin of replication from the conventional plasmid (No F1) resulted in more transfection conditions with higher EGFP-positive cell counts (i.e., Q1, more transgene expression) or higher total cell counts (i.e., Q4; Figure 4B) compared to conventional plasmids; however, conditions in which hMSCs were transfected with No F1 vectors generally had transgene expression data within Q3 (Figure 4B). Transgene expression data for the 16 MC conditions were also analyzed (Table 1; Figure 2). Conditions in which hMSCs were transfected with MCs generally produced transgene expression data that were within Q3 (i.e., low transgene expression and low total cell counts; Figure 4C). Conditions where hMSCs were transfected with MCs also produced a lower number of EGFP-positive cells (Figure 4C) compared to conditions where hMSCs were transfected with either conventional plasmids or No F1 vectors (Figures 4A and 4B, respectively). Finally, the transgene expression data for the 16 MIP conditions (Table 1; Figure 2) were analyzed. Conditions in which hMSCs were transfected with MIPs generally produced transgene expression data that were within Q3 (i.e., low transgene expression and low total cell counts; Figure 4D); however, conditions where hMSCs were transfected with MIPs produced more transgene expression data that were within Q2 (i.e., high transgene expression and high total cell counts; Figure 4D) compared to conditions where hMSCs were transfected with conventional plasmids (Figure 4A), No F1 vectors (Figure 4B), and MCs (Figure 4C). Analyzing EGFP-positive cell counts as a negative binomial variable with total cell counts as an offset term, indicated significant differences in EGFP-positive cell counts between vectors at the same total cell count within promoter ($p < 0.01$, Table S7), cationic carrier ($p < 0.0001$, Table S8), and donor ($p < 0.05$, Table S9). Furthermore, MIP vectors resulted in significantly higher EGFP-positive cell counts compared to all other vectors tested in hMSCs ($p < 0.001$, Table S9), except for D4 hMSCs transfected with plasmids ($p < 0.07$, Figure 4; Table S9).

Cationic carrier can affect hMSC transfection

In a similar manner used to compare promoters and bacterial elements, transgene expression data (i.e., number of EGFP-positive cells

Table 2. Normalization of DNA vector mass and moles of transgene

Vector name	Vector size (kbp)	Normalized expression cassette fraction	Fraction of expressionless vector for 1 μg/μL stocks
CMV	6.3	1	0
EF1a	6.9	1	0
CMV No F1	5.9	0.94	0.06
EF1a No F1	6.5	0.94	0.06
MC CMV	3.3	0.52	0.48
MC EF1a	3.9	0.57	0.43
MIP CMV	4.7	0.75	0.25
MIP EF1a	5.4	0.78	0.22

Kbp, kilobase pairs

and total cell counts) were grouped for the two commercially available cationic carriers (Figure 5). Conditions that made use of Turbofect, a polymer-based cationic carrier, generally had transgene expression data within Q3 (i.e., low transgene expression and low total cell counts; Figure 5A), however, seven transfection conditions (conditions in which hAMSCs were transfected with MIP CMV vectors) of the 192 conditions/replicates were contained within Q2 (i.e., high transgene expression and high total cell counts; Figure 5A). Conditions that made use of Lipofectamine 3000, a lipid-based cationic carrier, had one condition within Q2 (D1 hAMSC transfected with MIP CMV vectors; Figure 5B) but similar to Turbofect, the 64 conditions that made use of Lipofectamine 3000 (Figure 2) generally produced transgene expression data within Q3 (Figure 5B). Furthermore, analyzing EGFP-positive cell counts as a negative binomial variable, with total cell counts as an offset term, indicated a significant difference in EGFP-positive cell counts between Lipofectamine 3000 and Turbofect at the same total cell count within promoter ($p < 0.05$, Table S10), vector ($p < 0.01$, Table S11), and donor ($p < 0.01$, Table S12); however, due to our experimental design, it is difficult to conclude with any statistical confidence that Lipofectamine 3000 results in more EGFP-positive cells than Turbofect specifically between donors.

hMSC donor and tissue source can affect transfection

In a similar manner used to analyze promoters, bacterial elements, and cationic carriers, transgene expression data (i.e., number of EGFP-positive cell counts and total cell counts) for each hMSC donor and tissue source were grouped (Table S1; Figure 6). Transfection of hAMSCs generally resulted in transgene expression data within Q3 and Q4 (i.e., low transgene expression and varying total cell counts; Figure 6A) while transfection of hBMSCs resulted in all but one condition within Q3 (D4 hBMSCs transfected with No F1 CMV vector; Figure 6B). We further separated the transgene expression data by hMSC donor within each scatterplot in order to investigate transfection as a function of donor variability. For the two donors of hAMSCs, D1 (orange symbols) had transfection conditions with fewer EGFP-positive cells but higher total cell counts when compared to transfection conditions for D2 (Figure 6A; yellow symbols). However, there was little difference in transgene expression data between the two donors of hBMSCs (Figure 6B). Analyzing EGFP-positive cell counts as a negative binomial variable, with total cell counts as an offset term, indicated a significant difference in EGFP-positive cell counts between donors within promoter ($p < 0.05$, Table S13), vector ($p < 0.05$, Table S14), and cationic carrier ($p < 0.05$, Table S15); however, due to our experimental design in which we blocked by donor, further interpretation of statistical analysis on donor effects is not appropriate.

DISCUSSION

hMSCs are primary cells isolated from a variety of tissue with high clinical relevance,[1,2] which could be enhanced through genetic modification. However, gene delivery, particularly through nonviral routes, is inefficient.[8,12–16,24] We have previously reported enhanced nonviral gene delivery to hMSCs by priming with pharmacologic agents,[16] specifically with the glucocorticoid dexamethasone;[13–15] however, work remains to improve nonviral gene delivery to hMSCs, in particular through evaluation of key variables of the nonviral gene delivery system. This work systematically compares the key variables of nonviral gene delivery systems (e.g., DNA vector type, DNA vector bacterial elements, promoter, cationic carrier, and donor and tissue source) and the effects of these variables on transfection outcomes. The transfection outcomes varied widely for all 64 conditions tested (Tables 1; Table S1; Figure 2), therefore, deliberate grouping of variables was conducted in order to study the effects of each variable on hMSC transfection.

In order to investigate the effects of DNA vector modification on hMSC transfection, we first aggregated imaging transfection data (i.e., number of EGFP-positive cells and total cell counts) for all conditions tested and analyzed a single variable at a time. The first variable that we investigated was promoter used to drive expression of the transgene. The two promoters tested in this work (i.e., CMV and EF1a) are widely used promoters for gene delivery shown to produce high levels of transfection in numerous cell types.[25,27] Even so, the CMV promoter has shown significantly increased transfection levels compared to the EF1a promoter, especially in hMSCs.[14] Consistent with other published work, in this work, the CMV promoter did result in significantly increased EGFP-positive cell counts compared to the EF1a promoter when only the effects of the promoter were analyzed (Figure 3; Table S4–S6). This significant increase in transfection by the CMV promoter compared to the EF1a promoter may be from increased transcription of the transgene, as Antonova and colleagues have shown that the CMV promoter produces more transgenic mRNA transcripts compared to other promoters in mouse and primary human fibroblasts.[28] However, in this current report there was no significant increase in transgenic mRNA transcripts in hAMSCs from the CMV promoter compared to the EF1a promoter for any of the conditions tested at either 12 or 24 h after delivery of the transgene (Figure S3). While not significant, we did observe slight increases in transgenic mRNA transcripts in hAMSCs transfected with CMV DNA vectors compared to hAMSCs transfected with the same DNA vector with the EF1a promoter. However, these increases in transgenic mRNA transcripts likely do not contribute to the

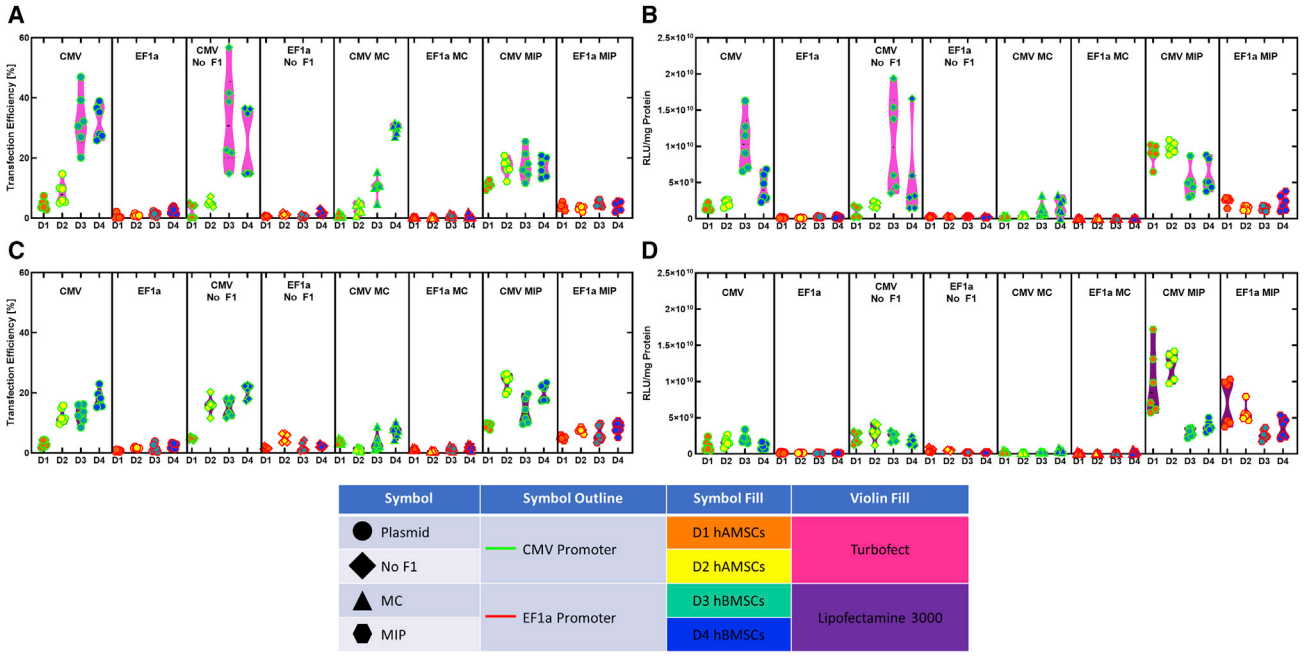

Figure 2. Transfection efficiency and production of transgene for all 64 conditions tested

(A) Violin plots of transfection efficiency for the 32 transfection conditions where Turbofect was used as the cationic carrier. (B) Violin plots of transgenic luciferase activity normalized to total protein amounts for the 32 transfection conditions where Turbofect was used as the cationic carrier. (C) Violin plots of transfection efficiency for the 32 transfection conditions where Lipofectamine 3000 was used as the cationic carrier. (D) Violin plots of transgenic luciferase activity normalized to total protein amounts for the 32 conditions that Lipofectamine 3000 was used as the cationic carrier. Parameters are identified within the legend provided.

significant increases in transfection efficiency and transgenic luciferase activity that we observed, and others have reported,[14] from the CMV promoter compared to the EF1a promoter. While this current study confirms that the CMV promoter produces more transfection than the EF1a promoter in hMSCs from multiple donors and tissue sources, the mechanism of enhancement for the CMV promoter needs further investigation.

Next, we investigated the effects of bacterial elements contained within the DNA vector for their effect on transfection outcomes in hMSCs. Conventional plasmids contain bacterial origins of replication and typically an antibiotic resistance gene for selection of plasmid-harboring bacteria during plasmid propagation. These bacterial components, while necessary for DNA vector production, have often been associated with an innate immune response through recognition of pathogen associated molecular patterns (PAMPs; e.g., unmethylated cytosine-phosphate-guanine [CpG]) by pattern recognition receptors (PPRs),[29,30] which may lead to transgene silencing.[31,32] Therefore, research into the development of highly efficient nonviral gene delivery systems has focused on removing bacterial elements from nonviral vectors.[8,29] While the experiments in this present work were not designed to study transgene silencing (i.e., transfection was assayed at a single time point following addition of DNA vectors), we did observe slight increases in transgenic luciferase activity when the F1 origin of replication (i.e., bacterial element) was removed from conventional plasmids, compared to conventional plasmids (Figures 2B and 2D). The F1 origin of replication is used in conventional plasmids to replicate and package single-stranded DNA into phages;[33] however, the F1 origin of replication is not necessary for conventional plasmid production or expression in mammalian cells. Furthermore, Johnson and colleagues[26] observed significant increases in bactofection (i.e., delivery of genetic cargo to mammalian cells using bacteria) of human breast cancer cells when the bacteria were harboring plasmids with no F1 origin of replication, presumably by rescuing DNA-induced stress. Therefore, removal of nonessential bacterial elements within DNA vectors may increase transfection in various cell types, particularly in hMSCs.

While removal of all bacterial elements is improbable for conventional plasmid production, Chen and colleagues[34] developed a DNA vector devoid of all bacterial elements, termed MCs, and showed increased transgene expression *in vivo* compared to conventional plasmids. MCs are devoid of all bacterial elements, while also having the ability to be propagated in engineered bacteria, through excision and recombination of the expression cassette from a parental plasmid, leaving a DNA vector that contains a promoter, transgene, and a terminator sequence.[34] MCs have since been shown to enhance transfection in hMSCs,[7,25,35–37] as well as stem cells from other species,[38,39] compared to conventional plasmids; however, in this current study, MCs produced the lowest transfection efficiencies and transgene expression observed, regardless of cationic carrier, promoter, donor, or hMSC tissue source (Figures 2, 3, 4, 5, and 6). The large

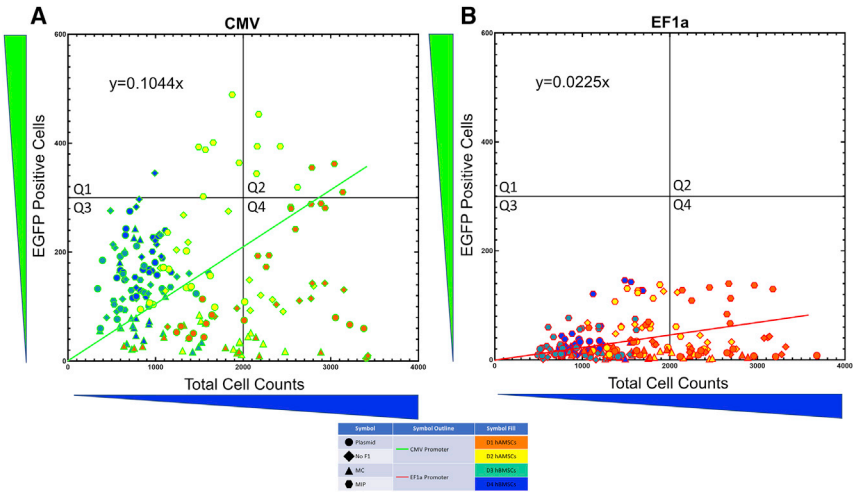

Figure 3. Transgene expression data as a function of DNA vector promoter in human mesenchymal stem cells (hMSCs)

(A) Scatterplot showing aggregated EGFP-positive cells and total cell counts for all transfection conditions (Table S1; Table 1) with the CMV promoter in all donors of hMSCs. (B) Scatterplot showing aggregated EGFP-positive cells and total cell counts for all transfection conditions (Table S1; Table 1) with the EF1a promoter in all donors of hMSCs. Quadrant 1 (Q1) represents high transgene expression but low total cell counts, which could be attributed to either transfection-induced toxicity and/or a reduction in proliferation. Q2 represents high transgene expression with high total cell counts, which could be attributed to either minimal transfection-induced toxicity and/or minimal reduction in proliferation. Q3 represents both low transgene expression and low total cell counts. Lastly, Q4 represents low transgene expression but high total cell counts. It should be noted that these quadrants were partitioned using the highest number of EGFP-positive cells and total cell counts that were observed in this current study; therefore, these quadrant boundaries should not be used to evaluate conditions and data from other studies. Lines represent the Poisson regression line that best fits the data. Parameters are identified within the legend provided.

discrepancy in transfection outcomes from MCs observed in this current study compared to other published studies may be from our normalization of both moles of expression cassette (i.e., transgene) and mass of DNA delivered (Table 2). For example, Mun and colleagues[25] observed higher transfection efficiencies in hAMSCs and hBMSCs using an EGFP expressing MC compared to an EGFP expressing plasmid when equal moles of expression cassette were delivered (i.e., higher mass of plasmid delivered than mass of MC). Alternatively, Boura and colleagues[36] delivered equal mass of MCs (i.e., higher molarity of expression cassette for MCs compared to plasmid) encoding for human leukocyte antigen-G1 (HLA-G1) to hBMSCs as plasmids carrying HLA-G1 and observed significantly higher expression of HLA-G1 from MCs in hBMSCs compared to a plasmid with the same promoter. Furthermore, Zimmermann and colleagues[7] showed significantly more alkaline phosphatase (ALP) activity in hBMSCs transfected with a bone morphogenetic protein 2 (BMP2) encoding MC compared to a conventional plasmid encoding BMP2, when equal mass of DNA was delivered (i.e., higher molarity of expression cassette for MCs compared to plasmid); however, when equal moles of expression cassette was delivered (i.e., higher mass of plasmid delivered than mass of MCs), BMP2 encoding MCs produced the same levels of ALP activity compared to BMP2 encoding plasmids. Indeed, we have observed increased transfection in hMSCs with MCs compared to conventional plasmids when equal mass of DNA vector was delivered but not equal moles of expression cassette (T.K., unpublished data); however, delivering equal mass of vectors with drastically different sizes is not a fair comparison as there will always be higher concentrations of expression cassette for the smaller vector (i.e., MC) than the larger vector (i.e., conventional plasmid), potentially increasing the probability of successful transfection for the smaller vector. Furthermore, delivering equal moles of expression cassette is also not a fair comparison for DNA vectors with drastically different sizes as the larger vector (i.e., conventional plasmid) will always have more mass of DNA than the smaller vector (i.e., MC), potentially leading to more toxicity than the smaller vector, as Zimmermann and colleagues observed a significant decrease in viability for conventional plasmids compared to MCs when equal moles of transgene were delivered (i.e., higher mass of conventional plasmid).[7] Therefore, we recommend that both moles of transgene and mass of DNA delivered need to be normalized in order to robustly compare DNA vectors with drastically different sizes. However, whether the transfection by MC observed in other studies is due to the lack of bacterial elements or the vectors' small size compared to conventional plasmids, or whether the lack of transfection observed in this work is due to lower copy numbers of the expression cassette for a given mass of DNA delivered, needs further investigation.

Another DNA vector with reduced bacterial components, which retains the ability to propagate in conventional bacteria, was developed by the Kay Lab.[19] These vectors, termed MIPs, contain all bacterial elements necessary for vector propagation in an engineered intron within the expression cassette.[19] The idea to incorporate bacterial elements within an engineered intron in the expression cassette stemmed from observations of *in vivo* transgene silencing when the extragenic space between the 5′ and 3′ ends of the expression cassette was greater than 1 kb.[31] The authors hypothesized that shortening the extragenic space between the 5′ and 3′ ends of the expression cassette could allow for more efficient gene looping, a mechanism in which the promoter and terminator regions are juxtaposed in a transcription-dependent manner,[40] thereby promoting efficient transcriptional elongation and recycling of RNA polymerase II from the terminator to the promoter. Their hypothesis that shortening the extragenic

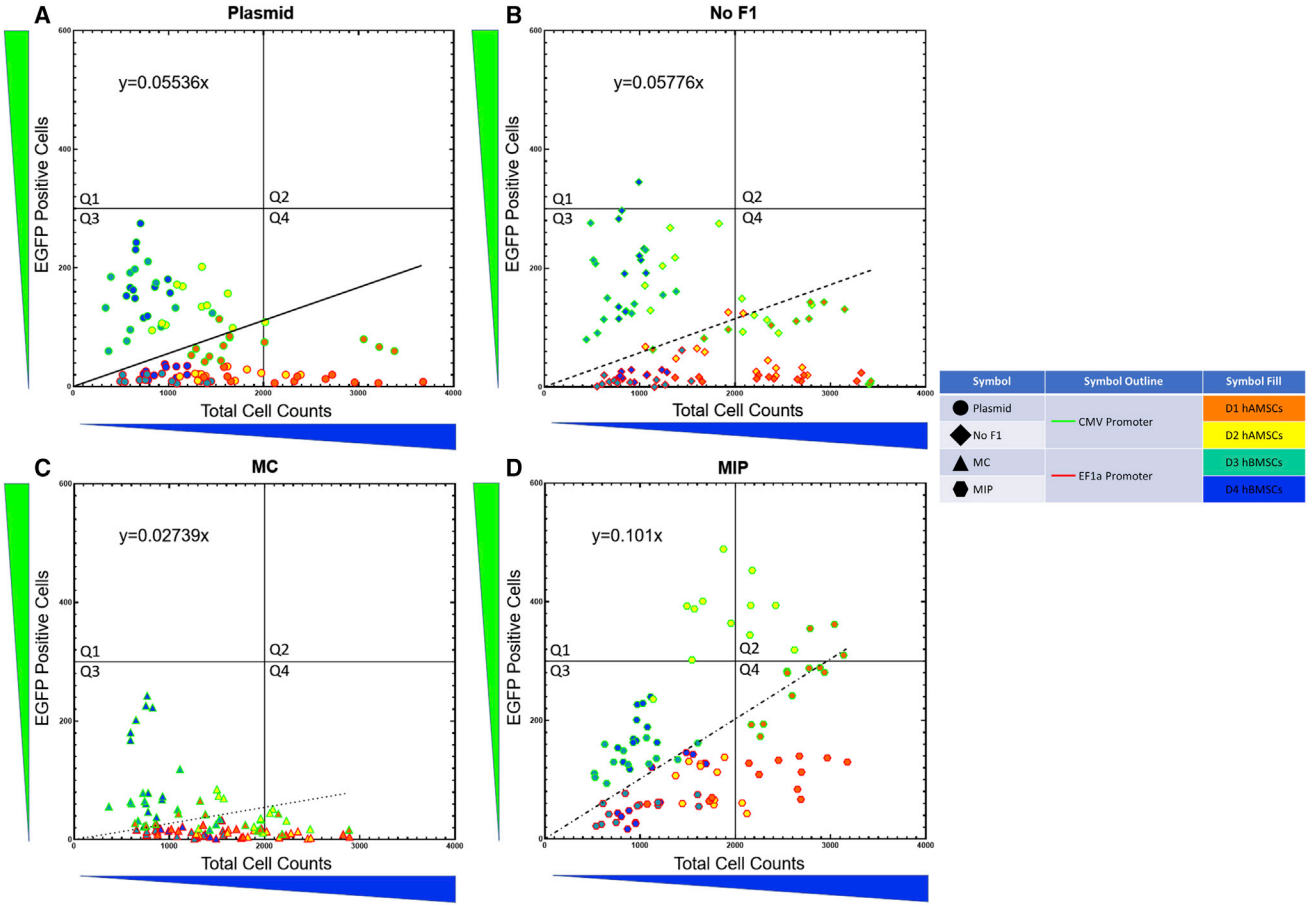

Figure 4. Transgene expression data as a function of DNA vector bacterial elements in hMSCs

(A) Scatterplot showing aggregated EGFP-positive cells and total cell counts for all plasmid vector conditions in all donors of hMSCs. (B) Scatterplot showing aggregated EGFP-positive cells and total cell counts for all plasmid conditions with the F1 origin of replication removed (No F1) in all donors of hMSCs. (C) Scatterplot showing aggregated EGFP-positive cells and total cell counts for all MC vector conditions in all donors of hMSCs. (D) Scatterplot showing aggregated EGFP-positive cells and total cell counts for all MIP conditions in all donors of hMSCs. Q1 represents high transgene expression but low total cell counts, which could be attributed to either transfection-induced toxicity and/or a reduction in proliferation. Q2 represents high transgene expression with high total cell counts, which could be attributed to either minimal transfection-induced toxicity and/or minimal reduction in proliferation. Q3 represents both low transgene expression and low total cell counts. Lastly, Q4 represents low transgene expression but high total cell counts. It should be noted that these quadrants were partitioned using the highest number of EGFP-positive cells and total cell counts that were observed in this current study, therefore, these quadrant boundaries should not be used to evaluate conditions and data from other studies. Lines represent the Poisson regression line that best fits the data. Parameters are identified within the legend provided.

space would allow for more efficient gene looping was never verified, but Lu and colleagues[19] did observe enhanced transfection with MIPs in mice and in human cells compared to plasmids and MCs. Indeed, MIPs produced the highest transfection efficiencies and transgene expression in this current study in both donors of hAMSCs compared to all other vectors, regardless of cationic carrier or promoter (Figures 2, 3, 4, 5, and 6). Additionally, we observed significantly more transgenic mRNA transcripts from hAMSCs transfected with MIP EF1a compared to hAMSCs transfected with either CMV or EF1a plasmids at 24 h (Figure S3); however, similar results were not observed for hAMSCs transfected with MIP CMV (Figure S3). The high transfection levels from MIPs observed in this current study, as well as other published work,[19,22,41] may be from the inclusion of an intron within the expression cassette, as others have shown increased transgene expression[42] or mRNA transcripts[43] when introns were inserted into the expression cassette. Introns have long been thought of as superfluous genetic material and were traditionally removed from transgenes prior to ligating into a DNA vector; however, introns have been shown to play vital roles in transgene expression, such as transcription,[43] polyadenylation,[44] and mRNA export and decay,[45] as well as translational efficiency.[46] Given the transfection levels observed in this current study by MIPs, as well as the transgenic mRNA transcript levels at 12 and 24 h after transfection, it is plausible that the engineered intron within the expression cassette of MIPs might be promoting transcription[42,43] or limiting mRNA decay (i.e., significantly higher transgenic mRNA transcripts for MIPs in

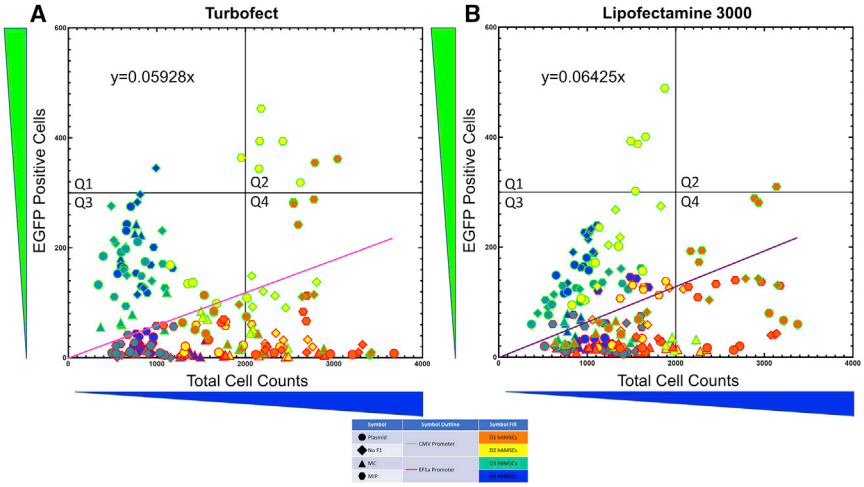

Figure 5. Transgene expression data as a function of cationic carrier in hMSCs

(A) Scatterplot showing aggregated EGFP-positive cells and total cell counts for all transfection conditions where the polymer transfection reagent Turbofect was used as the cationic carrier in all donors of hMSCs. (B) Scatterplot showing aggregated EGFP-positive cells and total cell counts for all vectors where the lipid transfection reagent Lipofectamine 3000 was used as the cationic carrier in all donors of hMSCs. Q1 represents high transgene expression but low total cell counts, which could be attributed to either transfection-induced toxicity and/or a reduction in proliferation. Q2 represents high transgene expression with high total cell counts, which could be attributed to either minimal transfection-induced toxicity and/or minimal reduction in proliferation. Q3 represents both low transgene expression and low total cell counts. Lastly, Q4 represents low transgene expression but high total cell counts. It should be noted that these quadrants were partitioned using the highest number of EGFP-positive cells and total cell counts that were observed in this current study, therefore, these quadrant boundaries should not be used to evaluate conditions and data from other studies. Lines represent the Poisson regression line that best fits the data. Parameters are identified within the legend provided.

D1 hAMSCs compared to both the CMV and EF1a conventional plasmid, regardless of promoter used; Figures S3B and S3D) or are enhancing translation in hAMSCs[42] (i.e., higher transfection efficiency and transgene expression by MIPs compared to other vectors tested regardless of promoter or cationic carrier in hAMSCs; Figure 4). However, in hBMSCs, increases in transfection efficiency and transgene expression by MIPs were only observed when the EF1a promoter was used (Figure 2), possibly due to the incorporation of a second intron within the EF1a promoter[42] or differences in intron processing by the cells.[47] However, studies comparing transcription and translation efficiency differences from either gene looping or incorporation of one or more introns are needed to fully elucidate the transfection enhancements observed by MIPs in hMSCs.

In addition to the above transfection parameters, research has shown that polymer- and lipid-mediated nonviral gene delivery efficacy can be dependent on cationic carrier formulation; however, limited research has been conducted on how polymer- and lipid-mediated transfection can be affected by different DNA vectors,[48] in particular within the context of hMSCs from multiple donors and tissue sources. Here, two commercially available transfection reagents were used, which represent both lipid- and polymer-based systems: Lipofectamine 3000 and Turbofect, respectively. These commercially available transfection reagents were chosen as they are readily available, widely used, and have shown moderate levels of transfection in hMSCs[14–16,24] (T.K., A.H., and L.S., unpublished data). This study did not include other modes of delivery (e.g., electroporation) given the complexities involved in comparing carrier-based systems to physical methods, but future studies should investigate other delivery strategies in the context of the parameters investigated here.

In this current study, there were differences in transfection efficiencies and transgene production between the two cationic carriers (Figure 2) and Poisson regressions of aggregated transgene expression data for each cationic carrier showed slight differences in overall transfection trends (Figure 5). Indeed, others have shown differences in transfection outcomes in hMSCs between polymer- and lipid-based systems, with either polymer-[49] or lipid-based[23] systems producing the highest transgene expression. Furthermore, we observed significantly different total cell ratios for tested cationic carriers (Turbofect total cell count divided by the total cell count for the same condition complexed with Lipofectamine 3000, which is an indirect measure of toxicity and/or proliferative effects of Turbofect relative to Lipofectamine 3000) between hAMSCs and hBMSCs (Figure S4), highlighting another transfection parameter that needs to be carefully considered in a hMSC nonviral gene delivery system. Indeed, our previous studies on hMSC transfection with lipid-based cationic carriers extensively characterized both cellular proliferation (through metabolic studies)[13] and transfection-induced toxicity,[15] and showed that rescuing transfection-induced metabolic shut down and toxicity could enhance transfection efficiency and transgene production.[13,15]. Taken together, cationic carrier selection does not have a large effect on overall transfection outcomes; however, transfection and total cell counts, which are an indirect measure of cytotoxicity and/or proliferative nature, can be optimized if the cationic carrier is selected based on hMSC tissue source.

Finally, hMSCs can be harvested from multiple tissues in the adult human body[50,51] and, due to their immunomodulatory effects,[5,52] have the potential for allogenic use,[53] making both donor and tissue source pertinent variables in this study. hMSCs have been shown to have

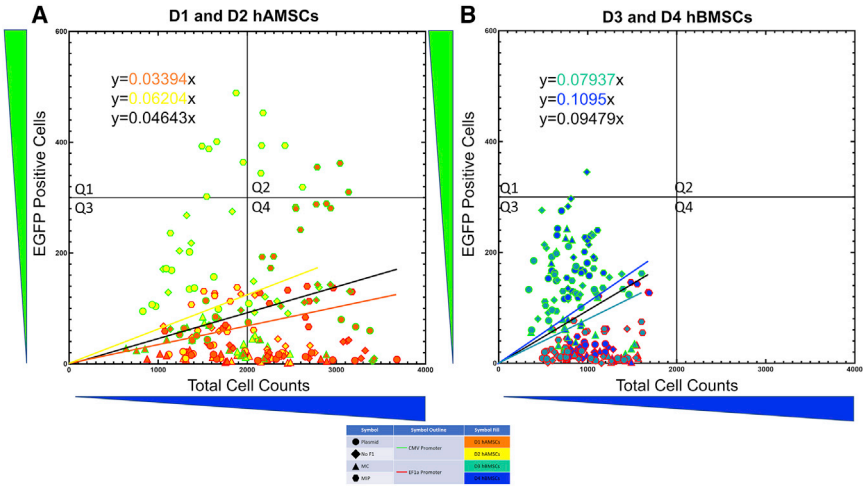

Figure 6. Transgene expression data as a function of hMSC tissue source and donor

(A) Scatterplot showing aggregated EGFP-positive cells and total cell counts for all transfection conditions in both donors of adiposed-derived hMSCs (hAMSCs). (B) Scatterplot showing aggregated EGFP-positive cells and total cell counts for all transfection conditions in both donors of bone-marrow-derived hMSCs (hBMSCs). Q1 represents high transgene expression but low total cell counts, which could be attributed to either transfection-induced toxicity and/or a reduction in proliferation. Q2 represents high transgene expression with high total cell counts, which could be attributed to either minimal transfection-induced toxicity and/or minimal reduction in proliferation. Q3 represents both low transgene expression and low total cell counts. Lastly, Q4 represents low transgene expression but high total cell counts. It should be noted that these quadrants were partitioned using the highest number of EGFP-positive cells and total cell counts that were observed in this current study; therefore, these quadrant boundaries should not be used to evaluate conditions and data from other studies. Lines represent the Poisson regression line that best fits the data. Parameters are identified within the legend provided.

large variability in gene expression, proliferative capacity, differentiation capacity, and transfection efficacy between the donor and tissue source from which they were obtained;[13–15,24,50,54] however, these parameters have not been studied in depth as they pertain to DNA vector modifications and transfection outcomes.[13,14] Here, the data show discrepancies in trends between transfection outcomes for each condition between the different donors and tissue sources (Figure 2), which may be partly attributed to the different proliferation rates between hMSCs from different donors and tissue source.[50] Generally, hAMSCs have higher proliferation rates compared to hBMSCs,[50] which may increase nuclear internalization of DNA vectors due to the increased nuclear breakdown, thereby giving hAMSCs a higher probability of successful transfection compared to hBMSCs. The slower proliferating hBMSCs may have lower probabilities of successful transfection due to less nuclear breakdown but have a higher DNA vector-to-cell ratio due to their lower cell numbers compared to hAMSCs (Figure 6), possibly causing an increase in transfection-induced toxicity (Figure S4) due to the higher DNA vector dose, as others have observed.[55] However, further studies are needed in order to elucidate the discrepancies in transfection efficiency and transgene expression observed in this study between different conditions on a hMSC donor and tissue source basis.

Conclusions

This work systematically investigated the effects of DNA vector modifications (i.e., promoter, bacterial element quantities, and positions within the vector) on transfection in hMSCs from different donors and tissue sources using two commercially available cationic carriers. Analyzing each variable separately, we observed differences in transfection outcomes based on promoter selection, DNA vector, and cationic carrier, as well as donor and tissue source. Notably, we observed the highest levels of transgene expression when MIPs, complexed with Lipofectamine 3000, were delivered to hAMSCs and transgene production was under control of the CMV promoter. Furthermore, the presented data provide valuable insight into the importance of hMSC donor and tissue source variability as they pertain to DNA vector modifications for nonviral gene delivery. This work demonstrates that transfection parameters may need to be tuned in an application- and patient-specific manner in order to achieve efficient transfection in hMSCs for clinical therapies.

MATERIALS AND METHODS

Cell culture

Cryopreserved hMSCs from four human donors and two tissue sources were purchased at passage two from Lonza (Lonza, Walkersville, MD, USA) and were used at passage six (see Table S1 for donor information). Adipose-derived hMSCs (hAMSCs) were positive for CD13, CD29, CD44, CD73, CD90, CD105, CD166, and negative for CD14, CD31, and CD45 cell surface markers. Bone-marrow-derived hMSCs (hBMSCs) were positive for CD29, CD44, CD105, and CD166 and negative for CD14, CD34, and CD45 cell surface markers. hMSCs were passaged and cultured in hMSC media, consisting of minimum essential medium alpha (MEM Alpha; GIBCO, Grand Island, NY, USA) supplemented with 10% heat-inactivated fetal bovine serum (FBS; GIBCO), 6 mM L-Glutamine (GIBCO), and 1% penicillin-streptomycin (Pen-Strep; 10,000 U/mL; GIBCO), and incubated at 37°C with 5% CO_2 until confluent. At confluence, hMSC media was removed and cells were washed with 1× phosphate-buffered saline (PBS) prior to the addition of 0.25% trypsin-ethylenediamine tetraacetic acid (EDTA; GIBCO) for cellular dissociation. After dissociation, an equal volume of hMSC media was added and total cellular suspension was removed for subsequent cell pelleting via

centrifugation to remove trypsin-EDTA. Cells were resuspended in warm hMSC media and counted via trypan blue exclusion using a hemocytometer prior to diluting in hMSC media for seeding, as described next.

For seeding of hAMSCs, cells were dissociated and counted, as described above, and 100 μL of 4.5×10^4 cells/mL cell suspension (4,500 cells/well; D1 and D2) was added to each well of clear bottom, black walled, 96-well plates (Corning Life Sciences, Corning, NY, USA). Immediately following seeding, plates were incubated at 37°C and 5% CO_2 and allowed to culture for 24 h. For seeding of hBMSCs, cells were dissociated and counted, as described above, and 100 μL of 4×10^4 cells/mL cell suspension (4,000 cells/well; D3 & D4) was added to each well of clear bottom, black walled, 96-well plates (Corning Life Sciences). Immediately following seeding, plates were incubated at 37°C and 5% CO_2 and allowed to culture for 48 h. The different seeding densities and culture times for hAMSCs (4.5×10^4 cells/mL, 24 h) and hBMSCs (4×10^4 cells/mL, 48 hours) were selected so all experimental conditions were at ~80% confluence before transfecting, as described below.

DNA vectors

All DNA vectors used in this screen encode for a fusion protein of EGFP and firefly luciferase (EGFPLuc, Figure 1 and Table 1). pTubb3-MC was a gift from Juan Belmonte (Addgene plasmid #87112; http://n2t.net/addgene:87112; RRID: Addgene_87112)[56] and was used to clone minicircle (MC) vectors MC.EGFPLuc-CMV, MC.EGFPLuc-EF1a, and MC.Expressionless (Genscript, Piscataway, NJ, USA). MIP 247 CoMIP 4in1 with shRNA p53 was a gift from Mark Kay and Joseph Wu (Addgene plasmid #63726; http://n2t.net/addgene:63726; RRID: Addgene_63726)[22] and was used to clone MIP vectors MIP.EGFPLuc-CMV, MIP.EGFPLuc-EF1a, and MIP.Expressionless (Genscript). The F1 origin of replication was removed from EGFPLuc-CMV (Clontech, Mountain View, CA, USA) and pEGFPLuc-EF1a (Genscript) in order to clone pEGFPLuc-CMV No F1 and pEGFPLuc-EF1a No F1, respectively (Genscript). MC vectors (MC.EGFPLuc-CMV, MC.EGFPLuc-EF1a, and MC.Expressionless) were propagated in the bacterial strain ZYCY10P3S2T (System Biosciences, Palo Alto, CA) under kanamycin selection following a published protocol,[57] with minor changes. Briefly, 100 mL of Terrific Broth (TB; Invitrogen) was inoculated with bacterial strain ZYCY10P3S2T containing MC vectors and cultured overnight at 37°C with shaking at 250 RPM. The overnight culture was then mixed with minicircle induction mix comprising 100 mL of Luria-Bertani broth (LB; Becton Dickinson, Franklin Lakes, NJ, USA), 4 mL of 1N NaOH, and 100 μL of 20% L-arabinose, and cultured for 5 h at 32°C with shaking at 250 RPM. All MIP vectors (MIP.EGFPLuc-CMV, MIP.EGFPLuc-EF1a, and MIP.Expressionless) were propagated in RNA-OUT competent cells (Nature Technologies, Lincoln, NE, USA)[58] using 6% sucrose selection media. All plasmids (pEGFPLuc-CMV, pEGFPLuc-CMV No F1, pEGPFLuc-EF1a, and pEGFPLuc-EF1a) were propagated in DH5α e. coli. (Invitrogen, Carlsbad, CA, USA) under kanamycin selection. All DNA vectors were isolated and purified using a Purelink High Purity Endotoxin free plasmid purification kit (Invitrogen). DNA quality and yield were measured using a Nanodrop (Thermo Fisher Scientific) and all DNA vectors were resuspended in Tris EDTA (TE) buffer at a concentration of 1 μg/μL.

In order to compare DNA vectors, an equal amount of transgene (i.e., molarity of expression cassette) and DNA mass was delivered to hMSCs for each DNA vector. Molarity of expression cassette for each DNA vector was normalized by dividing the size of each DNA vector (in kilobase pairs) by the size of the largest DNA vector (in kilobase pairs) for each promoter. DNA mass was then equalized by adding the remaining fraction of corresponding expressionless vector to make all DNA vector stocks be 1 μg/μL (Table 2).

hMSC transfection

24 h after seeding of hAMSCs, or 48 h after seeding of hBMSCs, as described above, all DNA vectors were complexed with either Lipofectamine 3000 (Invitrogen) at a DNA:lipid ratio of 1:2 in serum free Opti-MEM media (Invitrogen) following the manufacturer's protocol or complexed with Turbofect (Thermo Fisher Scientific) at a DNA:polymer ratio of 1:4 in serum free Opti-MEM media following manufacturer's protocol. After complex formation, 0.07 μg of Lipofectamine 3000 complexed DNA vector in 6.7 μL of Opti-MEM or 0.07 μg of Turbofect complexed DNA vector in 11.1 μL of Opt-MEM was delivered to each well, and plates were briefly centrifuged to ensure mixing of complexes with the hMSC media. Media were removed immediately after centrifugation and replaced with fresh, warmed, hMSC media lacking complexes. Following complex delivery, hMSCs were placed into incubators at 37°C and 5% CO_2 and allowed to culture for 48 h.

Cell staining and high content imaging for transfection efficiency assessment

48 h after delivery of complexes, cells were stained with Hoechst 33342 (Sigma-Aldrich, St. Louis, MO, USA) to enable nuclei counts for assessment of EGFP transfection efficiencies. After removing culture media from the cells, 50 μL of staining solution (1 μg/mL of Hoechst in hMSC media) was added to each well and incubated for 25 min at 37°C and 5% CO_2. After incubation, staining solution was removed, and cells were rinsed with 20 μL of 1× PBS on a multi-purpose rotator for 5 min, after which the rinse was removed and 100 μL of 1× PBS was added to each well for subsequent imaging.

Images of each well were acquired with a Cytation 1 Cell Imaging System (Biotek, Winooski, VT, USA), equipped with a laser autofocus cube and GFP (EGFP transgene production) and DAPI (nuclei count via Hoechst) filter cubes paired with 465 nm and 365 nm LED cubes, respectively. Two images, spaced 150 μm apart vertically, were taken of each well in each fluorescent channel, in addition to phase contrast images, using a 4× objective. Consistent fluorescence excitation LED intensity and camera exposure settings were used to allow for comparison of image intensities between wells in the same plate. After imaging, cells were washed with PBS and lysed with 150 μL per well of

1× reporter lysis buffer (Promega, Madison, WI, USA) by incubating at room temp for 10 min prior to storage at −80°C.

Assessment of transfection efficiency and transgene expression levels

Gen5 software (Biotek) was used for image preprocessing and deconvolution (to subtract background fluorescence from captured digital images), as well as object analysis (e.g., EGFP-positive cells and cell nuclei) in order to calculate transfection efficiencies. Object analysis identified objects of interest in all channels by their fluorescence intensity and size. DAPI and GFP intensity thresholds were set at 5,000 and 1,000 relative fluorescent units (RFUs), respectively, and minimum and maximum object size were set at 12 and 50 (DAPI) and 12 and 150 (GFP).

Transfection efficiency was calculated by dividing the number of EGFP objects (cells producing transgene) by the number of DAPI objects (cell nuclei) in the same well. Transgenic luciferase activity levels were quantified by measuring luciferase luminescence in RLUs with a Luciferase Assay kit (Promega) and a luminometer (Turner Designs, Sunnyvale, CA, USA). RLUs were normalized to total protein amount determined with a Pierce bicinchoninic acid (BCA) colorimetric assay (Pierce, Rockford, IL, USA) using an Epoch plate reader (Biotek) to measure absorbance at 562 nm.

Quantification of transgenic mRNA

To quantify relative mRNA transcript copy numbers of the EGFPLuc transgene from each DNA vector, we seeded D6 hAMSCs at 4.5×10^4 cells/mL (4,500 cells/well), as described above, and cultured at 37°C and 5% CO_2. 24 h after seeding, D1 hAMSCs were transfected with DNA vectors complexed with Turbofect transfection reagent, as described above. 12 and 24 h following transfection, mRNA was isolated for each condition using SingleShot Cell Lysis Kit (Bio-Rad, Hercules, CA, USA) following the manufacturer's protocol. Isolated mRNA was then reverse transcribed using iScript cDNA Synthesis Kit (Bio-Rad) following the manufacturer's protocol. qRT-PCR was performed on a QuantStudio 6 Flex Real-Time PCR System (Applied Biosystems, Foster City, CA, USA) with Power SYBR Green Master Mix (Thermo Fisher Scientific) and relative expression was calculated by the ΔΔCt method normalizing to the endogenous control RPL13A. See Table S2 for primer sequences (Integrated DNA Technologies, Coralville, IA, USA).

Data analysis and statistics

In this study, two promoters in eight DNA vectors complexed with two commercially available transfection reagents were investigated in four donors of hMSCs from two tissue sources (64 conditions). Our experimental design for this study was a split-plot design with the whole plot factor being the cationic carrier and the split plot factor being vector × promoter after blocking by donor. All data are reported as the mean of triplicate values for each condition on duplicate days (n = 6), except where noted. In order to compare each variable tested, the EGFP cell counts and total cell counts for all 64 conditions tested (Figure 2) were aggregated for that particular variable and presented in scatterplots (Figures 3, 4, 5, and 6) divided into four quadrants. Q1 represents high transgene expression but low total cell counts (which could be attributed to either transfection-induced toxicity and/or a reduction in proliferation). Q2 represents high transgene expression with high total cell counts (which could be attributed to either minimal transfection-induced toxicity and/or minimal reduction in proliferation). Q3 represents both low transgene expression and low total cell counts. Lastly, Q4 represents low transgene expression but high total cell counts. It should be noted that these quadrants were partitioned using the highest number of EGFP-positive cells and total cell counts that were observed in this current study; therefore, these quadrant boundaries should not be used to evaluate conditions and data from other studies. Poisson regressions, with the line forced through the origin, were performed for each scatterplot (i.e., variable) in order to visually identify differences in EGFP cell counts versus total cell counts for each variable tested. EGFP-positive cell count data represented in the scatterplots were analyzed as a negative binomial variable with the total cell counts as an offset term. Kenward-Roger adjustment was used on the degrees of freedom to account for the multiple error levels in the analysis. Transfection efficiency and transgenic luciferase activity fold changes were calculated for all pairwise comparisons for each donor by dividing the six transgene expression values for each column condition by the average (n = 6 for each condition) of the row condition (Figures S1 and S2). Relative transgenic mRNA transcript fold-changes were analyzed using an ANOVA with Dunnett's post hoc test. Statistical significance was accepted for p values less than 0.05. Statistics were evaluated using Prism GraphPad software (GraphPad Software, La Jolla, CA, USA) and SAS/STAT 14.2 software, version 9.4 of the SAS system for Windows. Copyright 2016 SAS Institute SAS and all other SAS Institute product or service names are registered trademarks or trademarks of SAS Institute (SAS Institute, Cary, NC, USA).

SUPPLEMENTAL INFORMATION

Supplemental information can be found online at https://doi.org/10.1016/j.omtn.2021.06.018.

ACKNOWLEDGMENTS

We would like to thank the National Institutes of Health (1 DP2 EB025760-01, 3 DP2 EB025760-01S1) for funding. The contents of this publication are the sole responsibility of the authors and do not necessarily represent the official views of the NIH. We would also like to thank Dr. Stephen D. Kachman and Kory Heier for their assistance with the statistical analysis.

AUTHOR CONTRIBUTIONS

Conceptualization, T.K. and A.K.P.; Methodology, T.K.; Investigation, T.K., A.H., L.S., and M.F.; Writing – Original Draft, T.K.; Writing – Review & Editing, T.K., A.H., L.S., M.F., and A.K.P.; Funding Acquisition, A.K.P.

DECLARATION OF INTERESTS

The authors declare no competing interests.

REFERENCES

1. Hosseini, S.A., Mohammadi, R., Noruzi, S., Mohamadi, Y., Azizian, M., Mousavy, S.M., Ghasemi, F., Hesari, A., Sahebkar, A., Salarinia, R., et al. (2018). Stem cell- and gene-based therapies as potential candidates in Alzheimer's therapy. J. Cell. Biochem. *119*, 8723–8736.
2. Lo Furno, D., Mannino, G., and Giuffrida, R. (2018). Functional role of mesenchymal stem cells in the treatment of chronic neurodegenerative diseases. J. Cell. Physiol. *233*, 3982–3999.
3. Ullah, I., Subbarao, R.B., and Rho, G.J. (2015). Human mesenchymal stem cells - current trends and future prospective. Biosci. Rep. *35*, e00191.
4. Goff, L.A., Boucher, S., Ricupero, C.L., Fenstermacher, S., Swerdel, M., Chase, L.G., Adams, C.C., Chesnut, J., Lakshmipathy, U., and Hart, R.P. (2008). Differentiating human multipotent mesenchymal stromal cells regulate microRNAs: prediction of microRNA regulation by PDGF during osteogenesis. Exp Hematol *36*, 1354–1369.
5. Gebler, A., Zabel, O., and Seliger, B. (2012). The immunomodulatory capacity of mesenchymal stem cells. Trends Mol. Med. *18*, 128–134.
6. Leng, Z., Zhu, R., Hou, W., Feng, Y., Yang, Y., Han, Q., Shan, G., Meng, F., Du, D., Wang, S., et al. (2020). Transplantation of ACE2-mesenchymal stem cells improves the outcome of patients with COVID-19 pneumonia. Aging Dis. *11*, 216–228.
7. Zimmermann, A., Hercher, D., Regner, B., Frischer, A., Sperger, S., Redl, H., and Hacobian, A. (2020). Evaluation of BMP-2 Minicircle DNA for Enhanced Bone Engineering and Regeneration. Curr. Gene Ther. *20*, 55–63.
8. Hamann, A., Nguyen, A., and Pannier, A.K. (2019). Nucleic acid delivery to mesenchymal stem cells: a review of nonviral methods and applications. J. Biol. Eng. *13*, 7.
9. Oggu, G.S., Sasikumar, S., Reddy, N., Ella, K.K.R., Rao, C.M., and Bokara, K.K. (2017). Gene delivery approaches for mesenchymal stem cell therapy: strategies to increase efficiency and specificity. Stem Cell Rev. Rep. *13*, 725–740.
10. Nayerossadat, N., Maedeh, T., and Ali, P.A. (2012). Viral and nonviral delivery systems for gene delivery. Adv. Biomed. Res. *1*, 27.
11. Jin, L., Zeng, X., Liu, M., Deng, Y., and He, N. (2014). Current progress in gene delivery technology based on chemical methods and nano-carriers. Theranostics *4*, 240–255.
12. Santos, J.L., Pandita, D., Rodrigues, J., Pêgo, A.P., Granja, P.L., and Tomás, H. (2011). Non-viral gene delivery to mesenchymal stem cells: methods, strategies and application in bone tissue engineering and regeneration. Curr. Gene Ther. *11*, 46–57.
13. Kelly, A.M., Plautz, S.A., Zempleni, J., and Pannier, A.K. (2016). Glucocorticoid cell priming enhances transfection outcomes in adult human mesenchymal stem cells. Mol. Ther. *24*, 331–341.
14. Hamann, A., Broad, K., Nguyen, A., and Pannier, A.K. (2019). Mechanisms of unprimed and dexamethasone-primed nonviral gene delivery to human mesenchymal stem cells. Biotechnol. Bioeng. *116*, 427–443.
15. Hamann, A., Kozisek, T., Broad, K., and Pannier, A.K. (2020). Glucocorticoid Priming of Nonviral Gene Delivery to Human Mesenchymal Stem Cells Increases Transfection by Reducing Induced Stresses. Mol. Ther. Methods Clin. Dev.
16. Kozisek, T., Hamann, A., Nguyen, A., Miller, M., Plautz, S., and Pannier, A.K. (2020). High-throughput screening of clinically approved drugs that prime nonviral gene delivery to human Mesenchymal stem cells. J. Biol. Eng. *14*, 16.
17. McCarthy, A. (2010). The NIH Molecular Libraries Program: identifying chemical probes for new medicines, http://nihsmr.evotec.com/evotec/.
18. Zheng, C., and Baum, B.J. (2005). Evaluation of viral and mammalian promoters for use in gene delivery to salivary glands. Mol. Ther. *12*, 528–536.
19. Lu, J., Zhang, F., and Kay, M.A. (2013). A mini-intronic plasmid (MIP): a novel robust transgene expression vector in vivo and in vitro. Mol. Ther. *21*, 954–963.
20. Darquet, A.M., Cameron, B., Wils, P., Scherman, D., and Crouzet, J. (1997). A new DNA vehicle for nonviral gene delivery: supercoiled minicircle. Gene Ther. *4*, 1341–1349.
21. Argyros, O., Wong, S.P., Fedonidis, C., Tolmachov, O., Waddington, S.N., Howe, S.J., Niceta, M., Coutelle, C., and Harbottle, R.P. (2011). Development of S/MAR minicircles for enhanced and persistent transgene expression in the mouse liver. J. Mol. Med. (Berl.) *89*, 515–529.
22. Diecke, S., Lu, J., Lee, J., Termglinchan, V., Kooreman, N.G., Burridge, P.W., Ebert, A.D., Churko, J.M., Sharma, A., Kay, M.A., and Wu, J.C. (2015). Novel codon-optimized mini-intronic plasmid for efficient, inexpensive, and xeno-free induction of pluripotency. Sci. Rep. *5*, 8081.
23. Cheung, W.Y., Hovey, O., Gobin, J.M., Muradia, G., Mehic, J., Westwood, C., and Lavoie, J.R. (2018). Efficient nonviral transfection of human bone marrow mesenchymal stromal cells shown using placental growth factor overexpression. Stem Cells Int. *2018*, 1310904.
24. Hamann, A., Thomas, A.K., Kozisek, T., Farris, E., Lück, S., Zhang, Y., and Pannier, A.K. (2020). Screening a chemically defined extracellular matrix mimetic substrate library to identify substrates that enhance substrate-mediated transfection. Exp. Biol. Med. (Maywood) *245*, 606–619.
25. Mun, J.-Y., Shin, K.K., Kwon, O., Lim, Y.T., and Oh, D.-B. (2016). Minicircle microporation-based non-viral gene delivery improved the targeting of mesenchymal stem cells to an injury site. Biomaterials *101*, 310–320.
26. Johnson, S.A., Ormsby, M.J., McIntosh, A., Tait, S.W.G., Blyth, K., and Wall, D.M. (2019). Increasing the bactofection capacity of a mammalian expression vector by removal of the f1 ori. Cancer Gene Ther. *26*, 183–194.
27. Raup, A., Jérôme, V., Freitag, R., Synatschke, C.V., and Müller, A.H. (2016). Promoter, transgene, and cell line effects in the transfection of mammalian cells using PDMAEMA-based nano-stars. Biotechnol. Rep. (Amst.) *11*, 53–61.
28. Antonova, D.V., Alekseenko, I.V., Siniushina, A.K., Kuzmich, A.I., and Pleshkan, V.V. (2020). Searching for Promoters to Drive Stable and Long-Term Transgene Expression in Fibroblasts for Syngeneic Mouse Tumor Models. Int. J. Mol. Sci. *21*, 6098.
29. Hardee, C.L., Arévalo-Soliz, L.M., Hornstein, B.D., and Zechiedrich, L. (2017). Advances in non-viral DNA vectors for gene therapy. Genes (Basel) *8*, 65.
30. Tan, Y., Li, S., Pitt, B.R., and Huang, L. (1999). The inhibitory role of CpG immunostimulatory motifs in cationic lipid vector-mediated transgene expression in vivo. Hum. Gene Ther. *10*, 2153–2161.
31. Lu, J., Zhang, F., Xu, S., Fire, A.Z., and Kay, M.A. (2012). The extragenic spacer length between the 5′ and 3′ ends of the transgene expression cassette affects transgene silencing from plasmid-based vectors. Mol. Ther. *20*, 2111–2119.
32. Chen, Z.Y., He, C.Y., Meuse, L., and Kay, M.A. (2004). Silencing of episomal transgene expression by plasmid bacterial DNA elements in vivo. Gene Ther. *11*, 856–864.
33. Russel, M., and Model, P. (1989). Genetic analysis of the filamentous bacteriophage packaging signal and of the proteins that interact with it. J. Virol. *63*, 3284–3295.
34. Chen, Z.-Y., He, C.-Y., Ehrhardt, A., and Kay, M.A. (2003). Minicircle DNA vectors devoid of bacterial DNA result in persistent and high-level transgene expression in vivo. Mol. Ther. *8*, 495–500.
35. Narsinh, K.H., Jia, F., Robbins, R.C., Kay, M.A., Longaker, M.T., and Wu, J.C. (2011). Generation of adult human induced pluripotent stem cells using nonviral minicircle DNA vectors. Nat. Protoc. *6*, 78–88.
36. Boura, J.S., Vance, M., Yin, W., Madeira, C., Lobato da Silva, C., Porada, C.D., and Almeida-Porada, G. (2014). Evaluation of gene delivery strategies to efficiently overexpress functional HLA-G on human bone marrow stromal cells. Mol. Ther. Methods Clin. Dev. *2014*, 1.
37. Jia, F., Wilson, K.D., Sun, N., Gupta, D.M., Huang, M., Li, Z., Panetta, N.J., Chen, Z.Y., Robbins, R.C., Kay, M.A., et al. (2010). A nonviral minicircle vector for deriving human iPS cells. Nat. Methods *7*, 197–199.
38. Bandara, N., Gurusinghe, S., Chen, H., Chen, S., Wang, L.X., Lim, S.Y., and Strappe, P. (2016). Minicircle DNA-mediated endothelial nitric oxide synthase gene transfer enhances angiogenic responses of bone marrow-derived mesenchymal stem cells. Stem Cell Res. Ther. *7*, 48.
39. Tidd, N., Michelsen, J., Hilbert, B., and Quinn, J.C. (2017). Minicircle mediated gene delivery to canine and equine mesenchymal stem cells. Int. J. Mol. Sci. *18*, 819.
40. O'Sullivan, J.M., Tan-Wong, S.M., Morillon, A., Lee, B., Coles, J., Mellor, J., and Proudfoot, N.J. (2004). Gene loops juxtapose promoters and terminators in yeast. Nat. Genet. *36*, 1014–1018.
41. Colluru, V.T., Zahm, C.D., and McNeel, D.G. (2016). Mini-intronic plasmid vaccination elicits tolerant LAG3^{+} CD8^{+} T cells and inferior antitumor responses. OncoImmunology *5*, e1223002.

42. Nott, A., Meislin, S.H., and Moore, M.J. (2003). A quantitative analysis of intron effects on mammalian gene expression. RNA *9*, 607–617.

43. Furger, A., O'Sullivan, J.M., Binnie, A., Lee, B.A., and Proudfoot, N.J. (2002). Promoter proximal splice sites enhance transcription. Genes Dev. *16*, 2792–2799.

44. Niwa, M., Rose, S.D., and Berget, S.M. (1990). In vitro polyadenylation is stimulated by the presence of an upstream intron. Genes Dev. *4*, 1552–1559.

45. Le Hir, H., Gatfield, D., Izaurralde, E., and Moore, M.J. (2001). The exon-exon junction complex provides a binding platform for factors involved in mRNA export and nonsense-mediated mRNA decay. EMBO J. *20*, 4987–4997.

46. Matsumoto, K., Wassarman, K.M., and Wolffe, A.P. (1998). Nuclear history of a pre-mRNA determines the translational activity of cytoplasmic mRNA. EMBO J. *17*, 2107–2121.

47. Xu, Y., Zhao, W., Olson, S.D., Prabhakara, K.S., and Zhou, X. (2018). Alternative splicing links histone modifications to stem cell fate decision. Genome Biol. *19*, 133.

48. Rahimi, P., Mobarakeh, V.I., Kamalzare, S., SajadianFard, F., Vahabpour, R., and Zabihollahi, R. (2018). Comparison of transfection efficiency of polymer-based and lipid-based transfection reagents. Bratisl. Lek Listy *119*, 701–705.

49. Yang, F., Green, J.J., Dinio, T., Keung, L., Cho, S.-W., Park, H., Langer, R., and Anderson, D.G. (2009). Gene delivery to human adult and embryonic cell-derived stem cells using biodegradable nanoparticulate polymeric vectors. Gene Ther. *16*, 533–546.

50. Mohamed-Ahmed, S., Fristad, I., Lie, S.A., Suliman, S., Mustafa, K., Vindenes, H., and Idris, S.B. (2018). Adipose-derived and bone marrow mesenchymal stem cells: a donor-matched comparison. Stem Cell Res. Ther. *9*, 168.

51. Zazzeroni, L., Lanzoni, G., Pasquinelli, G., and Ricordi, C. (2017). Considerations on the harvesting site and donor derivation for mesenchymal stem cells-based strategies for diabetes. CellR4 Repair Replace Regen Reprogram *5*, e2435.

52. Wada, N., Gronthos, S., and Bartold, P.M. (2013). Immunomodulatory effects of stem cells. Periodontol. 2000 *63*, 198–216.

53. Oliva, A.A., McClain-Moss, L., Pena, A., Drouillard, A., and Hare, J.M. (2019). Allogeneic mesenchymal stem cell therapy: A regenerative medicine approach to geroscience. Aging Med. (Milton) *2*, 142–146.

54. Qadan, M.A., Piuzzi, N.S., Boehm, C., Bova, W., Moos, M., Jr., Midura, R.J., Hascall, V.C., Malcuit, C., and Muschler, G.F. (2018). Variation in primary and culture-expanded cells derived from connective tissue progenitors in human bone marrow space, bone trabecular surface and adipose tissue. Cytotherapy *20*, 343–360.

55. Wang, W., Li, W., Ou, L., Flick, E., Mark, P., Nesselmann, C., Lux, C.A., Gatzen, H.H., Kaminski, A., Liebold, A., et al. (2011). Polyethylenimine-mediated gene delivery into human bone marrow mesenchymal stem cells from patients. J. Cell. Mol. Med. *15*, 1989–1998.

56. Suzuki, K., Tsunekawa, Y., Hernandez-Benitez, R., Wu, J., Zhu, J., Kim, E.J., Hatanaka, F., Yamamoto, M., Araoka, T., Li, Z., et al. (2016). In vivo genome editing via CRISPR/Cas9 mediated homology-independent targeted integration. Nature *540*, 144–149.

57. Kay, M.A., He, C.-Y., and Chen, Z.-Y. (2010). A robust system for production of minicircle DNA vectors. Nat. Biotechnol. *28*, 1287–1289.

58. Luke, J., Carnes, A.E., Hodgson, C.P., and Williams, J.A. (2009). Improved antibiotic-free DNA vaccine vectors utilizing a novel RNA based plasmid selection system. Vaccine *27*, 6454–6459.

OMTN, Volume *26*

Supplemental information

Comparison of promoter, DNA vector, and cationic carrier for efficient transfection of hMSCs from multiple donors and tissue sources

Tyler Kozisek, Andrew Hamann, Luke Samuelson, Miguel Fudolig, and Angela K. Pannier

Table S1: hMSC Donor Information				
Donor ID	Tissue Source	Age	Sex	Ethnicity/Race
D1	Adipose	22	M	Black
D2	Adipose	42	F	Black
D3	Bone Marrow	22	M	Not provided
D4	Bone Marrow	31	M	Black

Table S2: Sequences of Primers Used in qRT-PCR	
EGFP Forward	5'-ACGTAAACGGCCACAAGTTC-3'
EGFP Reverse	5'-AAGTCGTGCTGCTTCATGTG-3'
RPL-13A Forward	5'-CCTGGAGGAGAAGAGGAAAGAGA-3'
RPL-13A Reverse	5'-TTGAGGACCTCTGTGTATTTGTCAA-3'

Table S3: Type III Tests of Fixed Effects				
Effect	DF	Den DF	F Value	Pr > F
Cationic Carrier	1	4.134	15.05	0.0168
Donor	3	4.001	10.12	0.0244
Promoter	1	330.7	1455.64	<.0001
Vector	3	326	186.99	<.0001
Cationic Carrier*Donor	3	4.047	12.85	0.0156
Cationic Carrier*Promoter	1	321.4	85.87	<.0001
Cationic Carrier*Vector	3	310.9	8.16	<.0001
Donor*Promoter	3	321	18.07	<.0001
Donor*Vector	9	310	13.37	<.0001
Promoter*Vector	3	325.5	27.72	<.0001

EGFP positive cell counts for each effect (variable) were analyzed as a negative binomial with total cell count as an offset term. Kenward-Rogers adjustment was used on the degrees of freedom to account for the multiple error levels in our analysis. DF, degrees of freedom; Den DF, degrees of freedom associated with model errors; F-Value, F-test statistic; Pr > F, p-value associated with the F statistic. Significance was accepted at $p<0.05$.

Table S4: Pairwise Comparisons Between Promoters for Each Vector								
Vector	Promoter	_Promoter	Estimate	SE	DF	t Value	Pr > |t|	Adj P
Plasmid	CMV	EF1a	1.8122	0.09838	353	18.42	<.0001	<.0001
No F1	CMV	EF1a	1.9739	0.09191	316	21.48	<.0001	<.0001
MC	CMV	EF1a	1.8122	0.09838	353	18.42	<.0001	<.0001
MIP	CMV	EF1a	1.1076	0.08760	262.6	12.64	<.0001	<.0001

EGFP positive cell counts for each promoter were analyzed as a negative binomial with total cell count as an offset term. Promoter effects within each vector were compared using least square means with use of Tukey-Kramer to adjust for multiple comparisons. Estimate, logarithm of the ratio between the estimated responses for each promoter; SE, standard error; DF, degrees of freedom; t value, t-test statistic; Pr > |t|, p-value associated with the t statistic; Adj P, adjusted p-value. Significance was accepted at $p<0.05$.

Table S5: Pairwise Comparisons Between Promoters for Each Cationic Carrier

Cationic Carrier	Promoter	_Promoter	Estimate	SE	DF	t Value	Pr > |t|
Turbofect	CMV	EF1a	2.2020	0.06665	345.7	33.04	<.0001
Lipofectamine	CMV	EF1a	1.3440	0.06453	306.8	20.83	<.0001

EGFP positive cell counts for each promoter were analyzed as a negative binomial with total cell count as an offset term. Promoter effects within each cationic carrier were compared using least square means with use of Tukey-Kramer to adjust for multiple comparisons. Estimate, logarithm of the ratio between the estimated responses for each promoter; SE, standard error; DF, degrees of freedom; t value, t-test statistic; Pr > |t|, p-value associated with the t statistic. Significance was accepted at $p<0.05$.

Table S6: Pairwise Comparisons Between Promoters for Each Donor

Donor	Promoter	_Promoter	Estimate	SE	DF	t Value	Pr > |t|	Adj P
D1	CMV	EF1a	1.2843	0.09338	331.9	13.75	<.0001	<.0001
D2	CMV	EF1a	1.6203	0.09204	311.3	17.61	<.0001	<.0001
D3	CMV	EF1a	2.0922	0.09429	347.6	22.19	<.0001	<.0001
D4	CMV	EF1a	2.0951	0.09100	304.5	23.02	<.0001	<.0001

EGFP positive cell counts for each promoter were analyzed as a negative binomial with total cell count as an offset term. Promoter effects within each donor were compared using least square means with use of Tukey-Kramer to adjust for multiple comparisons. Estimate, logarithm of the ratio between the estimated responses for each promoter; SE, standard error; DF, degrees of freedom; t value, t-test statistic; Pr > |t|, p-value associated with the t statistic; Adj P, adjusted p-value. Significance was accepted at $p<0.05$.

Table S7: Pairwise Comparisons Between Vectors for Each Promoter

Promoter	Vector	_Vector	Estimate	SE	DF	t Value	Pr > |t|	Adj P
CMV	MC	MIP	-1.1961	0.08807	268.2	-13.58	<.0001	<.0001
CMV	MC	No F1	-0.8637	0.08838	272	-9.77	<.0001	<.0001
CMV	MC	Plasmid	-0.8924	0.08863	275	-10.07	<.0001	<.0001
CMV	MIP	No F1	0.3324	0.08651	250.1	3.84	0.0002	0.0009
CMV	MIP	Plasmid	0.3036	0.08677	253	3.50	0.0006	0.0031
CMV	No F1	Plasmid	-0.02875	0.08708	256.7	-0.33	0.7415	0.9876
EF1a	MC	MIP	-1.9006	0.09797	353	-19.40	<.0001	<.0001
EF1a	MC	No F1	-0.7020	0.1016	353	-6.91	<.0001	<.0001
EF1a	MC	Plasmid	-0.5063	0.1026	353	-4.93	<.0001	<.0001
EF1a	MIP	No F1	1.1987	0.09291	329.2	12.90	<.0001	<.0001
EF1a	MIP	Plasmid	1.3943	0.09413	347.9	14.81	<.0001	<.0001
EF1a	No F1	Plasmid	0.1956	0.09785	353	2.00	0.0463	0.1901

EGFP positive cell counts for each vector were analyzed as a negative binomial with total cell count as an offset term. Vector effects within each promoter were compared using least square means with use of Tukey-Kramer to adjust for multiple comparisons. Estimate, logarithm of the ratio between the estimated responses for each vector; SE, standard error; DF, degrees of freedom; t value, t-test statistic; Pr > |t|, p-value associated with the t statistic; Adj P, adjusted p-value. Significance was accepted at $p<0.05$. Red highlighted adjusted p-values indicate no significant difference at $\alpha=0.05$

Table S8: Pairwise Comparisons Between Vectors for Each Cationic Carrier

Cationic Carrier	Vector	_Vector	Estimate	SE	DF	t Value	Pr > |t|	Adj P
Turbofect	MC	MIP	-1.5044	0.09400	336.9	-16.00	<.0001	<.0001
Turbofect	MC	No F1	-0.5944	0.09662	353	-6.15	<.0001	<.0001
Turbofect	MC	Plasmid	-0.8299	0.09659	353	-8.59	<.0001	<.0001
Turbofect	MIP	No F1	0.9100	0.09115	303	9.98	<.0001	<.0001
Turbofect	MIP	Plasmid	0.6745	0.09114	303.4	7.40	<.0001	<.0001
Turbofect	No F1	Plasmid	-0.2355	0.09386	336.1	-2.51	0.0126	0.0604
Lipofectamine 3000	MC	MIP	-1.5923	0.09171	312.6	-17.36	<.0001	<.0001
Lipofectamine 3000	MC	No F1	-0.9712	0.09288	327.9	-10.46	<.0001	<.0001
Lipofectamine 3000	MC	Plasmid	-0.5689	0.09420	345.3	-6.04	<.0001	<.0001
Lipofectamine 3000	MIP	No F1	0.6211	0.08815	268.8	7.05	<.0001	<.0001
Lipofectamine 3000	MIP	Plasmid	1.0235	0.08956	285.5	11.43	<.0001	<.0001
Lipofectamine 3000	No F1	Plasmid	0.4023	0.09078	300.4	4.43	<.0001	<.0001

EGFP positive cell counts for each vector were analyzed as a negative binomial with total cell count as an offset term. Vector effects within each cationic carrier were compared using least square means with use of Tukey-Kramer to adjust for multiple comparisons. Estimate, logarithm of the ratio between the estimated responses for each vector; SE, standard error; DF, degrees of freedom; t value, t-test statistic; Pr > |t|, p-value associated with the t statistic; Adj P, adjusted p-value. Significance was accepted at $p<0.05$. Red highlighted adjusted p-values indicate no significant difference at $\alpha=0.05$

Table S9: Pairwise Comparisons Between Vectors for Each Donor

Donor	Vector	_Vector	Estimate	SE	DF	t Value	Pr > |t|	Adj P
D1	MC	MIP	-1.7418	0.1318	329.4	-13.22	<.0001	<.0001
D1	MC	No F1	-0.3901	0.1353	353	-2.88	0.0042	0.0216
D1	MC	Plasmid	-0.2420	0.1367	353	-1.77	0.0777	0.2898
D1	MIP	No F1	1.3517	0.1267	283.9	10.67	<.0001	<.0001
D1	MIP	Plasmid	1.4998	0.1283	298.4	11.69	<.0001	<.0001
D1	No F1	Plasmid	0.1481	0.1320	328.4	1.12	0.2624	0.6758
D2	MC	MIP	-2.3004	0.1325	328.6	-17.37	<.0001	<.0001
D2	MC	No F1	-1.5455	0.1338	340.6	-11.55	<.0001	<.0001
D2	MC	Plasmid	-1.2590	0.1355	353	-9.29	<.0001	<.0001
D2	MIP	No F1	0.7549	0.1242	264.7	6.08	<.0001	<.0001
D2	MIP	Plasmid	1.0413	0.1261	279.8	8.26	<.0001	<.0001
D2	No F1	Plasmid	0.2864	0.1277	292.2	2.24	0.0256	0.1142
D3	MC	MIP	-1.3379	0.1328	335	-10.08	<.0001	<.0001
D3	MC	No F1	-0.8160	0.1355	353	-6.02	<.0001	<.0001
D3	MC	Plasmid	-0.7892	0.1362	353	-5.79	<.0001	<.0001
D3	MIP	No F1	0.5220	0.1286	299.5	4.06	<.0001	0.0004
D3	MIP	Plasmid	0.5488	0.1294	306.3	4.24	<.0001	0.0002
D3	No F1	Plasmid	0.02683	0.1323	329	0.20	0.8394	0.9970
D4	MC	MIP	-0.8133	0.1273	290.7	-6.39	<.0001	<.0001
D4	MC	No F1	-0.3797	0.1298	310.1	-2.92	0.0037	0.0193
D4	MC	Plasmid	-0.5073	0.1296	309.4	-3.91	0.0001	0.0006
D4	MIP	No F1	0.4336	0.1269	284.9	3.42	0.0007	0.0040
D4	MIP	Plasmid	0.3060	0.1267	284.4	2.42	0.0164	0.0765
D4	No F1	Plasmid	-0.1276	0.1292	303.2	-0.99	0.3240	0.7565

EGFP positive cell counts for each vector were analyzed as a negative binomial with total cell count as an offset term. Vector effects within each donor were compared using least square means with use of Tukey-Kramer to adjust for multiple comparisons. Estimate, logarithm of the ratio between the estimated responses for each vector; SE, standard error; DF, degrees of freedom; t value, t-test statistic; Pr > |t|, p-value associated with the t statistic; Adj P, adjusted p-value. Significance was accepted at $p<0.05$. Red highlighted adjusted p-values indicate no significant difference at $\alpha=0.05$

Table S10: Pairwise Comparisons Between Cationic Carriers for Each Promoter

Promoter	Cationic Carrier	_Cationic Carrier	Estimate	SE	DF	t Value	Pr > |t|	Adj P
CMV	Lipofectamine 3000	Turbofect	-0.2017	0.07151	9.14	-2.82	0.0197	0.0197
EF1a	Lipofectamine 3000	Turbofect	0.6563	0.07772	12.74	8.45	<0.0001	<0.0001

EGFP positive cell counts for each cationic carrier were analyzed as a negative binomial with total cell count as an offset term. Cationic carrier effects within each promoter were compared using least square means with use of Tukey-Kramer to adjust for multiple comparisons. Estimate, logarithm of the ratio between the estimated responses for each cationic carrier; SE, standard error; DF, degrees of freedom; t value, t-test statistic; Pr > |t|, p-value associated with the t statistic. Significance was accepted at $p<0.05$.

Table S11: Pairwise Comparisons Between Cationic Carriers for Each Vector								
Vector	Cationic Carrier	_Cationic Carrier	Estimate	SE	DF	t Value	Pr > |t|	Adj P
Plasmid	Lipofectamine 3000	Turbofect	-0.08462	0.09949	32.95	-0.85	0.4012	0.4012
No F1	Lipofectamine 3000	Turbofect	0.5532	0.09832	31.46	5.63	<0.0001	<0.0001
MC	Lipofectamine 3000	Turbofect	0.1764	0.1038	38.9	1.7	0.0971	0.0971
MIP	Lipofectamine 3000	Turbofect	0.2643	0.09460	26.99	2.79	0.0095	0.0095
EGFP positive cell counts for each cationic carrier were analyzed as a negative binomial with total cell count as an offset term. Cationic carrier effects within each vector were compared using least square means with use of Tukey-Kramer to adjust for multiple comparisons. Estimate, logarithm of the ratio between the estimated responses for each cationic carrier; SE, standard error; DF, degrees of freedom; t value, t-test statistic; Pr > |t|, p-value associated with the t statistic. Significance was accepted at $p<0.05$. Red highlighted p-values indicate no significant difference at $\alpha=0.05$.								

Table S12: Pairwise Comparisons Between Cationic Carriers for Each Donor							
Donor	Cationic Carrier	_Cationic Carrier	Estimate	SE	DF	t Value	Pr > |t|
D1	Lipofectamine	Turbofect	0.5510	0.1174	4.157	4.69	0.0085
D2	Lipofectamine	Turbofect	0.6193	0.1163	4.006	5.33	0.0060
D3	Lipofectamine	Turbofect	-0.2048	0.1177	4.214	-1.74	0.1534
D4	Lipofectamine	Turbofect	-0.05621	0.1155	3.906	-0.49	0.6526
EGFP positive cell counts for each cationic carrier were analyzed as a negative binomial with total cell count as an offset term. Cationic carrier effects within each donor were compared using least square means with use of Tukey-Kramer to adjust for multiple comparisons. Estimate, logarithm of the ratio between the estimated responses for each cationic carrier; SE, standard error; DF, degrees of freedom; t value, t-test statistic; Pr > |t|, p-value associated with the t statistic. Significance was accepted at $p<0.05$. Red highlighted p-values indicate no significant difference at $\alpha=0.05$.							

Table S13: Pairwise Comparisons Between Donors for Each Promoter								
Promoter	Donor	_Donor	Estimate	SE	DF	t Value	Pr > |t|	Adj P
CMV	D1	D2	-0.6892	0.2325	4.565	-2.96	0.0351	0.1143
CMV	D1	D3	-1.2501	0.2325	4.566	-5.38	0.0039	0.0141
CMV	D2	D3	-0.5609	0.2322	4.546	-2.42	0.0655	0.2012
CMV	D4	D1	1.5946	0.2323	4.553	6.86	0.0014	0.0053
CMV	D4	D2	0.9054	0.2321	4.533	3.9	0.0138	0.0474
CMV	D4	D3	0.3445	0.2321	4.534	1.48	0.2037	0.5133
EF1a	D1	D2	-0.3532	0.236	4.852	-1.5	0.1966	0.5041
EF1a	D1	D3	-0.4423	0.2369	4.923	-1.87	0.1218	0.3474
EF1a	D2	D3	-0.0891	0.2366	4.9	-0.38	0.7223	0.9798
EF1a	D4	D1	0.7838	0.2358	4.832	3.32	0.022	0.0752
EF1a	D4	D2	0.4306	0.2355	4.81	1.83	0.1293	0.3634
EF1a	D4	D3	0.3415	0.2364	4.879	1.44	0.2095	0.5285

EGFP positive cell counts for each donor were analyzed as a negative binomial with total cell count as an offset term. Donor effects within each promoter were compared using least square means with use of Tukey-Kramer to adjust for multiple comparisons. Estimate, logarithm of the ratio between the estimated responses for each donor; SE, standard error; DF, degrees of freedom; t value, t-test statistic; Pr > |t|, p-value associated with the t statistic; Adj P, adjusted p-value. Significance was accepted at $p<0.05$. Red highlighted adjusted p-values indicate no significant difference at $\alpha=0.05$

Table S14: Pairwise Comparisons Between Donors for Each Vector

Vector	Donor	_Donor	Estimate	SE	DF	t Value	Pr > |t|	Adj P
Plasmid	D1	D2	-0.8555	0.2521	6.311	-3.39	0.0135	0.0509
Plasmid	D1	D3	-1.2511	0.2531	6.404	-4.94	0.0022	0.0088
Plasmid	D2	D3	-0.3956	0.252	6.3	-1.57	0.1652	0.4558
Plasmid	D4	D1	1.6229	0.252	6.298	6.44	0.0005	0.0023
Plasmid	D4	D2	0.7674	0.251	6.194	3.06	0.0214	0.0779
Plasmid	D4	D3	0.3718	0.2519	6.287	1.48	0.1882	0.5018
No F1	D1	D2	-0.9938	0.2504	6.14	-3.97	0.007	0.0272
No F1	D1	D3	-1.1298	0.2519	6.284	-4.49	0.0037	0.0148
No F1	D2	D3	-0.136	0.2507	6.17	-0.54	0.6065	0.9454
No F1	D4	D1	1.3472	0.2513	6.227	5.36	0.0015	0.0062
No F1	D4	D2	0.3534	0.2501	6.113	1.41	0.2066	0.5351
No F1	D4	D3	0.2174	0.2516	6.256	0.86	0.4195	0.8230
MC	D1	D2	0.1616	0.257	6.807	0.63	0.55	0.9195
MC	D1	D3	-0.7039	0.2565	6.754	-2.74	0.0298	0.1074
MC	D2	D3	-0.8655	0.2568	6.786	-3.37	0.0125	0.048
MC	D4	D1	1.3576	0.2541	6.506	5.34	0.0014	0.0056
MC	D4	D2	1.5192	0.2545	6.545	5.97	0.0007	0.003
MC	D4	D3	0.6537	0.2539	6.491	2.57	0.0393	0.1370
MIP	D1	D2	-0.397	0.2477	5.876	-1.6	0.1611	0.4438
MIP	D1	D3	-0.3001	0.2484	5.946	-1.21	0.2729	0.6446
MIP	D2	D3	0.09696	0.2484	5.941	0.39	0.7099	0.9780
MIP	D4	D1	0.4291	0.2481	5.915	1.73	0.1351	0.3875
MIP	D4	D2	0.03209	0.248	5.91	0.13	0.9013	0.9991
MIP	D4	D3	0.1291	0.2488	5.98	0.52	0.6226	0.9515

EGFP positive cell counts for each donor were analyzed as a negative binomial with total cell count as an offset term. Donor effects within each vector were compared using least square means with use of Tukey-Kramer to adjust for multiple comparisons. Estimate, logarithm of the ratio between the estimated responses for each donor; SE, standard error; DF, degrees of freedom; t value, t-test statistic; Pr > |t|, p-value associated with the t statistic; Adj P, adjusted p-value. Significance was accepted at $p<0.05$. Red highlighted adjusted p-values indicate no significant difference at $\alpha=0.05$

Table S15: Pairwise Comparisons Between Donors for Each Cationic Carrier								
Cationic Carrier	Donor	_Donor	Estimate	SE	DF	t Value	Pr > |t|	Adj P
Turbofect	D1	D2	-0.4871	0.2402	5.11	-2.03	0.0972	0.2897
Turbofect	D1	D3	-1.2241	0.2404	5.127	-5.09	0.0035	0.0132
Turbofect	D2	D3	-0.737	0.2402	5.113	-3.07	0.0271	0.0925
Turbofect	D4	D1	1.4928	0.2398	5.078	6.22	0.0015	0.0056
Turbofect	D4	D2	1.0057	0.2397	5.064	4.2	0.0083	0.0301
Turbofect	D4	D3	0.2687	0.2399	5.081	1.12	0.3127	0.6941
Lipofectamine 3000	D1	D2	-0.5553	0.239	5.003	-2.32	0.0677	0.2113
Lipofectamine 3000	D1	D3	-0.4683	0.2395	5.05	-1.96	0.1074	0.3142
Lipofectamine 3000	D2	D3	0.08698	0.2391	5.02	0.36	0.7309	0.9817
Lipofectamine 3000	D4	D1	0.8856	0.2389	5.003	3.71	0.0139	0.0492
Lipofectamine 3000	D4	D2	0.3303	0.2386	4.973	1.38	0.2252	0.5576
Lipofectamine 3000	D4	D3	0.4173	0.2391	5.019	1.74	0.1412	0.3926

EGFP positive cell counts for each donor were analyzed as a negative binomial with total cell count as an offset term. Donor effects within each cationic carrier were compared using least square means with use of Tukey-Kramer to adjust for multiple comparisons. Estimate, logarithm of the ratio between the estimated responses for each donor; SE, standard error; DF, degrees of freedom; t value, t-test statistic; Pr > |t|, p-value associated with the t statistic; Adj P, adjusted p-value. Significance was accepted at $p<0.05$. Red highlighted adjusted p-values indicate no significant difference at $\alpha=0.05$

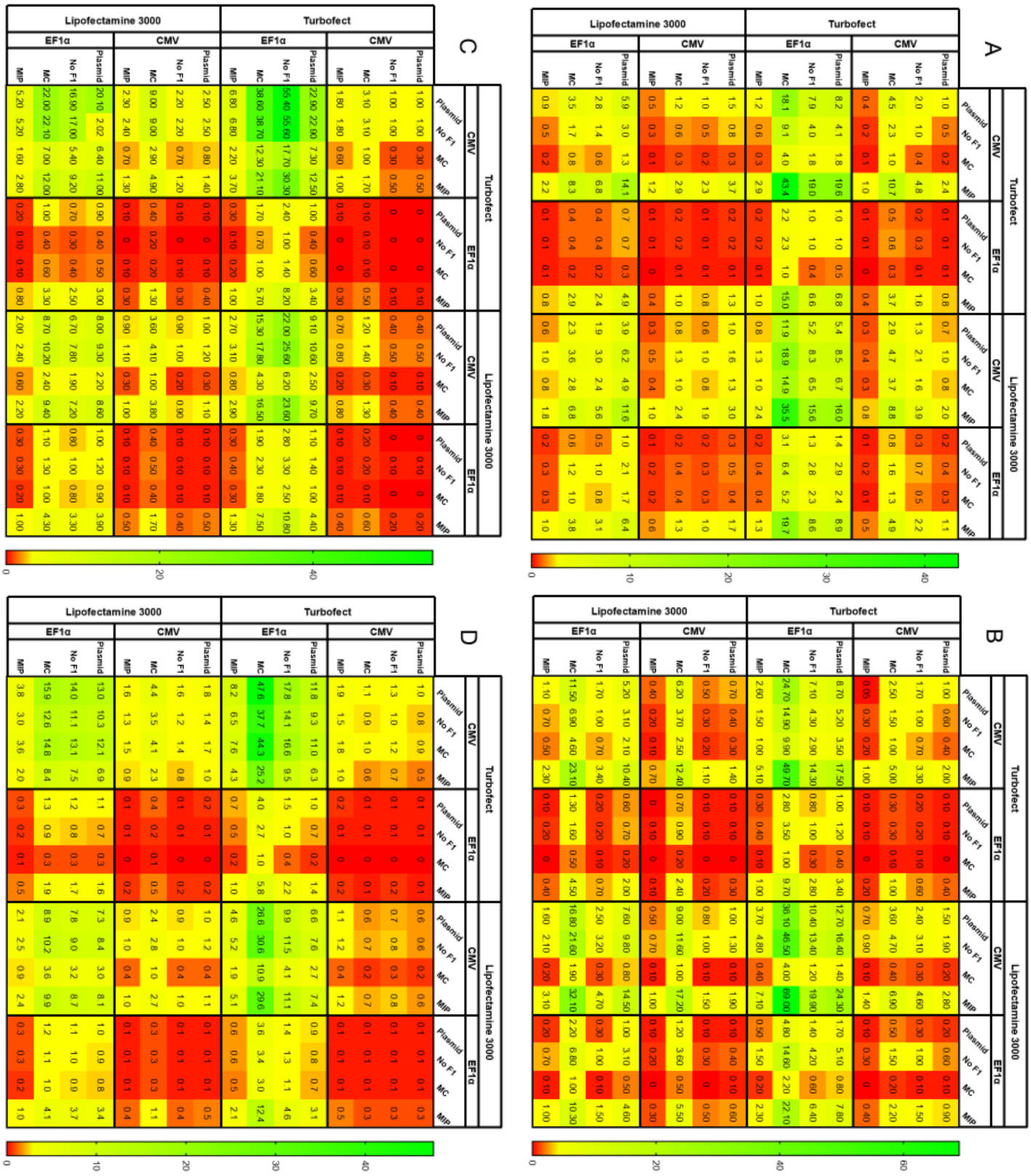

Figure S1. Donor specific transfection efficiency fold changes for all pairwise comparisons of transfection conditions. (A) Transfection efficiency fold changes for all pairwise comparisons of transfection

conditions in D1 hAMSCs. (B) Transfection efficiency fold changes for all pairwise comparisons of transfection conditions in D2 hAMSCs. (C) Transfection efficiency fold changes for all pairwise comparisons of transfection conditions in D3 hBMSCs. (D) Transfection efficiency fold changes for all pairwise comparisons of transfection conditions in D4 hBMSCs. Fold changes are presented relative to column conditions.

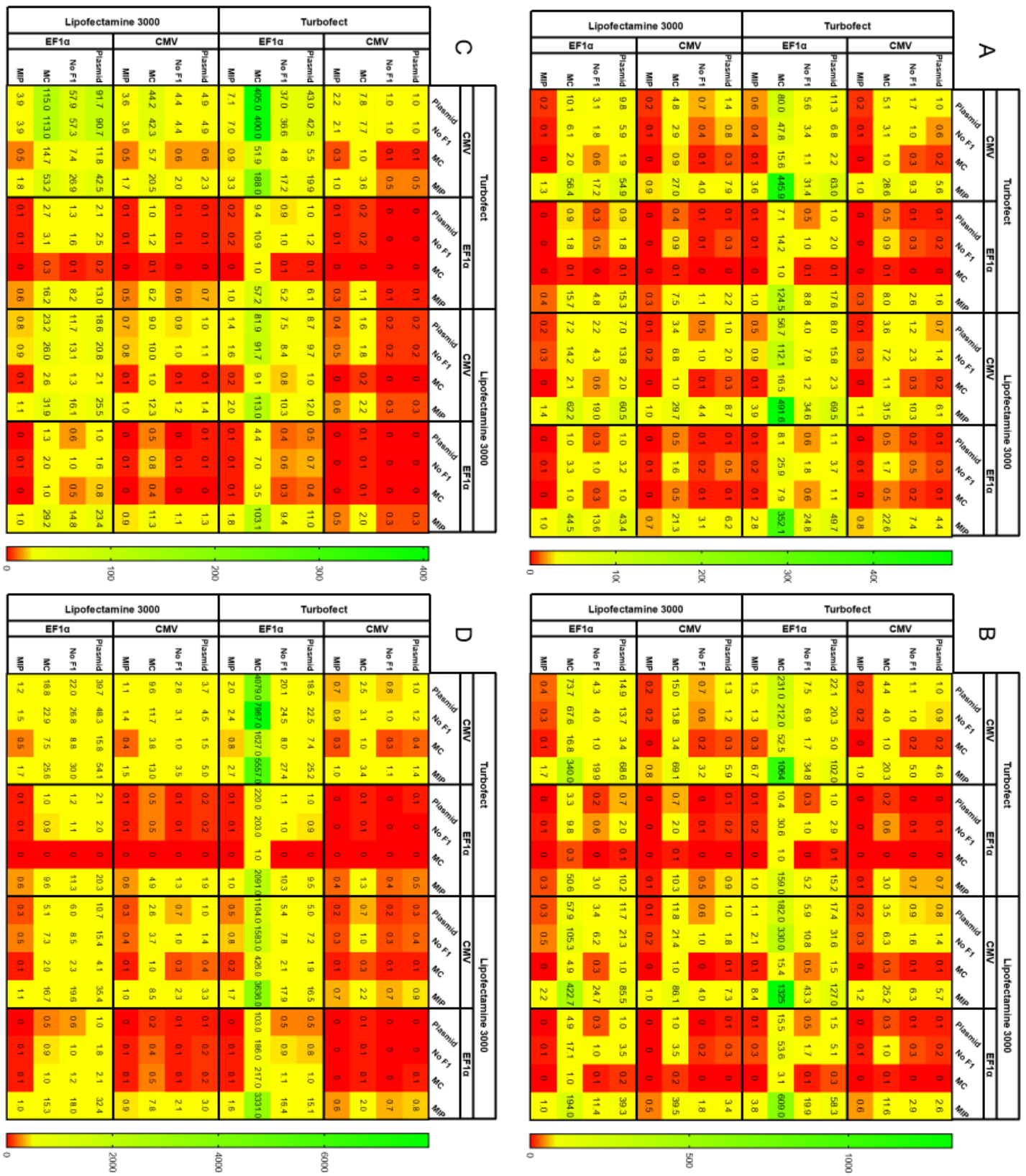

Figure S2. Donor specific transgenic luciferase activity fold changes for all pairwise comparisons of

transfection conditions. (A) Transgenic luciferase activity fold changes for all pairwise comparisons of transfection conditions in D1 hAMSCs. (B) Transgenic luciferase activity fold changes for all pairwise comparisons of transfection conditions in D2 hAMSCs. (C) Transgenic luciferase activity fold changes for all pairwise comparisons of transfection conditions in D3 hBMSCs. (D) Transgenic luciferase activity fold changes for all pairwise comparisons of transfection conditions in D4 hBMSCs. Fold changes are presented relative to column conditions.

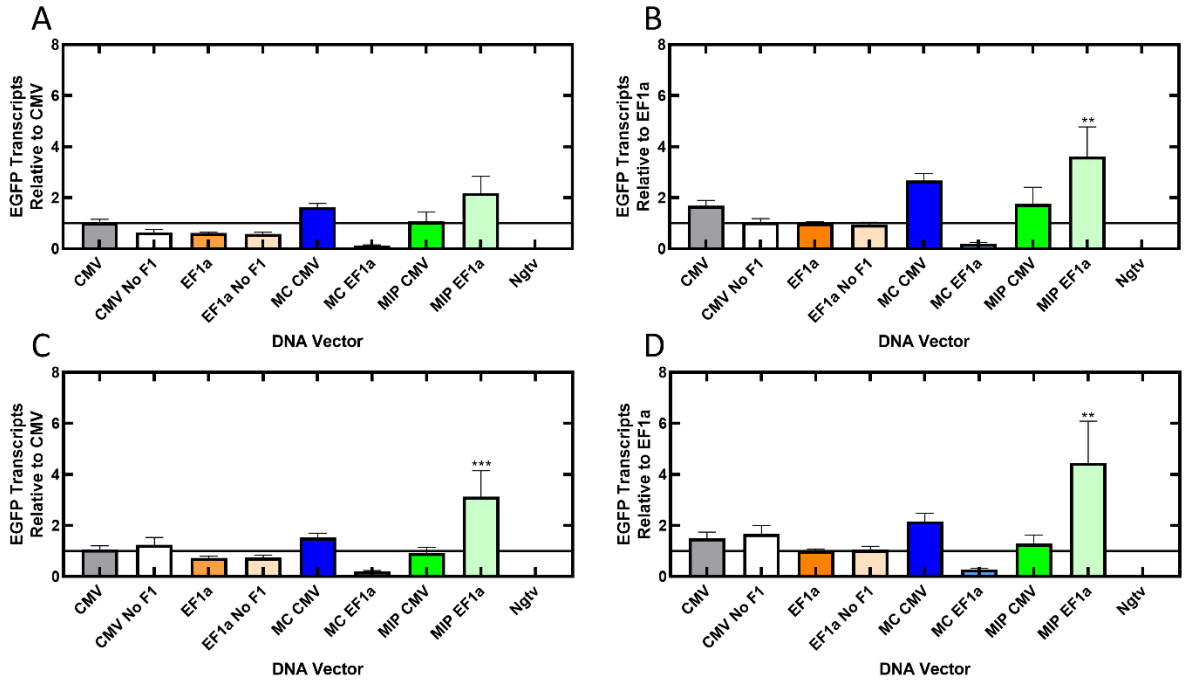

Figure S3. Relative transgenic mRNA transcripts at 12- and 24-hours following delivery of complexes as a function of DNA vector and promoter. (A) Transgenic mRNA transcripts, relative to the plasmid vector with the CMV promoter, for D1 hMSCs 12 hours after delivery of DNA vectors complexed with Turbofect. (B) Transgenic mRNA transcripts, relative to the plasmid vector with the EF1a promoter, for D1 hMSCs 12 hours after delivery of DNA vectors complexed with Turbofect. (C) Transgenic mRNA transcripts, relative to the plasmid vector with the CMV promoter, for D1 hMSCs 24 hours after delivery of DNA vectors complexed with Turbofect. (D) Transgenic mRNA transcripts, relative to the plasmid vector with the EF1a promoter, for D1 hMSCs 24 hours after delivery of DNA vectors complexed with Turbofect. Data in bar graphs are represented as mean ± SEM (n=6). *, $p<0.05$; **, $p<0.01$; ***, $p<0.001$; ****, $p<0.0001$.

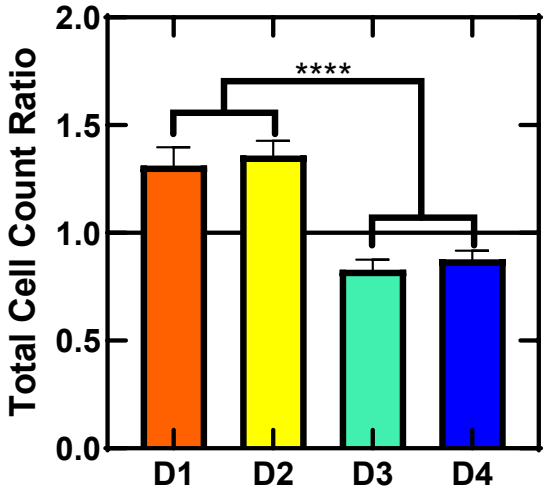

Figure S4. Cationic carrier effects on total cell counts in different donors of hMSCs derived from adipose tissue and bone marrow. Total cell counts for a DNA vector complexed with Turbofect were divided by total cell counts for the same DNA vector complexed with Lipofectamine 3000 for each donor to calculate total cell count ratios, which is an indirect measure of toxicity and/or proliferative effects of Turbofect relative to Lipofectamine 3000. Data in bar graphs are represented as mean ± SEM (n=48/donor). ****, $p<0.0001$